STUDIES IN RS CANUM VENATICORUM TYPE STARS

THESIS SUBMITTED IN PARTIAL FULFILMENT OF THE REQUIREMENTS FOR THE DEGREE OF DOCTOR OF PHILOSOPHY IN THE FACULTY OF SCIENCE, PANJAB UNIVERSITY, CHANDIGARH

1992

S. MOHIN

Acknowledgements

I am extremely grateful to Prof.R.K.Kochhar for suggesting the topic, and for his encouragement throughout the work. I am also grateful to Prof.S.K.Trehan who took special interest and helped me in various ways for the successful completion of this work.

My thanks are due to late Prof.M.K.V.Bappu who introduced me to the field of observational astronomy in 1972.

The invaluable help of my friends Raveendran and Mekkaden for generously sharing their scientific insight with me and their patience in going through the entire manuscript are gratefully acknowledged. I also thank Prof.T.P.Prabhu and Dr.G.C.Anupama for making me familiar with their computer program for spectroscopic reduction.

Mr.S.Muthukrishnan prepared the line drawings and the offset work was done by Mr.R.Krishnamoorthy. Mr.M.G.Chandrasekharan Nair and Mr.B.A.Varghese helped me at the computer centre. I thank them.

Finally, I am very grateful to all my friends at Kavalur and Bangalore who took special interest in providing all the necessary help for this study.

Summary

It had been customary to divide variable stars into three classes: eruptive, pulsating, and eclipsing. It has recently been realized that there exists a fourth class of 'rotating variable stars' to which RS Canum Venaticorum systems belong. The most important characteristic of RS CVn systems in the optical region is the variable light curve arising from rotational modulation by spotted areas on the stellar photosphere.

The present work was started with the aim of obtaining multiband photometric observations covering the entire phases of light curve for a few selected RS CVn stars and to use our database in conjunction with published observations to numerically model the light curves with a view to deriving physical parameters. Though RS CVn characteristics were first detected in double-lined spectroscopic binaries, later many single-lined spectroscopic binaries were found. We have selected two single-lined and two double-lined binaries for our investigation. All four are non-eclipsing close binaries: DM UMa and II Peg are single-lined, whereas V711 Tau and UX Ari are double-lined. All these objects are known to show Hα as pure emission feature above the continuum at all times. This is a clear signature of chromospheric activity. So it was decided to supplement the photometric data with $H\alpha$ spectroscopy.

The thesis has been divided into eight chapters. The first chapter contains a general introduction to RS CVn systems and a short description of their observational characteristics at wide wavelength regions. This chapter also includes a brief discussion of other variable stars which mimic RS CVns in chromospheric activity and irregular light variation. A report of the present study is also given. The second chapter describes the method of

observations and data reduction.

The method of least squares using differential correction was employed to solve the light curves. Chapter 3 deals with the method. It gives a short review of the existing spot models available in the literature, the mathematical formulation of our method and some of its salient features. When observations are available in more than one wavelength band, the present method allows the simultaneous determination of the spot temperature along with the other parameters. In this respect our method is superior to other published methods. The computer program in Fortran developed by us is fairly general; there is no restriction either on the number of discrete spots, or on their latitudes or longitudes. Further, the temperature of the spots may be treated as either known or unknown, in which case it may be either the same for all the spots or different for different spots.

BV photometry of DM UMa was obtained on a total of 96 nights. It is analysed along with the observations available from 1979 onwards. The results are presented in chapter 4. All the data are analysed in terms of the spot model. This is the first time that such an extensive dataset has been used for an RS CVn star. The modelling indicates a slow migration of the spots in latitude towards the equator from 1984 onwards, and a decrease in the spot area during the same period. Note that this result is contrary to what is observed in the sun. Phases of light minima of DM UMa lie on four well separated lines and all of them show migrations towards decreasing orbital phases. We find that the lifetime of a spot group can be as short as about two years. During the period of our observations the $H\alpha$ emission is well correlated with the photometric phase in the sense that the emission is more intense near the light curve minimum. An optical flare event has also been detected in this object.

Chapter 5 deals with the other non-eclipsing single-lined spectroscopic binary, II Peg. An analysis of the data shows that on most occasions during the period 1974–91 there were two prominent spots or spot groups present on the surface of the active component. We could identify a total of six spot groups and their lifetimes range from two to seven years. The migration of the phase of light minimum has both direct and retrograde motions; this is in

contrast to the behaviour of the other objects studied. At larger amplitudes the brightness at minimum is found to decrease and the brightness at maximum to increase. Chugainov's observations in 1974 however do not conform to this trend. The maximum light level in V was close to 7.35 mag during 1976–85. From 1986 onwards we find that it has secularly increased; it was 7.25 mag during 1989. The $H\alpha$ observations indicate that II Peg, like DM UMa, also shows a very strong and asymmetrical emission line. The emission is variable and modulated with the photometric phase. Our $H\alpha$ data show that the star has a tendency for flaring up during the photometric minimum.

The observations and analysis of the double-lined spectroscopic binary V711 Tau are discussed in chapter 6. BV photometry was obtained on a total of 120 nights. The mean light level of the system during 1982–91 was found to be about 0.05 mag brighter than that during 1975–82. We attribute this to a global reduction in the spot area. Phases of light minima lie on two independent near-straight lines, implying that spots are predominantly confined to two different latitude belts. The lifetime of a centre of activity is more than 15 years. The amplitude of the light curve is highly variable and shows a cyclic behaviour with a period of about three years. At larger amplitudes the brightness at maximum and minimum shows the same behaviour as that of II Peg; both of them converge to $\Delta V \sim 1.55$ mag at very low amplitudes. The possible scenarios are discussed. The $H\alpha$ observations indicate that the emission strengths are variable. No modulation either with orbital phase or with photometric phase is found during the period of our observations.

UX Ari is the subject of chapter 7. The star was observed photometrically on a total of 101 nights. We find that $B-V$ is phase dependent with the system being reddest at the light maximum. The investigation shows that the $B-V$ variations arise as a result of the variable fractional contribution by the hotter component (G5 V) to the total light of the system. At larger amplitudes of the light curves the behaviour of both light maximum and minimum is quite similar to that of V711 Tau. The spectroscopic observations at $H\alpha$ region show a sudden drop in the emission equivalent width around the phases 0.8–1.0.

Finally in chapter 8 the results of the present study are summarized, and

further prospects briefly touched upon. Doppler imaging technique would give independent information on the distribution of spots on the stellar surface. However this can be applied to only fast rotators. We stress the need for coordinated multiwavelength observations to answer some of the related problems.

Chapters, figures and tables are numbered sequentially all throughout. The references are given at the end.

Contents

1

INTRODUCTION

1. Historical introduction

The recognition that RS Canum Venaticorum type stars form a separate subgroup of variable stars came in 1946 when Struve pointed out that these binaries show *Ca II H* and *K* emission lines ($\lambda\lambda$ 3933, 3969) (Struve 1946). In these objects the emissions are much stronger than would be expected in typical single stars of the same spectral type. The emissions arise from a late G or early K component of the binary and reflect the orbital motion of that component. The candidates for this group of stars increased with the work of Hiltner (1947) and Gratton (1950). Later in a study of the absolute dimensions of eclipsing binaries Plavec & Grygar (1965) found that a few of them, namely RS CVn, WW Dra, Z Her, AR Lac, and SZ Psc stood apart from the rest of the binaries; in these systems both the components are late-type and detached; and the mass ratios are about unity. Further studies by Popper (1970) and Oliver (1974) strengthened the arguments in favour of the existence of this group. Extensive photometric studies of the eclipsing binary RS CVn by Chisary & Lacona (1965) and Catalano & Rodono (1967, 1969) paved the way for the classification of a new group of variable stars with RS CVn as the prototype.

Hall (1976) suggested the following observational criteria to pick out

RS CVn systems after examining the various characteristics of 24 similar well observed systems then available: (i) Orbital periods range from 1-14 days. (ii) Strong *Ca II H* and *K* emissions. (iii) The hotter star is of spetral type F or G, and luminosity class V or IV. The cooler star is of spectral type late G or early K, and luminosity class III-IV.

An increase in the number of RS CVn candidates has highlighted the inadequacy of Hall's criteria. It is now known that a number of these systems are single-lined spectroscopic binaries (e.g., II Peg, DM UMa) where the nature of the secondary is not known. Moreover, there are systems with periods longer than 14 days (e.g., ζ And, λ And). The active components in the above systems have the same observational characteristics of the binaries considered by Hall.

Thus we can distinguish an RS CVn from the rest of variables if it exhibits the following observational characteristics (Fekel, Moffett & Henry 1986).

(i) Binarity with a late-type giant-subgiant component.

(ii) Variable light curves arising from the rotational modulation not attributable to pulsation, eclipses, or ellipticity.

(iii) Variable and enhanced chromospheric activity.

RS CVn stars have attracted much attention due to their peculiarities at wide wavelength regions. Apart from the presence of strong *Ca II H* and *K* emissions in the optical region, these objects show intense coronal X-ray emission and very strong radio flares (Spangler et al. 1977; Feldman et al. 1978; Walter et al. 1980; Linsky 1988).

2. X-ray and ultraviolet emissions

RS CVn systems are the most luminous nondegenerate late-type stellar X-ray sources. After the discovery of strong soft X-ray emission from the RS CVn system UX Ari by HEAO-1 (Walter, Charles & Bowyer 1978), regular X-ray observations of these objects have been started. Charles (1983) has reviewed the 'high energy picture' of RS CVn systems. These systems exhibit greatly enhanced coronal activity. The X-ray emission indicates a coronal temperature of 10^7 K which is almost an order of magnitude higher than the

values found for the quiet sun coronal structures.

X-ray spectroscopy of the highly active RS CVn systems shows multi-temperature spectra indicating that the emission originates from two physically distinct regions, one of which is at a typical solar temperature while the other is at a considerably higher temperature. The line emission is consistent with solar abundances of the heavy elements. Observations of X-ray flares from six RS CVn systems namely, V711 Tau, DM UMa, II Peg, HD 8357, HD 101379, and V532 Cen suggest extremely energetic events with peak soft X-ray luminosities ranging from 6×10^{30} to 10^{33} erg s^{-1}. Similar flare events have been detected as enhanced ultraviolet emission line fluxes in several systems (Weiler et al. 1978; Simon et al. 1980; Baliunas et al. 1984; Buzasi et al. 1987; Simon & Sonneborn 1987; Linsky 1988).

High resolution International Ultraviolet Explorer spectra have provided important informations on RS CVn stars. The study of the inhomogeneous structure of stellar atmosphere by making use of chromospherically active stars in a binary system has received a fillip from IUE observations. It is expected that as a result of the star's rotation, the active regions, if they exist, can modulate the fluxes in the emission lines arising from the high temperature transition regions. This modulation due to rotation which connects the photosphere and the associated active regions in the upper atmosphere became clear only with IUE observations. Simultaneous optical photometry and coordinated IUE observations of several RS CVn objects revealed that the emission line flux is a function of the photometric phase. The strength of emission lines such as *C II* (λ 1335), *C IV* ($\lambda\lambda$ 1548, 1530), and *Si IV* ($\lambda\lambda$ 1394, 1403) originating in transition region is 30-50 % higher at photometric light minimum than it is at light maximum. Flare spectra of RS CVn stars show that these high temperature lines are strengthened by larger factors as compared to the low temperature chromospheric lines like *C I* (λ 1657) and *Mg II* ($\lambda\lambda$ 2796, 2803) (Rodono, Romeo & Strazzula 1980; Ayres & Linsky 1982; Baliunas & Dupree 1982; Marstad et al. 1982; Ayres, Simon & Linsky 1984; Dorren et al. 1986; Rodono et al. 1987).

3. Radio emission

Many RS CVn stars exhibit strong and variable emission on time scales of minutes to several days. The flare luminosities observed in some of these systems occasionally exceed $L_R = 10^8$erg s^{-1}Hz^{-1} which is about 10^5 times that of a typical solar radio flare. The important radio properties of these objects are listed by Bookbinder (1988). Morris & Mutel (1988) have detected 54 objects out of 93 systems observed at 6 cm, while Drake et al. (as quoted in Bookbinder 1988) have detected over 70 of the 110 observed systems. Slee et al. (1987) have reported the detection of 25 systems out of 37 at 8.4 GHz in a survey of southern objects. It is yet unclear whether a true quiescent emission level exists or whether the emission is the result of the superposition of many small flares.

The radio emission is often circularly polarized, and its apparent correlation with the observing frequency, luminosity, and orbital inclination suggests the existence of large-scale magnetic field structure in these systems (Mutel et al. 1987). In the Drake et al. sample the mean radio luminosity (10^{16} erg s^{-1} Hz^{-1}) is found to be independent of the period of the system. Morris & Mutel (1988) have also found no correlation of rotation period with radio luminosity except perhaps for systems with periods shorter than about 10 days. The apparent lack of an activity–rotation relation for these systems is puzzling in view of the presumed role of the 'dynamo' as the ultimate driving mechanism for the radio emission.

Using Very Large Baseline Interferrometric techniques, the sizes of the radio emitting regions have been measured for several systems. These sources are often resolved on the milliarcsec level and have brightness temperatures of the order of a few 10^{10} K. The structures revealed by these observations also indicate that there are two characteristic sizes: (i) an optically thin emission component, with moderate polarization, that has a size comparable to the binary separation, and (ii) an unresolved, unpolarized 'core'. The combination of high brightness temperature and moderate degree of circular polarization suggests that the radiation is probably due to gyrosynchrotron emission from MeV electrons in a magnetic field between 10 and 100 Gauss.

4. Chromospheric phenomena

The *Ca II H* and *K* emission lines are recognized as the signature of the presence of stellar chromosphere which, in analogy with the sun, is defined as the atmospheric layer between the photosphere and the corona (that is between the visible surface and the extremely hot outermost extension of its atmosphere). At present it is generally accepted that nonradiative heating is responsible to a large extent for the existence of the solar chromosphere, although direct momentum transfer to the gas by mechanical waves or $L\alpha$ radiation pressure may be important in cool giants and supergiants. It is in this region that the emission lines of neutral and singly ionized atoms originate (cf. Linsky 1980).

If the sun, which is a typical average star (G2V), has a chromosphere, we should expect that stars of different luminosities and masses that have effective temperature comparable to the solar value will display features indicative of similar phenomena and perhaps on a grander scale. A difficulty that we encounter when we go over to survey other stars is that we have no more the advantage of the availability of a disc for close scrutiny that the sun represents. The manifestation of a chromosphere and chromospheric activity in the case of stars can be identified only from the integrated spectrum or from monochromatic light intensity variations, if they exist. In the case of cool stars usually the existence of chromosphere has been recognized through the presence of emission components in the *Ca II H* and *K* lines.

The Wilson–Bappu empirical relation between the widths of the *Ca II H* and *K* emission cores and stellar absolute magnitude enables one to express the properties of stellar chromosphere as a function of spectral type and luminosity. It is well known that the magnetic fields control the structures of outer atmosphere of the sun and sun-like stars. Extension of the studies of solar magnetic activity to stars of different masses, ages, metallicities, evolutionary status, and rotation rates has yielded many new results. In the case of lower main sequence stars, observations indicate that both stellar rotation and chromospheric emission decay proportionately to the square root of stellar age (Skumanich 1972; Soderblom 1982). However, Simon et

al. (1985) have shown that the decline with age is better fit by an exponential law with e-folding times shorter for the high-excitation transition region lines than for the low-excitation chromospheric lines. Wilson (1978) has made a study of the long term behaviour of stellar chromospheric activity variations in the main sequence stars, apparently single or widely spaced binary systems of spectral types F, G, K, and M. The study has since been extended by others to cover nearly 100 lower main sequence stars. Baliunas (1986) has summarized the result of these investigations. About 85% of the stars are found to be variable, and 60% of the total have cyclic behaviour that is periodic or likely to be periodic. A few stars have multiple periods. Cyclic periods shorter than five years only occur as the primary period for stars more massive than the sun.

With the introduction of modern detectors like CCD the studies of RS CVn objects have received a new impetus. The recent observational information regarding chromospheric emission features in RS CVn stars is reviewed by Bopp (1990) and Ramsey (1990).

The first search for the *Ca II H* and *K* emission variability in RS CVn stars (Weiler 1978) indicated a correlation between emission intensity and orbital phase in the case of three stars: UX Ari, the prototype RS CVn and Z Her. However, the correlation is only moderately strong for the prototype, and marginal for the other two. Observations of λ And show that the relative flux at *K* is larger by 25 - 100 % at light minimum than at light maximum. Also there are rapid variabilities of *K* line emission by as much as 10% on a time scale of 10 minutes and they are several magnitudes larger than the total radiative output of typical solar flares (Baliunas et al. 1981; Baliunas & Dupree 1982). The spectrophotometric study of a few objects indicates that there is no strong correlation of chromospheric loss rate at *Ca II H* and *K* and $H\alpha$ (λ 6563) and rotational velocity. Also an active RS CVn type star V711 Tau does not show any significant variation in the *Ca II* flux (Bopp 1983).

It has been known that $H\alpha$ is also an important indicator of chromospheric activity in RS CVn stars (Bopp 1990 and references therein). Early surveys indicated $H\alpha$ to be completely or partially filled by emission in most

RS CVn stars (Weiler 1978; Bopp & Talcot 1978). It was argued that the complex spatial behaviour of the $H\alpha$ line in the sun cannot be compared with the observation of the integrated stellar line to study the chromospheric activity in stars (Linsky 1983). The recent high resolution studies of this line in stars have proved that the $H\alpha$ line is a feature which may exhibit complex temporal behaviour (Fekel, Moffett, & Henry 1986; Bopp et al. 1989). There are a few systems (V711 Tau, UX Ari, II Peg, and DM UMa) which are known to show $H\alpha$ as a pure emission feature above the continuum, or as a completely filled in absorption feature at all times. The above four systems have been extensively monitored in $H\alpha$ by several investigators who report strong net emission with large nightly variations and the variablity in the net flux showing stellar flares (Dorren et al. 1981; Fraquelli 1984; Nations & Ramsey 1986).

5. RS CVn stars in perspective

It had been customary to divide variable stars in three classes: eruptive, pulsating, and eclipsing. In a variable star, in addition to its light variability, its spectral type (or colour) and radial velocity may also vary. The discovery of chromospheric activity along with detection of soft X-ray emission, ultraviolet and infrared excess in a number of variable stars made it necessary to include these phenomena in the classification scheme of variable stars. A new class called 'rotating variables' was introduced comprising of candidates showing the above listed phenomena. In a rotating variable, the light variation is assumed to be due to a nonuniform surface brightness distribution arising from the presence of spots, or regions of low or high surface brightness. When the rotational axis of the star does not coincide with the direction of line of sight, the net surface brightness of its hemisphere turned towards the observer can vary. RS Canum Venaticorum systems belong to this recently recognized group of variable stars called 'rotating variable stars' (Kholopov 1984). There are many variables observationally similar to RS CVn stars by way of their chromospheric activity and irregular light variation, though they are of at different stages of stellar evolution. W-type W Ursa Majoris binaries, BY Draconis stars, T Tauri stars and FK Comae stars are the systems

most often compared with RS CVn stars.

Evolutionary studies have shown that RS CVn systems consist of evolved stars; both the components have evolved from main-sequence through processes not radically different from normal single-star evolution. When a component of the system has exhausted its core hydrogen and developed a convective envelope as it moves along the red-giant branch of H-R diagram, instabilities develop which manifest themselves in many irregularities in the electromagnetic spectrum from radio to X-ray. During this period evolution is accelerated through mass exchange and perhaps mass loss (Popper & Ulrich 1977). Studies based on stellar evolution calculations of binaries with periods in the range 1-30 days show that the evolutionary status of components of RS CVn binaries is due to normal nuclear evolution (Morgan & Eggleton 1979).

W UMa binaries are contact eclipsing systems and consist of cool dwarfs with orbital periods less than one day. Their masses are unequal and they are spectroscopically similar in optical region. It is generally believed that both stars are inside a common envelope; in these the more massive one generates most of the luminosity and then transfers to the outer envelope of the secondary (Eaton 1986).

BY Dra stars consist of both single and binary main-sequence stars of spectral types K and M having strong $Ca\ II\ \ H$ and K as well as Balmer emission lines. Their light curves have a low amplitude variability with period of a few days (Bopp & Fekel 1977).

FK Comae stars are single late-type giants with very high rotational velocity ($\geq$ 100 km s^{-1}). They also show strong $Ca\ II\ \ H$ and K, and $H\alpha$ in emission and are photometrically variable with a period of a few days to nearly a week (Bopp & Stencel 1981).

T Tauri stars are the low-mass pre-main-sequence stars. Their evolutionary phases are characterised by irregular brightness variations on time scales from minutes to decades with appreciable amplitudes of up to about $\Delta m \approx 6$ mag. The great majority of the known T Tauri stars show enhanced chromospheric activity and it is generally assumed that these stars have large-scale surface inhomogenity (Appenzellar & Mundt 1989).

There are several other groups of objects which are chromospherically active and which mimic the RS CVn stars in one or the other observational characteristics (Hall 1989). A much better understanding of all these systems, which represent objects in different stages of stellar evolution, can become possible, only when all the relevant phenomena concerning both observation and theory are better explored (Popper 1980).

6. Starspots

The most important characteristic of RS CVn systems in the optical region is the variable light curve arising from rotational modulation. Not only does the light curve change in shape, but it changes in mean light level, amplitude, and phases of the light maximum and minimum also. In most of these systems the light curve has a period nearly equal to the binary orbital period. The evolution of light curves, based on many years of observation of several systems, is available now. The light curves of a typical RS CVn star DM UMa are shown in Figure 1.

It is now widely accepted that one of the hemispheres of the active star is predominantly covered by starspots, analogous to sunspots, which rotationally modulate the observed flux and give rise to the photometric light curve (Hall 1976). Slow changes in the phase of light curves are attributed to the differential rotation of the active star in the binary. The variations seen in the amplitude of the light curves presumably arise due to changes in size, number, area of spots, etc. The fractional area which the spots are expected to cover in order to account for the enormous optical variation exhibited by these binaries is indeed on a far greater scale than that is seen on the sun even during the sunspot maximum.

The spot hypothesis was first introduced by Kron (1947, 1952) to explain the light variation of AR Lac and YY Gem. However, it did not receive much attention then because of the limited observational data. The starspot model was resurrected by Hall (1972) with a view to explaining the irregularities noticed in the light curves of the prototype RS CVn accumulated for more than 10 years by the Catania astronomers (Chisary & Lacona 1965; Catalano & Rodono 1967, 1969).

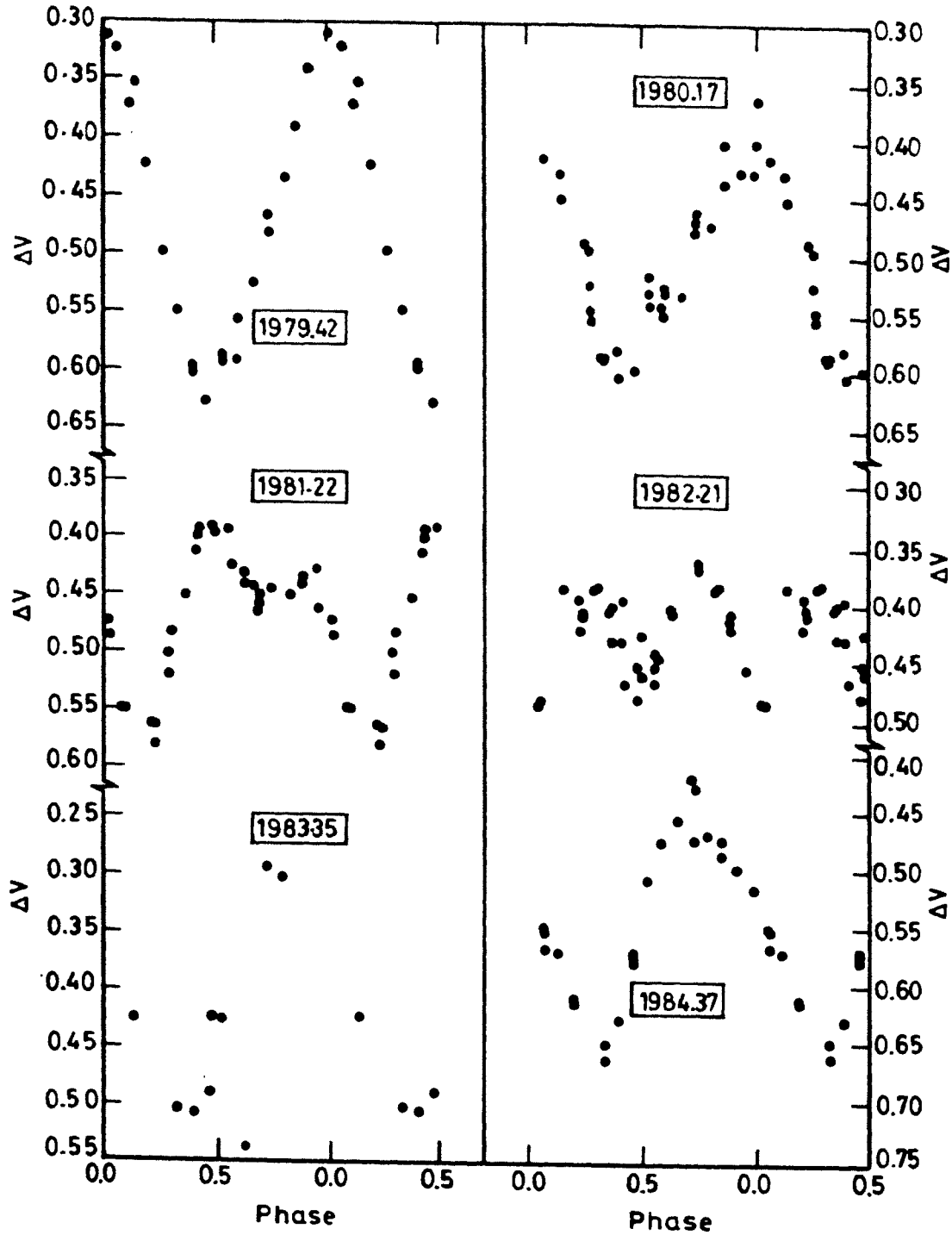

Figure 1. *V* light curves of a typical RS CVn star DM UMa (Chapter 4).

Initially, evidence in support of the presence of the inhomogenities on the surface of the cool star came only from broadband photometry in the optical region. Later, many coordinated multi-wavelength observations supported the model of a star with starspots and associated active regions in the RS CVn systems (Bopp 1983, 1990; Linsky 1984, 1988; Ramsey 1990). A few pieces of the observational evidence are listed below:

(i) Spectroscopic observations of V711 Tau (= HR 1099) showed that TiO bands have enhanced absorption near the photometric minimum (Ramsey & Nations 1980).

(ii) In the case of λ And it was found that the fluxes of $Ca\ II\ \ K$ line and the transition region emission lines are larger at light minimum than at light maximum (Baliunas & Dupree 1982).

(iii) Coordinated IUE and optical photometry of II Peg show a clear enhancement of chromospheric and transition region lines during the light minimum (Rodono et al. 1987)

(iv) Simultaneous photometry and TiO spectroscopy for II Peg show an orbital modulation of absorption in TiO bandhead similar to the light modulation (Huenemoerder, Ramsey & Buzasi 1989).

(v) High resolution spectra show phase-dependent asymmetry in absorption line profiles in objects with large rotational velocities $\geq$ 30 km s^{-1} (Fekel 1983); Doppler imaging technique uses this information to deduce the surface distribution of spots (Vogt & Penrod 1983; Gondoin 1986).

7. Present study

The general picture that has emerged is that the characteristics of RS CVn systems can be understood in terms of sun-like activity. In these systems we are seeing exceptionally large chromospheric, coronal and flare activity as compared to the sun. RS CVn stars provide a link between solar and stellar phenomenology.

As we have seen, the most important photometric characteristic of these systems is the light curve arising from the rotational modulation by spotted areas on the stellar photosphere. For a proper understanding of these systems it is necessary to have an extended photometric coverage during all phases of

the light curve which spans several orbital periods. Our observational programme was dictated by the existing facilities at Vainu Bappu Observatory, Kavalur. The number of clear-sky nights and available telescope time had their share in defining the programme.

Our main aim has been to obtain multi-band photometric observations covering the entire phase of the light curve for selected objects giving special attention to four RS CVn systems, namely, DM UMa, II Peg, V711 Tau and UX Ari. All four are non-eclipsing close binaries; DM UMa and II Peg are single-lined spectroscopic binaries, whereas V711 Tau and UX Ari are double-lined. These four objects are available at Kavalur during the best part of the observing season (Nov−Apr). These objects have been observed several nights in a month and some times several times in a night to be sure of their variations. A 34-cm telescope at Kavalur was dedicated for the programme. Its small size was not a serious handicap since the selected objects are fairly bright enough. The photometer, filters, detector and the recording units were kept the same throughout for the observational programme. Thus the resulting data have been free from any systematic errors. Since all these binaries have short periods, of about a week or less, it has been possible to subject them to a thorough photometric investigation.

We have supplemented our photometric data with the spectroscopic data wherever possible. All these binaries are known to show $H\alpha$ as pure emission feature above the continuum, or as a completely filled-in absorption feature at all times. Spectroscopic monitoring of these systems at high resolution ($\lambda/\Delta\lambda \approx 10000$) in the $H\alpha$ region is a valuable aid in understanding the chromospheric activity. Moreover, spectroscopic observations have been obtained in such a way as to have a full coverage of the orbital phases of these systems and to remain close to the photmetric monitoring days. We have used our database in conjunction with published observations to numerically model the light curves with a view to deriving physical characteristics of starspots.

2

OBSERVATIONAL TECHNIQUES

8. BV photometry

Observations were made with the 34-cm reflector of Vainu Bappu Observatory, Kavalur (VBO) using a conventional single channel photoelectric photometer through the two filters: B (1mm BG12 + 2mm GG13) and V (Corning 3384). An uncooled RCA 1P21 photomultiplier tube kept at 900 V was used for the entire observations. The output from the PMT was amplified using a d.c. amplifier specifically built for this purpose and then registered on a strip chart recorder (Raveendran & Mohin 1987).

A typical sequence of observations of a star consisted of the following: star plus sky in filter V; sky in V; star plus sky in B; and sky in B. During the observations, if the photometric quality of the sky was found to be poor, the sequence was repeated in the reverse order for standard stars. The sequence, comparison–variable–check star, was repeated at least four times during each night of observation, essentially to bring down the errors caused by variations in sky transparency and poor telescope tracking.

The combination of the telescope, filter and light detector defines its own set of magnitude and colours, normally referred to as the observer's system quantities. From the system magnitudes v and b, the system colour $(b-v)$ was calculated for each object observed.

9. Extinction correction

From the mean time of observation through V and B filters, the airmass X through which the object was observed was obtained using (Hardie 1962)

$$X = secZ - 0.0018167\,(secZ - 1) - 0.002875\,(secZ - 1)^2 - 0.0008083\,(secZ - 1)^3.$$

The zenith distance Z of the object is given by

$$secZ = (sin\phi sin\delta + cos\phi cos\delta cosh)^{-1},$$

where h and δ are the known hour angle and declination of the object, and ϕ is the latitude, taken to be 12° 34' 32" for Kavalur. The magnitude v_o and $(b-v)_o$ corrected for the atmospheric extinction are usually obtained from

$$v_o = v - \{k_v + k'_v\,(b-v)\}\,X, \tag{1}$$

and

$$(b-v)_o = (b-v) - \{k_{bv} + k'_{bv}\,(b-v)\}\,X, \tag{2}$$

where k_v and k'_v are the first and second order magnitude extinction coefficients, and k_{bv} and k'_{bv} are the corresponding quantities for the $(b-v)$ colour. The second order coefficient in yellow band V is negligible (Hardie 1962), and hence equation (1) reduces to

$$v_o = v - k_v\,X. \tag{3}$$

On many nights on which the programme stars were observed, it was not possible to determine the extinction coefficients owing to several reasons, the presence of intermittent clouds being one of them. Hence, for consistency the mean extinction coefficients representing an entire observing season were used for the data reduction.

In variable star photometry, all the measurements are made differentially with respect to a close-by comparison star at a nearly identical airmass. In terms of the differences, equation (3) can be written as

$$\Delta v_o = \Delta v - k_v\,\Delta X. \tag{4}$$

The mean difference in the airmasses of the variable star and the comparison star at the times of observation normally does not exceed 0.02. A maximum uncertainty of ~ 0.1 in k_v will affect the magnitude difference by less than 0.002 mag which is negligible compared to other sources of error. Hence, the use of an average value for k_v in place of the particular night's extinction coefficient would not introduce any significant error in the results of differential photometry.

According to equation (4), k_v can be obtained by observing the difference in magnitudes of two nonvariable stars through a range of differential airmasses. This procedure can be advantageously used to determine a mean extinction coefficient representing an entire observing season by combining several nights' data. This is so because it essentially removes the effects due to any variation in the zero-point of magnitude that arises from the changes in several parameters like high tension voltages, reflectivity of the telescope optics, transmittance of the various optical components in the photometer, etc. Similarly, if there are two or more observations of a standard star on any single night, data obtained on several nights can be combined to derive a mean value of k_v. In this case equation (3) reduces to

$$k_v \Delta X = \Delta v.$$

In differential photometry, equation (2) becomes

$$\Delta(b-v)_o = \Delta(b-v) - k_{bv} \Delta X - k'_{bv} (b-v) \Delta X - k'_{bv} \Delta(b-v) X.$$

The second order term k'_{bv} is nearly constant for a particular site, being $\sim$ 0.02 for Kavalur. Usually, the chosen comparison star will have a colour very similar to that of the variable. This, together with $\Delta X < 0.02$ makes the contribution by the second order terms negligibly small. So, the second order terms have been completely neglected in the data reduction, and the following equation was used

$$\Delta(b-v)_o = \Delta(b-v) - k_{bv} \Delta X. \qquad (5)$$

Unlike the magnitude extinction coefficient, the colour extinction coefficient does not vary significantly from night to night (Oke 1965). Hence, as in

the case of differential magnitudes use of mean k_{bv} will not introduce any appreciable error in the differential colour.

10. System calibration

The system magnitude and colour obtained were next transformed to the standard UBV system (Johnson 1963). This was achieved by observing a number of stars with well-defined standard UBV values along with the programme stars and deriving the system transformation coefficients using the following relations (Hardie 1962):

$$(B-V) = \mu(b-v)_o + \zeta_{bv}, \tag{6}$$

$$V = v_o + \epsilon(B-V) + \zeta_v. \tag{7}$$

Table 1. Mean extinction and system coefficients

Season	k_v	k_{bv}	ϵ	μ	ζ_{bv}
1984-85	0.20	0.14	0.025±0.005	0.977±0.007	0.586±0.004
1985-86	0.25	0.15	0.059±0.010	0.997±0.009	0.483±0.003
1986-87	0.25	0.15	0.021±0.003	0.987±0.006	0.490±0.002
1987-88	0.22	0.12	0.042±0.004	1.037±0.005	0.282±0.003
1988-89	0.14	0.14	0.026±0.003	0.977±0.005	0.606±0.002
1989-90	0.24	0.17	0.031±0.002	0.973±0.003	0.566±0.002
1990-91	0.20	0.14	0.043±0.002	0.989±0.002	0.461±0.001

The transformation coefficients μ, ζ_{bv}, and ϵ do not vary significantly during a particular observing season, whereas the magnitude zero-point term ζ_v might change appreciably from night to night. An accurate knowledge of the extinction coefficient is essential for an adequate determination of ζ_v. Mean values of μ and ζ_{bv}, representing an entire season, can be obtained by combining data on standard stars obtained on several nights spread over the whole observing season. But ϵ has to be determined using a particular night's

data, and then a suitable average value can be derived by consolidating the values obtained on several nights during the observing season. The system transformation coefficients derived for the various seasons are given in Table 1 along with the mean extinction coefficients k_v and k_{bv}.

11. Standard differential quantities

As already mentioned, in variable star photometry all the measurements are done with respect to a nearby comparison star. Equations (6) and (7) can be written using differences as

$$\Delta(B-V) = \mu\,\Delta(b-v)_o,$$

$$\Delta V = \Delta v_o + \epsilon\,\Delta(B-V).$$

If σ_μ and $\sigma_{\Delta bv}$ are the probable errors in μ and $\Delta(b-v)_o$, the error in $\Delta(B-V)$ is given by

$$\sigma_{\Delta BV} = \{\Delta(b-v)_o^2\,\sigma_\mu^2 + \mu^2\,\sigma_{\Delta bv}^2\}^{\frac{1}{2}}. \tag{8}$$

Similarly, if $\sigma_{\Delta v}$ and σ_ϵ are the probable errors in Δv_o and ϵ, probable error in ΔV is given by

$$\sigma_{\Delta V} = \{\sigma_{\Delta v}^2 + \epsilon^2\,\sigma_{\Delta BV}^2 + \Delta(B-V)^2\,\sigma_\epsilon^2\}^{\frac{1}{2}}. \tag{9}$$

The only unknowns in the above expressions are $\sigma_{\Delta v}$, and $\sigma_{\Delta bv}$. Usually, along with the comparison one more nonvariable, called the check star, is also observed and the probable errors in Δv_o and $\Delta(b-v)_o$ are calculated from the standard deviations in the observed differential magnitudes and colours of the comparison and check stars. These quantities, evaluated from the data for an entire season, include the uncertainties in several parameters like the extinction coefficients, gain step calibrations of the d.c. amplifier, etc. involved in the reduction of the data.

The differential magnitudes and colours of the variable can be directly converted to magnitudes and colours if standard UBV values are available for either the comparison or the check star. Otherwise, another nearby non-variable with well determined UBV values should be observed differentially

with respect to the comparison on a couple of nights. Using the mean differential magnitude and colour thus determined, the standard magnitude and colour of the comparison can be calculated. These values in turn can be used to convert the differential magnitudes and colours of variable star to magnitudes and colours.

12. $H\alpha$ observations

Spectroscopic observations were made with the Zeiss Cassegrain 102-cm telescope of the VBO using Carl-Zeiss Universal Astronomical Grating Spectrograph (UAGS) with a Bausch and Lomb 1800 lines mm^{-1} grating blazed at 5000Å in the first order. The detector used was a Thomson–CSF TH 7882 CCD chip coated for enhanced sensitivity to ultraviolet radiation and mounted in a liquid-nitrogen-cooled dewar. The data acquisition was done through 'Photometrics CCD system' supplied by Photometrics Ltd., U.S.A. The UAGS setup with a 250-mm Schmidt camera gives a dispersion of ≈ 0.50Å per pixel at $H\alpha$ region. The slit width was set to give a projected width of around two pixels. Wavelength calibrations were carried out using a Fe–Ne hollow cathode tube.

The spectroscopic data were analysed on a VAX 11/780 computer using the interactive package RESPECT developed locally at VBO (Prabhu & Anupama 1991). The spectrum extraction procedures in RESPECT are based on optimal extraction algorithm discussed by Horne (1986). The extraction of the one-dimensional spectrum from the two-dimensional image involves the following procedure:

(i) The correction for electronic bias and thermal background

Electronic bias needs to be subtracted to correct the data counts for the mean d.c. voltage offset given to the detector electronics to avoid negative counts from the Analogue to Digital Converter. The image also needs to be corrected for the signal registered by the detector in the absence of exposure to light *i.e.* dark counts due to detector white noise. In the case of the Photometrics CCD system in use at Kavalur, it was found that for an operating temperature of −120 C the mean dark count value was not significant even for a 30 minute integration. Hence, a mean of the bias and dark values along

with the mean scattered light in the spectrograph were subtracted out from the raw data image at each wavelength.

(ii) The correction for sky background

The recorded spectrum contains contribution from the background sky. By keeping the slit height larger than the stellar image size the sky spectrum was exposed on either side of the star-plus-sky spectrum. A smooth continuous sky spectrum was estimated first and the resultant spectrum was scaled to account for the difference in the effective number of pixels of object and sky spectra, and then subtracted from the star-plus-sky spectrum to yield the required object spectrum.

(iii) The correction for pixel-to-pixel sensitivity variations (flat-fielding)

Though CCD has got an excellent linearity, it suffers from substantial pixel-to-pixel sensitivity variations, largely caused by the variations in the collection area of the pixels in the device. The telescope dome was illuminated by a continuum source of tungsten filament to provide uniform brightness. Many images of the dome were then taken in an observing night and the flat-field constructed from good exposures was used to correct for the nonuniform sensitivity across the pixels.

The corrected spectrum was first obtained by subtracting the electronic bias and thermal background from the observed raw spectrum and then dividing the result with the flat field spectrum. The final stellar spectrum was obtained by subtracting the corrected sky background from the corrected star-plus-sky spectrum. The wavelength calibration of the stellar spectrum was established using the coefficients obtained by fitting a polynomial of order 3 to the comparison spectrum. The standard deviation of fit was $\sim$ 0.015Å in the wavelength calibration.

Only observations with a signal to noise ratio S/N $\sim$ 100 were included in the analysis. The integration times ranged from 30 to 45 minutes for these spectra. In a few cases individual spectra with poor S/N ratio were co-added to improve the S/N ratio. In such cases each spectrum was individually extracted and then added after wavelength calibration. All the spectra were normalized to the continuum level defined in each spectrum by a straight line fit to the relatively line-free stable points.

Table 2. Equivalent widths (EW2) for standard stars

Star	JD 2440000.+	EW2 (Å)
ρ Gem (F0 V)	8265.3111	5.354
	8265.3236	5.145
	8295.2361	5.425
	8322.1792	5.502
ϵ Vir (K0 III)	8294.3889	3.195
	8295.4826	3.080
	8296.5028	3.036
α Tau (K5 III)	8224.4111	2.471
	8225.4000	2.642
	8294.1694	2.774
	8295.1229	2.639
α Boo (K0 III)	8295.4951	2.476
	8296.4958	2.522

The observed $H\alpha$ emission line profile comprises of the true $H\alpha$ emission profile superposed on the $H\alpha$ absorption line profile. In the case of double-lined spectroscopic binaries, photospheres of both components contribute to the absorption line profile and form a complex continuum under the emission profile. The variation in the absorption line profile due to the orbital motion of the stars introduces significant phase dependent distortions in the observed emission profiles. In the case of RS CVn stars the contribution from the underlying absorption lines can be removed either theoretically or empirically by using one of the following techniques:

(i) For the same spectral types as the programme stars the theoretical absorption line profiles are constructed from model atmosphere calculations and then subtracted from the observed $H\alpha$ line profiles (Fraquelli 1984).

(ii) A high signal/noise spectrum of a standard star similar to the program star in spectral type is artificially broadened, aligned in wavelength and suitably normalized, and then subtracted from the observed spectrum of the program star (Ramsey & Nations 1984; Buzasi, Ramsey & Huenemoerder 1991).

The resolution employed in the present observations is not good enough for a detailed profile analysis and hence we have concentrated our efforts only on the equivalent width measurements. The program stars in the present study are all non-eclipsing binaries and so the equivalent width of the underlying $H\alpha$ absorption profiles is independent of orbital phase.

Two different estimates of H_α equivalent widths have been made from the programme star spectra; the first (denoted by EW1) was obtained by integrating the H_α emission profile above the continuum, and the second (denoted by EW2) by subtracting the area below the continuum from the area above the continuum in the fixed wavelength interval $\lambda\lambda$ 6550-6580.

In order to estimate the errors in the measurement of equivalent width of programme stars, a few standard stars of late spectral types were also observed on several nights. The equivalent widths EW2 obtained for these objects are given in Table 2 which shows that the method entails an uncertainty of $\sim$ 0.2Å. In both cases EW1 and EW2, the wavelengths for the integration were visually set on the computer monitor. To ascertain the consistency of the method independent measurements were made on the same spectra. It is encouraging to note that the EWs did not differ by more than 0.05Å in any case.

3

SPOT MODELLING

13. General remarks

The extensive observational materials on RS CVn systems at wide wavelength regions from radio to X-rays that has accumulated over recent years indicate the existence of starspots analogous to sunspots on the active component. Several attempts have been made to reproduce the light curves of RS CVn systems assuming starspots to be responsible for the observed light variation (Eaton & Hall 1979; Kimble, Kahn & Bowyer 1981; Dorren & Guinan 1982; Vogt 1983; Poe & Eaton 1985; Rodono et al. 1986; Zeilik et al. 1990 and the references therein).

There are two different approaches that have been followed to reproduce the light curves using starspot models : (i) a continuous distribution of small spots within an equatorial belt (Eaton & Hall 1979; Kimble, Kahn & Bowyer 1981), and (ii) a small number of large discrete, usually one or two spots, in most cases at high latitudes (Dorren & Guinan 1982; Poe & Eaton 1985; Rodono et al. 1986; Zeilik et al. 1990). There is no solar analogue for the high latitude spots; however there are no compelling theoretical reasons to rule them out. The simple solutions of Doppler imaging techniques using high resolution spectra suggest a small number of large spots, sometimes even close to the poles (Rodono et al. 1986; Vogt & Hatzes 1991). Another

indirect evidence suggesting the presence of large discrete spots comes from the recent detection of a localized magnetic field in the RS CVn binary HR 1099 by Donati et al. (1990). The above suggestions are model-dependent. A large body of observations, both spectroscopic and photometric, obtained during several seasons is expected to give important clues to the nature of starspots.

There are many difficulties in modelling the observed light curves. One of the basic parameters involved in spot modelling is the brightness of the immaculate or the unspotted photosphere. It is very difficult to assign the unspotted magnitude since the brightness at light curve maximum has been found to vary in almost all well observed systems (see the following Chapters). On the basis of the starspot model, the variation in brightness at light maximum can be accounted for by either of the two likely phenomena occurring on the surface of the active star: (i) Changes in the longitudinal distribution of spots present in the equatorial region, or (ii) changes in the area of spots present in the polar region.

Specifically, in the case of DM UMa (Chapter 4) for which the model is applied to reproduce all the available observed light curves till date, the brightness at light maximum observed in 1984 was fainter by $\sim$0.20 mag than that observed during 1989-90. Assuming that the light maximum observed on the latter occasion corresponds to the unspotted star, the change in the brightness at light maximum observed on the former occasion can be accounted for on the assumption of four nearly equal equatorial spots at longitudes separated by $\sim$90°. If the spots are cooler by $\sim$1300 K than the undisturbed photosphere they should cover a total fractional area of $\sim$0.28 (assuming orbital inclination $i = 40°$). The total fractional area within a belt of $\pm$30°about the equator is 0.50. Therefore restricting the spots to equatorial regions will leave no room to accommodate the spots needed for the light modulation in addition to the change in the brightness at light maximum. It is to be noted that a change of about 0.20 mag in the light maximum can be produced by a single spot covering a fractional area about 0.07, if situated at a higher latitude.

In light curve modelling, usually the spot parameters are derived by

varying the different parameters systematically until acceptable approximation to the observations is obtained. In almost all cases the temperatures of the spots were fixed initially, and only a single-wavelength band data were made use of (Rodono et al. 1986; Budding & Zeilik 1987; Zeilik et al. 1988). Poe & Eaton (1985) have derived starspot areas and temperatures in several binary systems with late-type components; they first determined the best fit latitude, longitude and size for the spots that reproduce the shape and amplitude of the V curve, and then used the amplitude of a colour curve, usually $V-I$, to define the spot temperature. In the case of BH Vir, a short period RS CVn binary, Zeilik et al. (1990) have determined the spot temperature using multiband photometry. They used the V band data to determine the size of the spot (assuming T = 0 K) and then adjusted the ratio of the flux of the spot to that of the photosphere at I band to derive the spot temperature. Similarly they have compared the B and R band observations also.

The present approach employs the method of least squares using differential correction to the parameters to arrive simultaneously at the best fit values for the various parameters, including the temperature, assuming that the light variation is caused by a limited number of large discrete spots. The presence of a strict minimum in the sum of the squares of the deviations in the multidimensional parameter space is indicated by the absolute convergence of the solution on iteration; the problem of choosing the final parameters from a set of possible values does not arise in this method because all the spot parameters are optimized simultaneously instead of optimizing each one of them independently. Apart from avoiding any personal bias thus, this method also allows the simultaneous determination of the spot temperature when observations are available in more than one wavelength band. In this respect the present method is better than the other spot modelling methods existing in the literature.

14. Mathematical formulation

We make the following assumptions: (i) The spotted star is spherical, (ii) both the undisturbed and spotted regions radiate like blackbodies and (iii) limb-darkenings in the two regions follow quadratic laws. The monochro-

matic luminosity of the undisturbed star is then given by

$$L_\lambda = R^2 B_\lambda(T_*) \int \{1 - A_*(1 - cos\theta) - B_*(1 - cos\theta)^2\} cos\theta \, dA,$$

where R is the stellar radius; T_* is the effective temperature; $B_\lambda(T_*)$ the Planck function; A_* and B_* are the limb-darkening coefficients; dA is an element of surface area; and θ is the angle between the line of sight and the radius along dA; the integration is carried over the visible hemisphere. The change in luminosity due to the presence of a spot of effective temperature T_s is given by

$$\Delta L_\lambda = R^2 B_\lambda(T_*) \int \{1 - A_*(1 - cos\theta) - B_*(1 - cos\theta)^2\} cos\theta \, dA$$
$$- R^2 B_\lambda(T_s) \int \{1 - A_s(1 - cos\theta) - B_s(1 - cos\theta)^2\} cos\theta \, dA,$$

where A_s and B_s are the limb-darkening coefficients of the spotted region, and the integrations are over the visible spot area. If several discrete spots are present, the total change in luminosity is obtained using

$$\Delta L_\lambda^T = \sum_{spots} \Delta L_\lambda.$$

The magnitude of the star at photometric phase ϕ is given by

$$m_\lambda(\phi) = -2.5 log \frac{L_\lambda - \Delta L_\lambda^T(\phi)}{L_\lambda} + M_\lambda, \qquad (1)$$

where M_λ is the unspotted magnitude of the star. In the case of light contribution by a nearby companion, L_λ in equation (1) should be replaced by $L_\lambda(1 + R_\lambda)$, R_λ being the luminosity ratio of the components at λ.

The above considerations are general to the extent that no assumptions are made either on the specific shape of the spots or on their nature whether cool or hot. For the present analysis we have assumed that the spots are circular in shape so that the spot is completely described by the four parameters, spot radius (θ_R), polar distance (θ_P), longitude (θ_L) and temperature (T_s). The assumptions are simplistic. The fact that there is always a clear rotational modulation, in most cases with well defined one or two minima, indicates that most of the light variation is due to a prominent spot or spot

group. There may be additional spots or spot groups scattered over the surface contributing negligibly to the over all light modulation. An irregular spot, or spot group can be replaced by an 'equivalent' circular spot, and the spot parameters thus determined would refer to this equivalent spot. Under such an approximation, modelling a single light curve would not be of much significance; but modelling a series of light curves obtained during several successive seasons would be helpful in determining the average spot characteristics and spot evolution. Spot parameters can also be obtained spectroscopically through the techniques of Doppler imaging (Vogt & Penrod 1983). But in systems like DM UMa, where the rotational velocities are low, this technique would be very difficult. The observed magnitude is a function of ΔL_λ^T which in turn is a function of the above parameters of the various spots. If we denote these parameters by θ_i (i = 1, n where n is four times the number of spots) equation (1) can be written in the functional form as

$$m_\lambda = m_\lambda(\phi, \theta_i, ...). \tag{2}$$

For a least square solution of the spot parameters, we follow the method outlined in Scarborough (1964) for a nonlinear function. Expanding equation (2) about the initial guess values for the spot parameters θ_i', using Taylor's theorem, we obtain

$$m_\lambda = m_\lambda(\phi, \theta_i', ...) + \left(\frac{\partial m_\lambda}{\partial \theta_i}\right)_0 \delta\theta_i + ... \tag{3}$$

The derivatives $\left(\frac{\partial m_\lambda}{\partial \theta_i}\right)_0$, are obtained at $\theta_i = \theta_i'$. Equation (3) is linear in $\delta\theta_i$ and using the observational data normal equations which are equations of condition to minimize the sum of the squares of residuals are derived. Here $\delta\theta_i$ are the corrections to the initial guess values, and the procedure is repeated by replacing θ_i' by $\theta_i' + \delta\theta_i$ until convergence is reached. The various derivatives are numerically evaluated using

$$\left(\frac{\partial m_\lambda}{\partial \theta_i}\right)_0 = \frac{m_\lambda(\phi, \theta_i' + \Delta\theta_i, ...) - m_\lambda(\phi, \theta_i' - \Delta\theta_i, ...)}{2\Delta\theta_i}.$$

The monochromatic luminosities at the effective wavelengths of observation were numerically evaluated by taking about 200 surface area elements, and

a similar number of area elements were taken inside the region of a spot to compute ΔL_λ. On doubling these numbers the change in the net magnitude is found to be less than 1.0×10^{-4}. To compute the derivatives we used a value of 2° for $\Delta\theta_R, \Delta\theta_P$ and $\Delta\theta_L$, and a value of 20 K for ΔT. The resulting normal equations were solved using the Cracovian matrix method (Kopal 1959), since along with the coefficients it gives the uncertainties involved in their evaluation. The derivatives can also be derived using these uncertainties for $\Delta\theta_R, \Delta\theta_P$, etc. after the first iteration, but we found no additional advantage; the convergence is reached faster, but the computation time increases since after each iteration the standard deviation of fit has to be calculated for the evaluation of the uncertainties.

The computer program in Fortran developed by us is fairly general; there is no restriction either on the number of discrete spots or on their latitudes or longitudes. Further, the temperature of the spots may be treated as either known or unknown, in which case it may be either the same for all the spots or different for different spots. The determinancy of the spot parameters is indicated by their absolute convergence on iteration from the starting initial guess values; otherwise divergence occurs with the spot area or temperature finally becoming negative. Our trials with synthetic data indicate that the choice of the initial guess values are not critical for achieving the convergence of the solution.

15. Results and discussion

In Figure 2, we have plotted the synthetic V and B light curves due to a circular spot of radius $\theta_R = 31.5°$at a polar distance of $\theta_P = 11.5°$(typical values derived for DM UMa, Chapter 4) for a few selected spot temperatures. The orbital inclination was taken as $i = 40°$, and the limb-darkening coefficients in V and B were taken as A = 0.78 and A = 0.92, respectively; the photospheric temperature was taken as $T_* = 4700$ K. The calculations show that the amplitude of light variation in V band is 0.14 mag and the corresponding amplitude of $B - V$ modulation is around 0.026 mag due to a spot of temperature $T_S = 3400$ K. Out of this the contribution due to the differential limb-darkening estimated using the case $T_S = 0$ K is 0.018 mag,

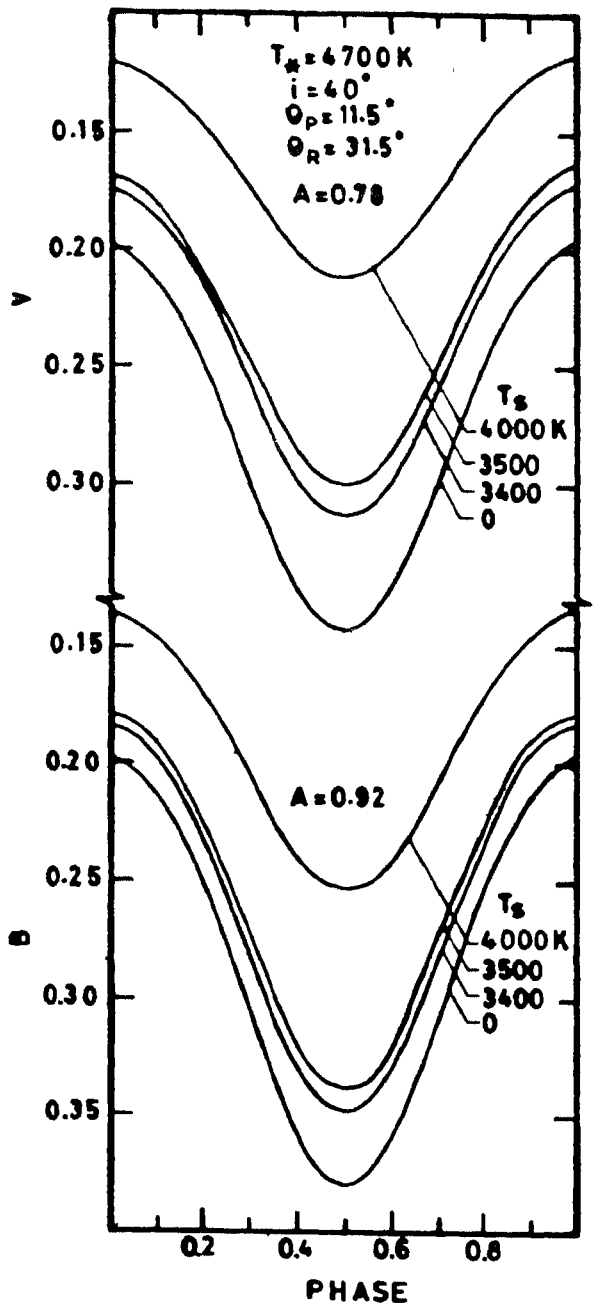

Figure 2. Synthetic V and B light curves for different assumed spot temperatures. The assumed spot parameters are indicated in the figure. The spotted V and B magnitudes are taken as 0.0 mag.

indicating that any determination of temperature separately from the amplitude of $B-V$ modulation is meaningless. Poe & Eaton (1985) have clearly demonstrated that the wavelength dependence of limb-darkening contributes a large fraction of the variation in the colours $U-B$, $B-V$ and even $V-R$, and they have suggested that only the $V-I$ colour curve can be used as a reliable indicator of spot temperature.

We find from Figure 2 that the shape of the light curve does not change substantially with change in temperature and it depends mainly on the spread of the spotted region; however, the mean light level changes appreciably with the spot temperature. The changes in the amplitudes of the light curves are much larger than the changes in the amplitude of the colour curve. From the figure we also find that larger changes occur in V band than in B band indicating that observations at longer wavelength bands are more suitable for the determination of the spot parameters, especially the spot temperature.

In the bottom panel of Figure 3, we have plotted the expected amplitudes of modulations of $B-V$, $V-R$, and $V-I$ colours. The limb-darkening coefficients in R and I bands were taken as A = 0.57 and A = 0.45, respectively (Poe & Eaton 1985). From the figure we find that largest modulations in colours are produced by spots of temperature $\sim$ 3500 K on a photosphere of temperature 4700 K. The differential limb-darkening contributes a large fraction of the variation in all the colours including $V-I$. The effects due to temperature in $B-V$ and $V-R$ colours are nearly the same (< 0.01 mag), indicating that $V-R$ observations do not have any appreciable advantage over $B-V$ observations (see also the top panel of Figure 2); but in the $V-I$ colour, the effect due to the temperature is larger (~ 0.02) making it the more suitable for the determination of spot temperature. It is clear from the figure that even an uncertainty of ~ 0.01 mag in the determination of colour amplitude would lead to a rather large uncertainty (> 500 K) in the determination of spot temperature, if spot temperature is determined separately from the colour modulation.

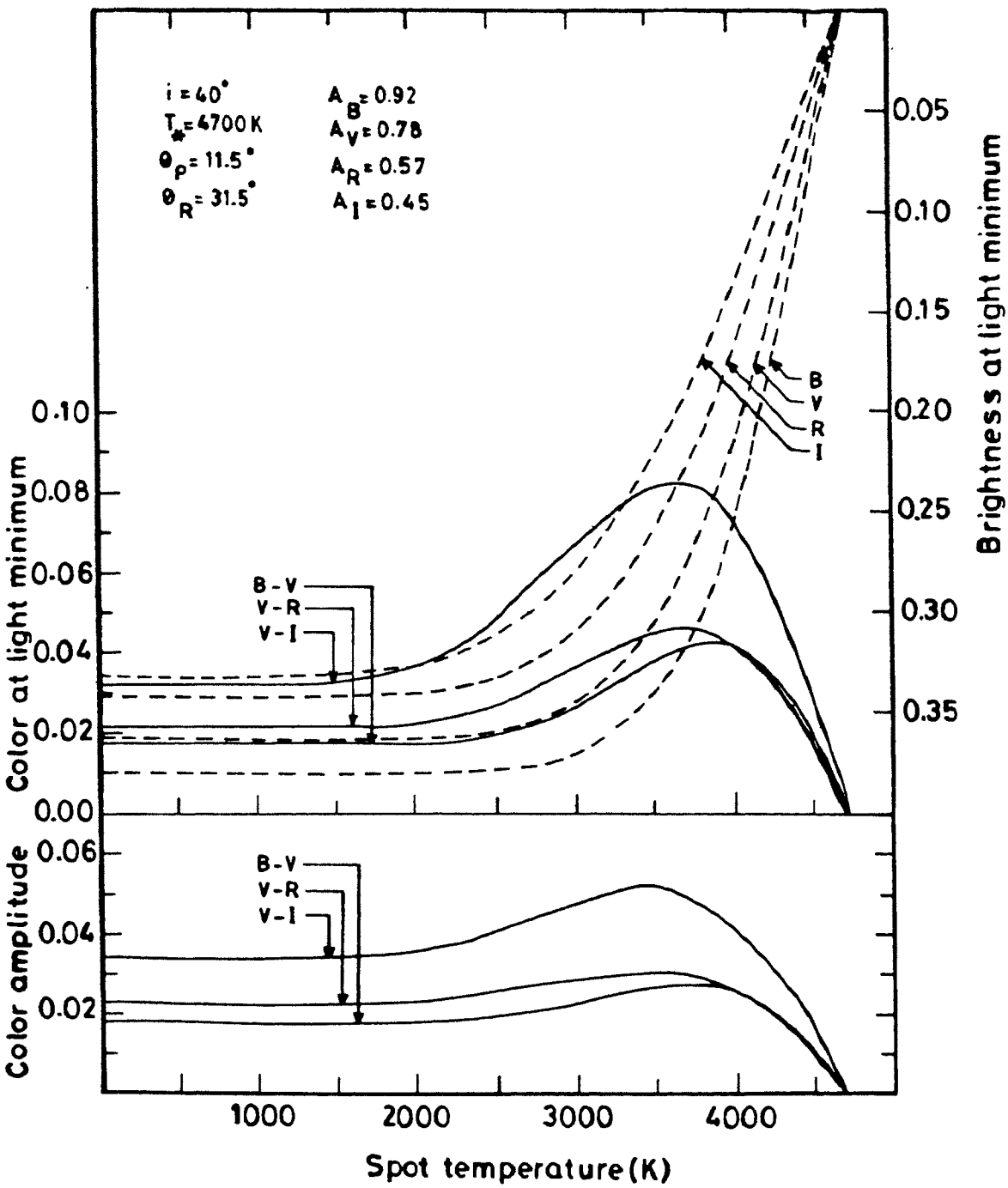

Figure 3. Top panel shows the variation in various colours and brightness at light minimum in $BVRI$ bands. The expected amplitudes of various colour modulations with spot temperature are shown in the bottom panel. The unspotted magnitudes in all bands are assumed to be 0.0 mag.

In the top panel of Figure 3 we have plotted the various colours and the brightnesses in $BVRI$ bands at the light minimum. The unspotted magnitudes were assumed to be zero at all bands. It is clear that a substantial fraction of the changes in colours result from the differential limb darkening and the change in brightness at light minimum is appreciably large at all bands for spot temperatures larger than 3000 K. For spots cooler than 3000 K the changes in V and B magnitudes are less.

In the present case the B and V observations were directly and simultaneously used instead of using the amplitudes of the V and $B-V$ modulations separately. Also, the spot temperature was treated as an unknown in the least square solution along with the other spot parameters. Both B and V observations were given equal weight in the solution of spot parameters. The temperature determination relies upon the over all fit of both V and B light curves, and hence on the information contained in the entire light curve. The program was tested with synthetic BV data, and we could retrieve the input spot temperature along with the other spot parameters.

4

DM URSA MAJORIS

16. Historical introduction

The ninth magnitude star BD +61°1211 (= SAO 015338), now known by its variable star designation DM UMa, was first proposed as the prime optical counterpart of the X-ray source 2A 1052+606 (Liller 1978; Schwartz et al. 1979). X-ray observations indicate that this star is a fairly bright soft X-ray source with a luminosity of $8.2\pm0.3\times10^{27}$ D^2(pc) erg s^{-1}, similar to that in hard X-rays, and an effective temperature of 10^7K (Walter et al. 1978; Schwartz et al. 1979). Subsequent spectroscopic observations of this star revealed the presence of highly variable *Ca II H* and *K*, and $H\alpha$ emission lines (Charles et al. 1979; Schwartz et al. 1979). A detailed spectroscopic study has shown that DM UMa is a single-lined spectroscopic binary with an orbital period of 7.492 days and a mass function of 0.016 $M_\odot$ (Crampton et al. 1979). The visible component of the binary has a spectral type of K2 III–IV. An inspection of the Harvard archival plate collection showed the star to be a variable with an amplitude around 0.3 mag (Schwartz et al. 1979).

The first photometric light curve was obtained by Kimble et al. (1981) who found that the photmetric period is approximately the same as the spectroscopic orbital period. They assigned a spectral type K0-K1 III-IV

to the visible component and classified the object to be an RS CVn. Thus DM UMa has got the unique distinction of becoming the very first member among the RS CVn class of stars to be recognized via its X-ray emission.

Mohin et al. (1985) has shown that the light curves of DM UMa obtained during any two seasons do not agree in shape, amplitude, phases of light maximum and minimum, and mean light level. From the change in the colour $B-V$ over the photometric period, they have argued that the hemisphere visible during the light minimum is cooler than that seen during the light maximum. The mean colour $B-V = 1.065 \pm 0.002$ mag obtained by them is consistent with a spectral type K1 III or K2 IV. The phases of light minima obtained during 1979–84 were found to lie on two well separated lines with different slopes, indicating similar rotation periods, but shorter than the 7.492 orbital period. On the basis of starspot hypothesis they have argued that there were two spot groups present during that time, one waning and the other waxing producing respectively maximum amplitudes of 0.32 and 0.23 mag.

17. BV photometry

DM UMa was observed on a total of 96 nights during the seven observing seasons: 1984–85 (11 nights), 1985–86 (4 nights), 1986–87 (30 nights), 1987–88 (13 nights), 1988–89 (7 nights), 1989–90 (12 nights) and 1990–91 (19 nights). The comparison stars were BD +60°1301 and BD +61°1210. All the observations were made differentially with respect to BD +60°1301 and transformed to the UBV system. The mean differential magnitudes and colours of the comparison stars, in the sense BD +60°1301 minus BD +61°1210, obtained during six of the seasons are given in Table 3 along with the corresponding number of observations (n) obtained during each season; the values are consistent and indicate their nonvariability. Table 4 gives the results for the variable star, in the sense DM UMa minus BD +60°1301. Each value given in Table 4 is a mean of three to four independent measurements; the typical error in ΔV is ± 0.010 mag and in $\Delta(B-V)$ ± 0.014 mag. The photometric properties derived from the present observations, together with those compiled from other sources, are given in Table 5. All the quantities

given in the table are evaluated from the graphical plots of the observations except the phase of light minimum which is derived from the spot modelling.

Table 3. The mean differential magnitudes and colours of comparison stars, in the sense BD + 60°1301 minus BD + 61°1210

Season	ΔV	n	$\Delta(B-V)$	n
1984–85	−0.462±0.007	11	+0.751±0.004	9
1986–87	−0.470±0.002	22	+0.745±0.003	13
1987–88	−0.450±0.002	5	+0.742±0.007	5
1988–89	−0.465±0.003	7	+0.757±0.004	7
1989–90	−0.464±0.003	10	+0.747±0.004	10
1990–91	−0.462±0.002	19	+0.753±0.003	18

In the case of DM UMa the observations of Kimble et al. (1981) show an orbital modulation of $B-V$ with an amplitude of about 0.04 mag. Mohin et al. (1985) confirmed the change in $B-V$ with change in V in the sense that the star becomes redder as it becomes fainter. Because of the low amplitudes (< 0.20 mag against the 0.32 mag in V band observed by Kimble et al.) and slightly larger error our data do not show up the $B-V$ variation as strikingly as the data of Kimble et al. do. In Fig. 4 we have plotted the values of $\Delta(B-V)$ against the corresponding values of ΔV taken from Table 4. The correlation between $B-V$ and V is not that apparent from the figure. The slope of the assumed linear relationship derived using the least square technique is 0.125±0.014, which is consistent with that reported by Mohin et al. (1985).

In Fig. 5 we have plotted the brightness at maximum ΔV_{max} and minimum ΔV_{min} taken from Table 5 against the corresponding amplitude. Both ΔV_{max} and ΔV_{min} show a large range in magnitudes (about 0.30 mag). Apparently, the change in amplitude is uncorrelated with a change in either ΔV_{max} or ΔV_{min}. Fig. 6 is the plot of ΔV_{max} and ΔV_{min} given in Table 5 against the corresponding epoch of observations. The figure shows that both

Table 4. The differential magnitudes and colours of DM UMa

JD (Hel.) 2440000.+	ΔV	Δ(B−V)	JD (Hel.) 2440000.+	ΔV	Δ(B−V)
6055.4601	0.635	−0.098	6056.4580	0.640	−0.093
6084.3898	0.540	...	6086.4002	0.579	...
6088.3666	0.439	−0.134	6090.3591	0.485	−0.120
6095.3834	0.459	−0.127	6118.2387	0.455	−0.136
6120.2888	0.497	−0.110	6120.3939	0.493	−0.130
6121.2346	0.526	−0.138	6122.3535	0.552	−0.118
6123.2669	0.585	−0.132	6471.4080	0.583	...
6473.3927	0.565	...	6505.3019	0.449	...
6506.3071	0.443	...	6817.4329	0.424	...
6819.3579	0.381	−0.140	6820.3401	0.415	−0.125
6821.3202	0.468	...	6825.3777	0.417	−0.121
6825.4813	0.403	−0.137	6828.3195	0.457	...
6828.3288	0.456	...	6828.3425	0.470	...
6828.3580	0.453	...	6829.3517	0.543	...
6830.3098	0.521	...	6830.3462	0.522	−0.125
6830.3694	0.539	−0.131	6831.3714	0.458	...
6832.3246	0.446	−0.133	6833.4003	0.409	...
6834.2975	0.396	...	6835.3052	0.420	...
6836.2854	0.504	...	6846.2664	0.466	...
6847.2806	0.428	−0.105	6850.3460	0.407	−0.118

Table 4. continued

JD (Hel.) 2440000.+	ΔV	Δ(B−V)	JD (Hel.) 2440000.+	ΔV	Δ(B−V)
6851.2975	0.471	−0.104	6852.2884	0.527	−0.114
6853.3386	0.479	−0.126	6857.3351	0.395	...
6858.2536	0.450	−0.121	6859.3459	0.524	−0.136
6860.2573	0.506	−0.110	6861.2438	0.463	−0.120
6862.2502	0.436	−0.131	6877.2767	0.436	...
6883.1848	0.481	...	6884.2116	0.471	−0.138
6892.2755	0.430	...	7157.4257	0.452	...
7178.3509	0.574	...	7179.3813	0.489	...
7183.3386	0.437	...	7184.3705	0.524	−0.099
7185.4286	0.564	−0.128	7198.3102	0.461	...
7200.3523	0.566	...	7201.3099	0.544	−0.091
7230.2368	0.605	−0.102	7232.3000	0.430	−0.131
7233.2821	0.412	...	7238.2963	0.595	...
7556.4260	0.311	−0.155	7557.3616	0.324	−0.130
7558.4298	0.404	−0.113	7559.3064	0.437	−0.126
7560.3367	0.481	−0.135	7561.3781	0.418	−0.126
7572.4274	0.334	−0.119	7852.4624	0.446	−0.149
7853.4286	0.364	−0.132	7855.4626	0.270	...
7856.4210	0.313	−0.130	7869.4159	0.275	−0.197
7912.3177	0.389	−0.127	7913.3303	0.329	−0.119

Table 4. continued

JD (Hel.) 2440000.+	ΔV	Δ(B−V)	JD (Hel.) 2440000.+	ΔV	Δ(B−V)
7915.3238	0.232	−0.149	7916.4041	0.287	−0.138
7917.3413	0.318	−0.157	7918.3846	0.347	−0.131
7922.3211	0.237	−0.178	8296.4220	0.156	−0.152
8297.4090	0.192	−0.138	8298.3780	0.205	−0.131
8299.3679	0.256	−0.159	8300.4229	0.334	−0.171
8301.3839	0.358	−0.123	8302.3329	0.271	−0.141
8303.4189	0.187	−0.186	8304.3991	0.151	−0.134
8305.3491	0.194	...	8325.2711	0.227	−0.126
8327.2609	0.168	−0.105	8328.2670	0.220	−0.113
8329.3012	0.276	−0.141	8331.2447	0.341	−0.104
8332.2521	0.253	−0.124	8333.2169	0.151	−0.161
8334.2072	0.132	−0.151	8335.2081	0.163	−0.084

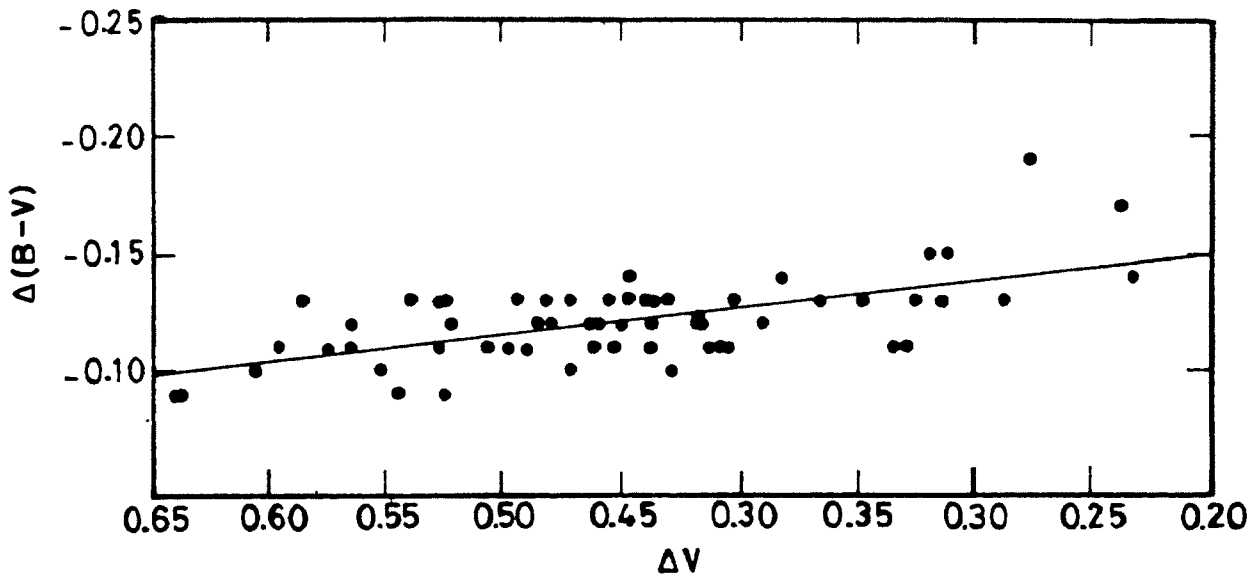

Figure 4. Plot of $\Delta(B\text{-}V)$ against the corresponding ΔV given in Table 4.

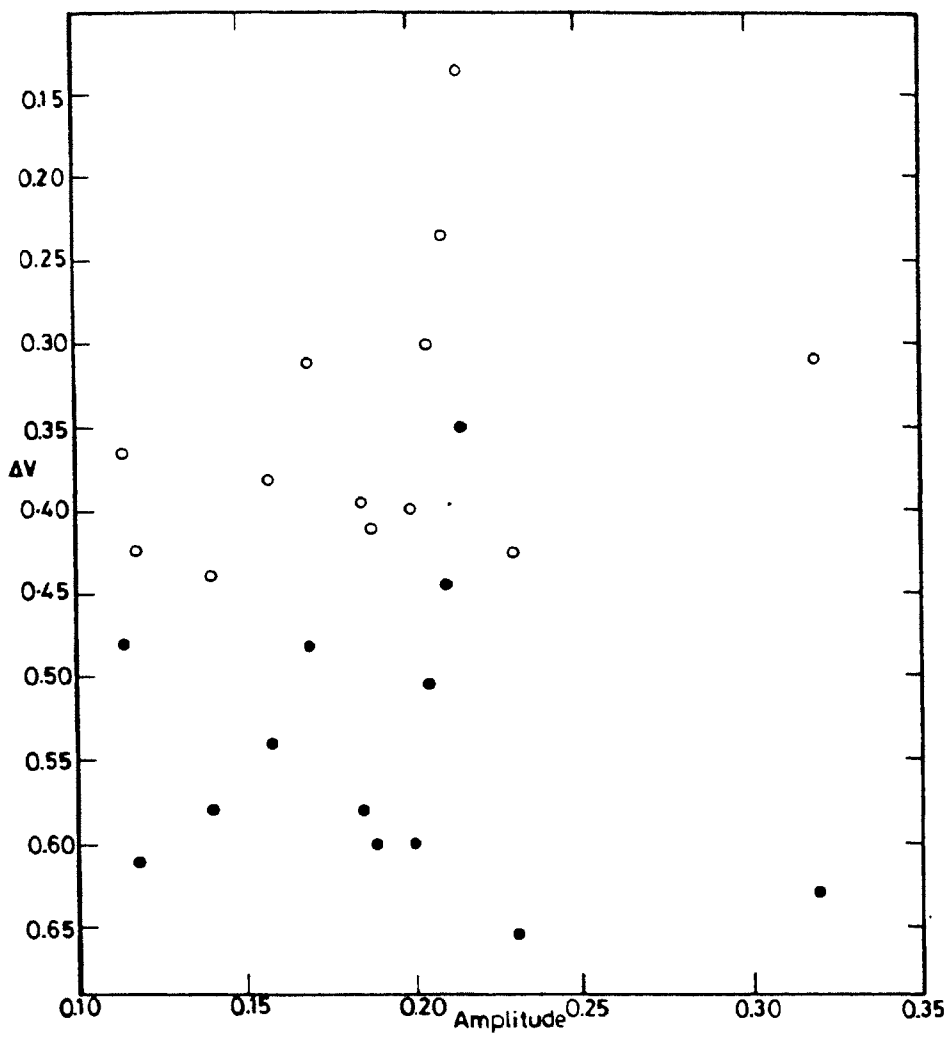

Figure 5. Plot of the brightness at light maximum (open circles) and light minimum (filled circles) against the V amplitude.

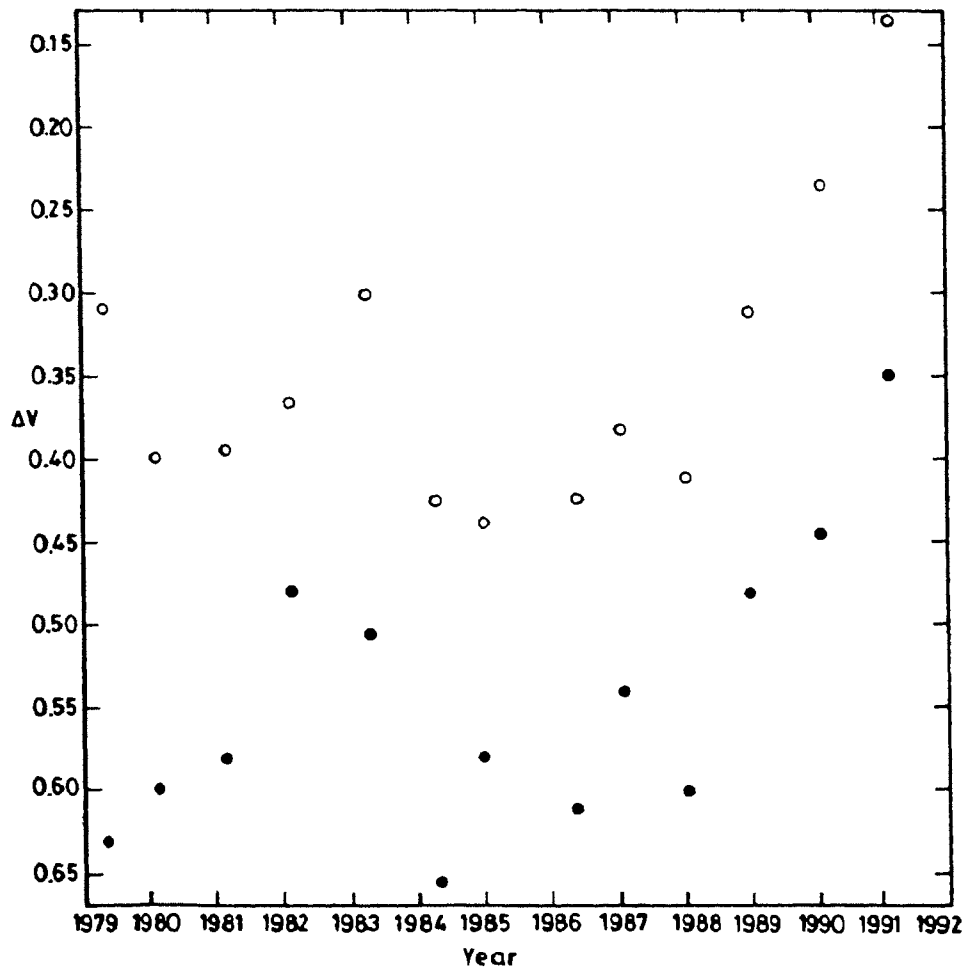

Figure 6. Plot of the brightness at light maximum (open circles) and light minimum (filled circles) against the mean epoch of observation.

ΔV_{max} and ΔV_{min} show nearly similar trends in their behaviour; in general an increase in ΔV_{max} is followed by an increase in ΔV_{min} and a decrease in ΔV_{max} by a decrease in ΔV_{min}. Both show monotonic increase from 1987 onwards.

Table 5. Photometric characteristics of DM UMa

Epoch	Amplitude	ΔV_{max}	ΔV_{min}	Phase Min	References
1979.42	0.320	0.310	0.630	0.50	Kimble et al. (1981)
1980.17	0.200	0.400	0.600	0.45	Mohin et al. (1985)
1981.22	0.185	0.395	0.580	0.19	Mohin et al. (1985)
				0.75	
1982.21	0.115	0.365	0.480	0.03	Mohin et al. (1985)
				0.49	
1983.35	0.205	0.300	0.505	0.35	Mohin et al. (1985)
1984.37	0.230	0.425	0.655	0.26	Mohin et al. (1985)
1985.06	0.141	0.439	0.580	0.15	Present study
1986.46	0.186	0.424	0.610	0.62	Heckert et al. (1988)
1987.10	0.158	0.382	0.540	0.57	Present study
1988.07	0.188	0.412	0.600	0.00	Present study
1989.02	0.170	0.311	0.481	0.00	Present study
1990.09	0.210	0.235	0.445	0.96	Present study
1991.16	0.215	0.135	0.350	0.90	Present study

18. Phase of light minimum

Fig. 7 is a plot of the phase of light minima taken from Table 5 against the corresponding mean epoch of observation. It is interesting to see that the phases of the light minima fall on four well separated lines. The minimum first observed in 1979 (which we identify as group A) could be traced until

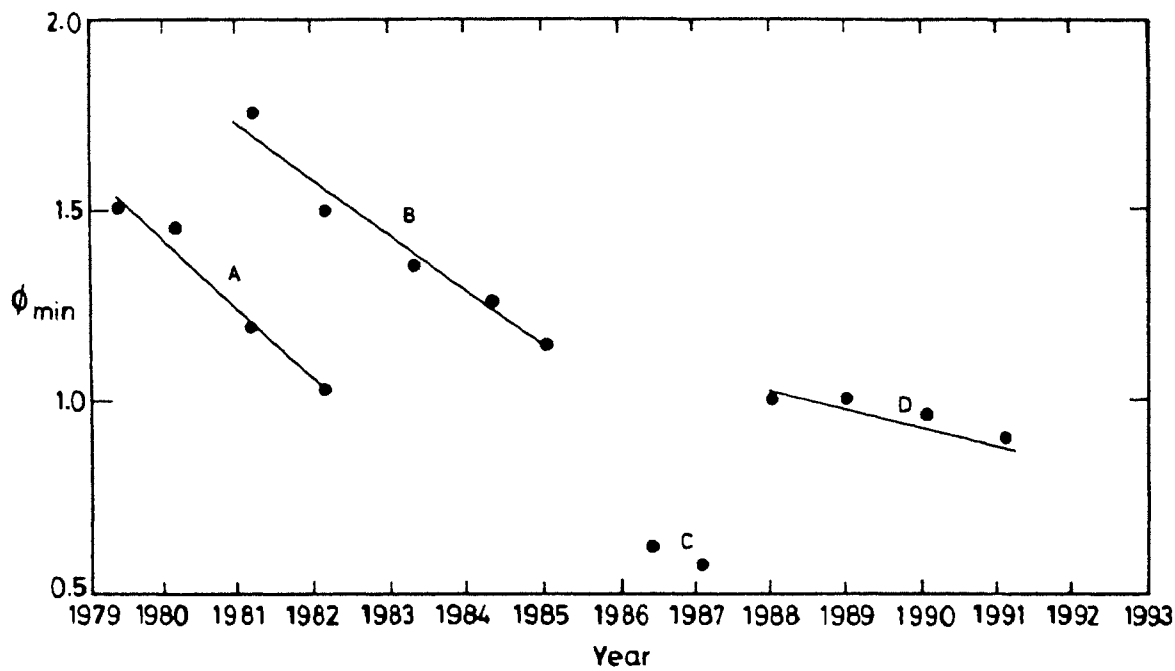

Figure 7. Plot of the phase of light minimum versus mean epoch of observation.

1982. A second minimum which first appeared sometime in 1981 (group B) could be traced until 1985. During 1986−87 there was a short-lived minimum (group C). The minima identified as group D had its origin sometime in 1988 and was still in existence in 1991. From an analysis of the photometry available during 1979−84, Mohin et al. (1985) have put a lower limit of about four years for the lifetime of a centre of activity (spot or spot group). But Fig. 7 indicates that the lifetime of a spot or spot group can be as short as about two years (group C). It is interesting to see that all groups show migrations towards decreasing orbital phases. The photometric periods for group A, B, and D derived using least square technique are 7.465±0.002, 7.470±0.002 and 7.487±0.001 days, respectively. If the equator is synchronized to the orbital rotation, this would imply that higher latitude regions are rotating faster than the equatorial region as suggested by Vogt & Hatzes (1991) in the case of UX Ari.

19. Results of spot modelling

We have pooled our data with other published data (Kimble et al. 1981; Mohin et al. 1985; and Heckert et al. 1988) and discuss it in the framework of spot model described in Chapter 3. The Julian days of observation were converted into orbital phases using the following ephemeris (Crampton et al. 1979):

$$\text{JD (Hel.)} = 2443881.4 + 7^d.492\ \text{E},$$

where the initial epoch corresponds to the time of maximum of positive radial velocity, and the period is the orbital period mentioned above. Both B and V observations were given equal weights in the solution of spot parameters. The computed best fit B and V light curves are shown in Figures 8−18 along with the available B and V band observations.

We could not precisely determine the V magnitude of the comparison star; however our measurements yield a mean $B - V$=1.183±0.013 for it. To convert the differential magnitude and colour of the variable to V and B magnitudes that are needed for the analysis, we have assumed V=0.0 mag for the comparison star . With this, for the variable star ΔV becomes V, and $(\Delta(B - V) + \Delta V + 1.183)$ becomes B; the ordinates in Figures 8−18

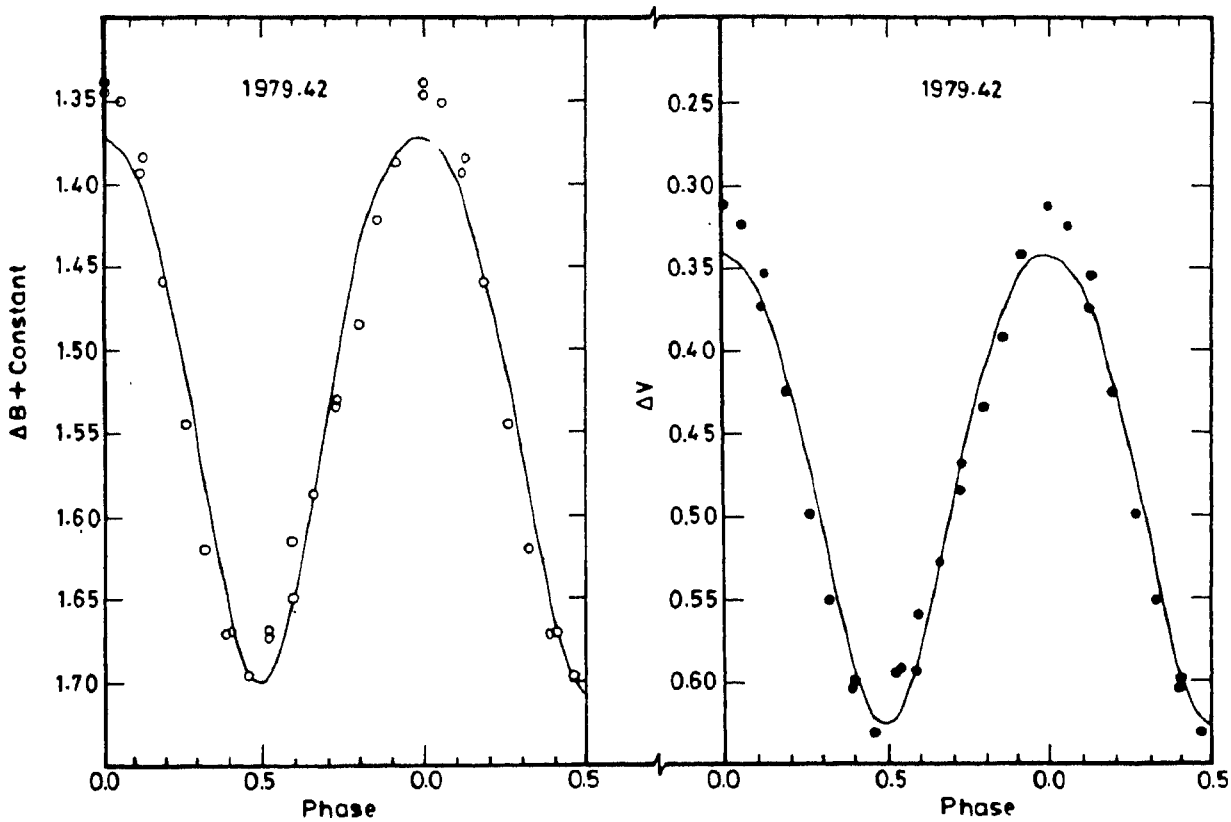

Figure 8. The 1979.42 light curve of DM UMa (Kimble et al. 1981) along with the corresponding best fit computed curves. Observations in B and V bands are indicated by open and filled circles respectively. Phases are reckoned from JD (Hel.) 2443881.4 using the period $7^d.492$.

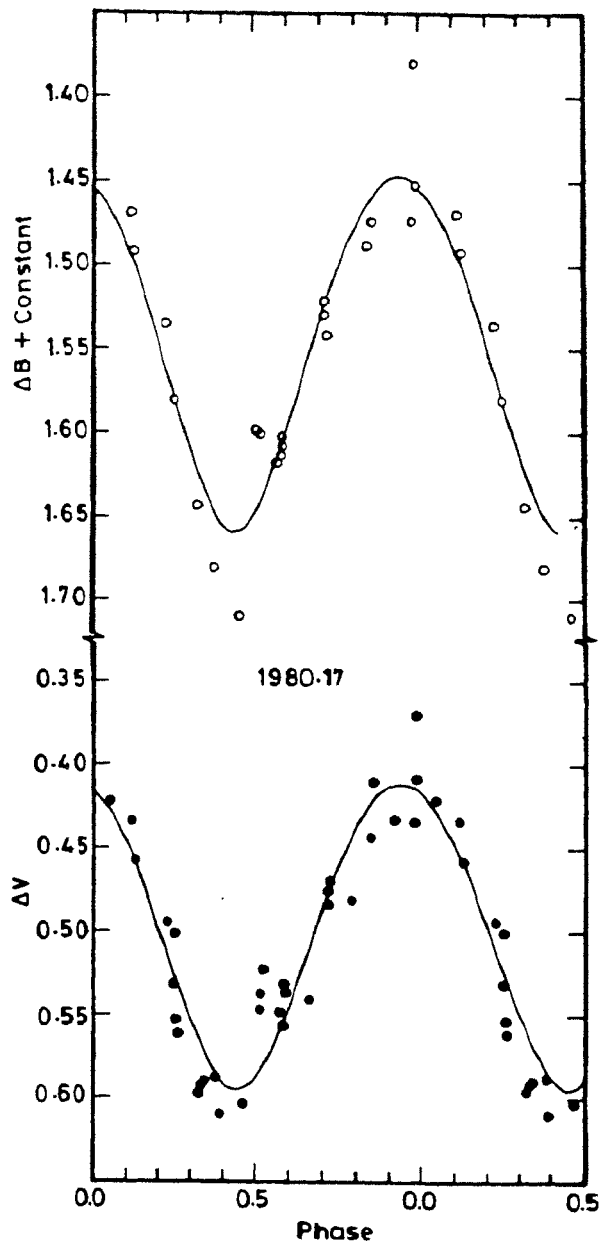

Figure 9. The 1980.17 light curve of DM UMa (Mohin et al. 1985). The descriptions are as in Fig. 8.

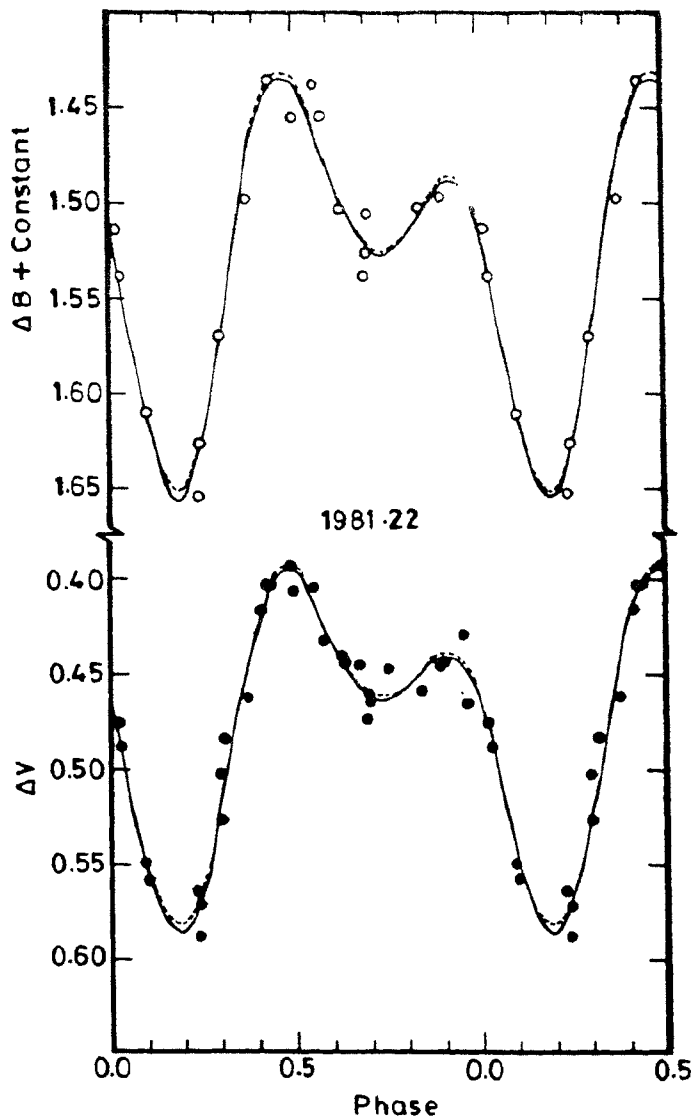

Figure 10. The 1981.22 light curve of DM UMa (Mohin et al. 1985). The descriptions are as in Fig. 8. The results for the same set of spot parameters for quadratic limb-darkening laws for the spotted and unspotted regions are also shown as dashed curves.

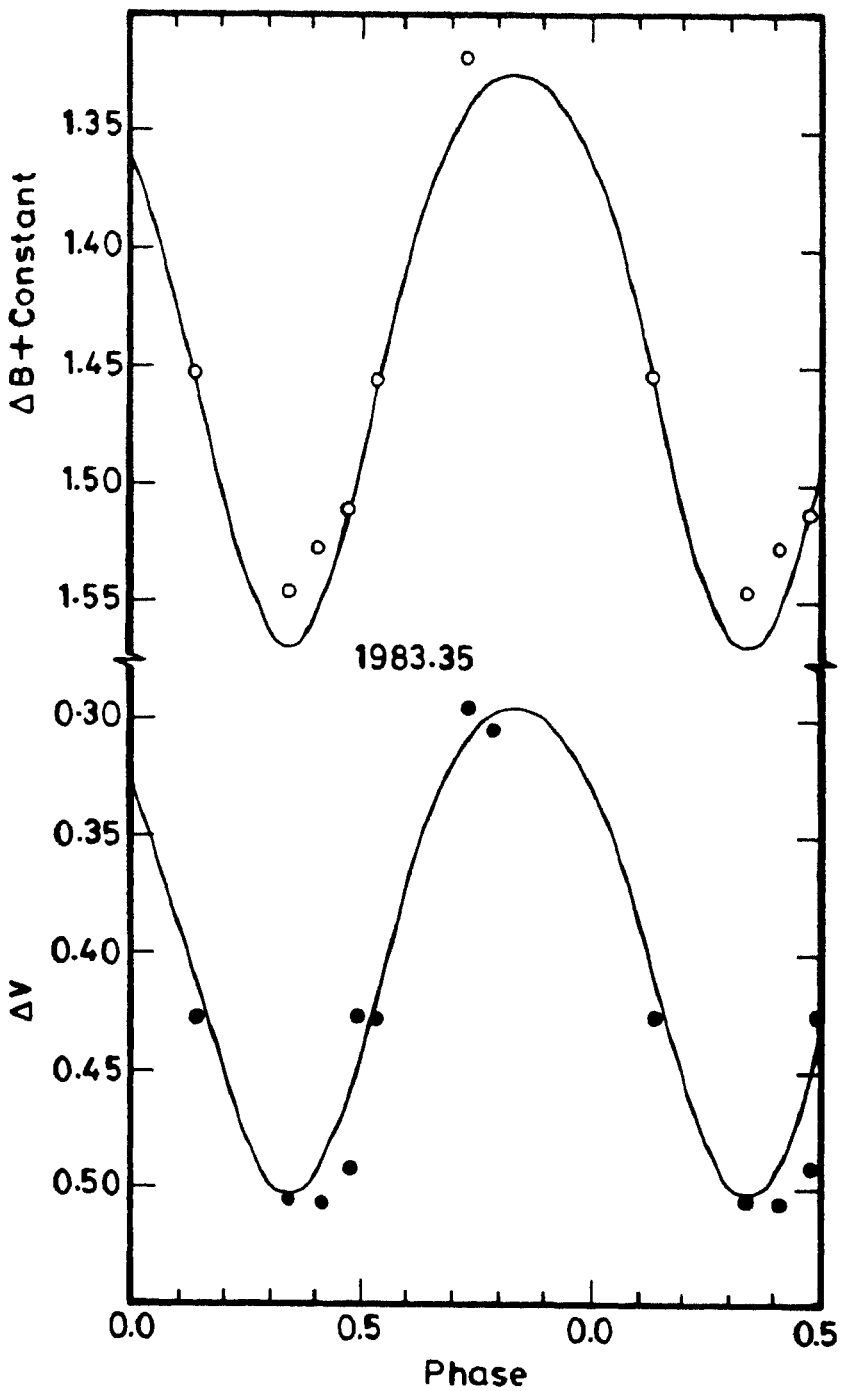

Figure 11. The 1983.35 light curve of DM UMa (Mohin et al. 1985). The descriptions as in Fig. 8.

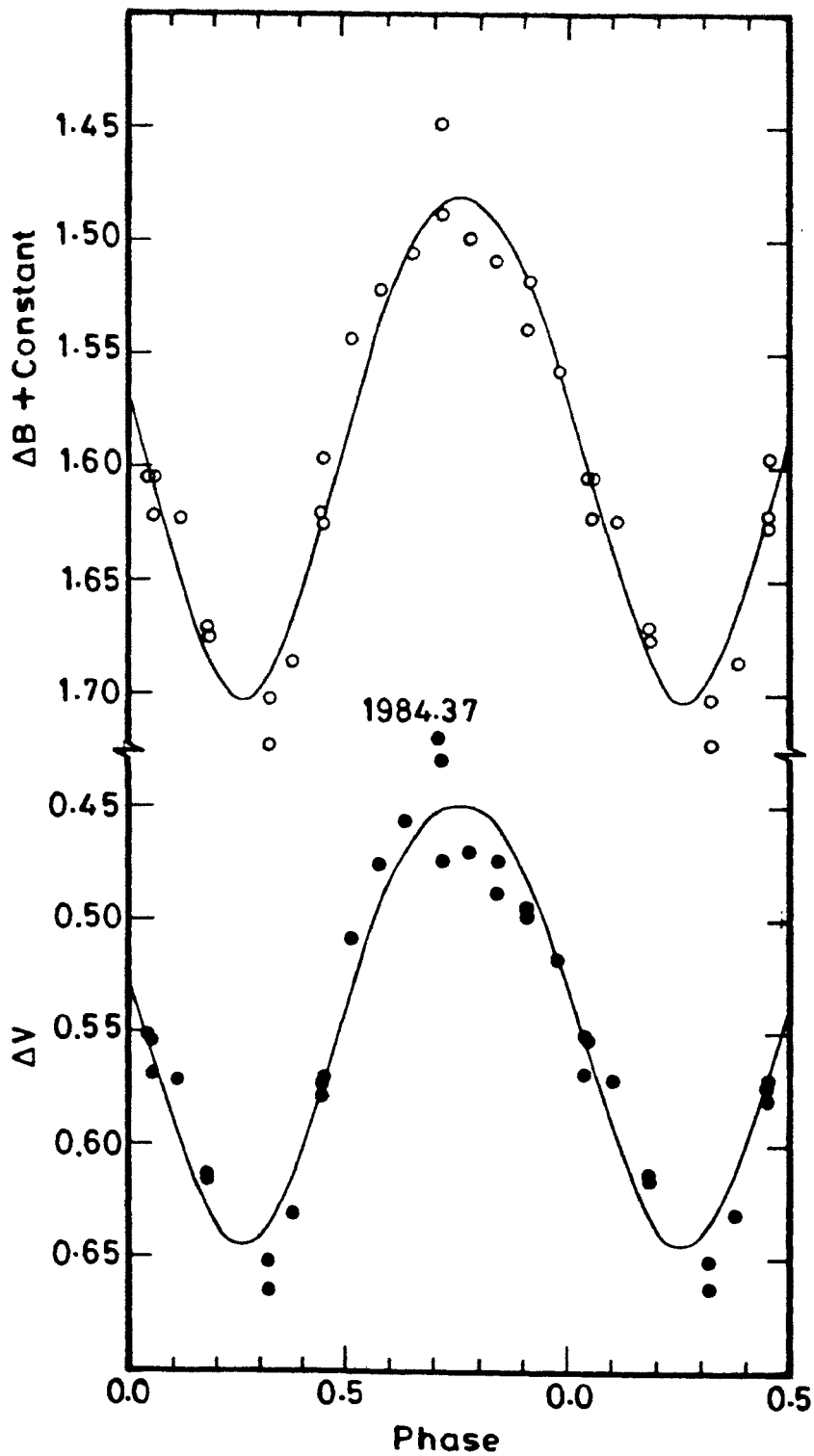

Figure 12. The 1984.37 light curve of DM UMa (Mohin et al. 1985). The descriptions are as in Fig. 8.

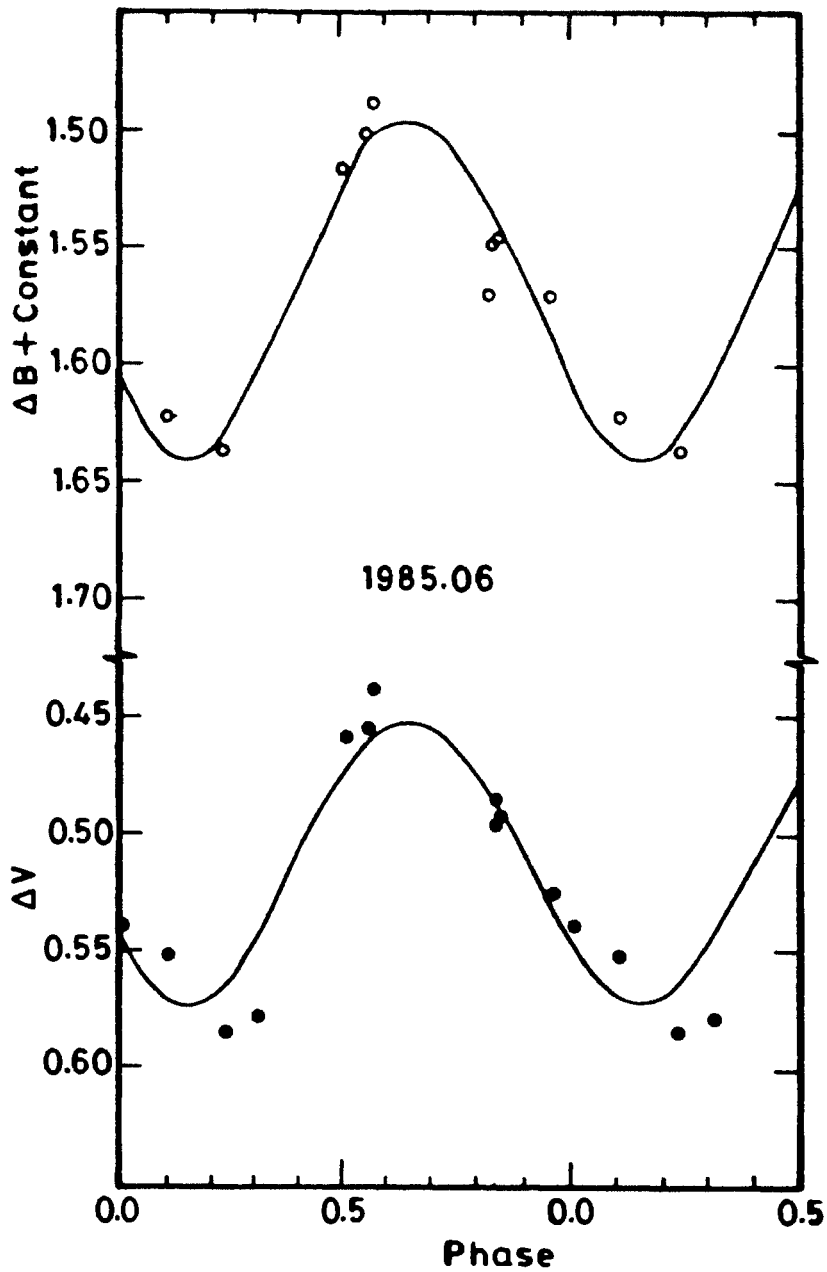

Figure 13. The 1985.06 light curve of DM UMa (present study). The descriptions as in Fig. 8.

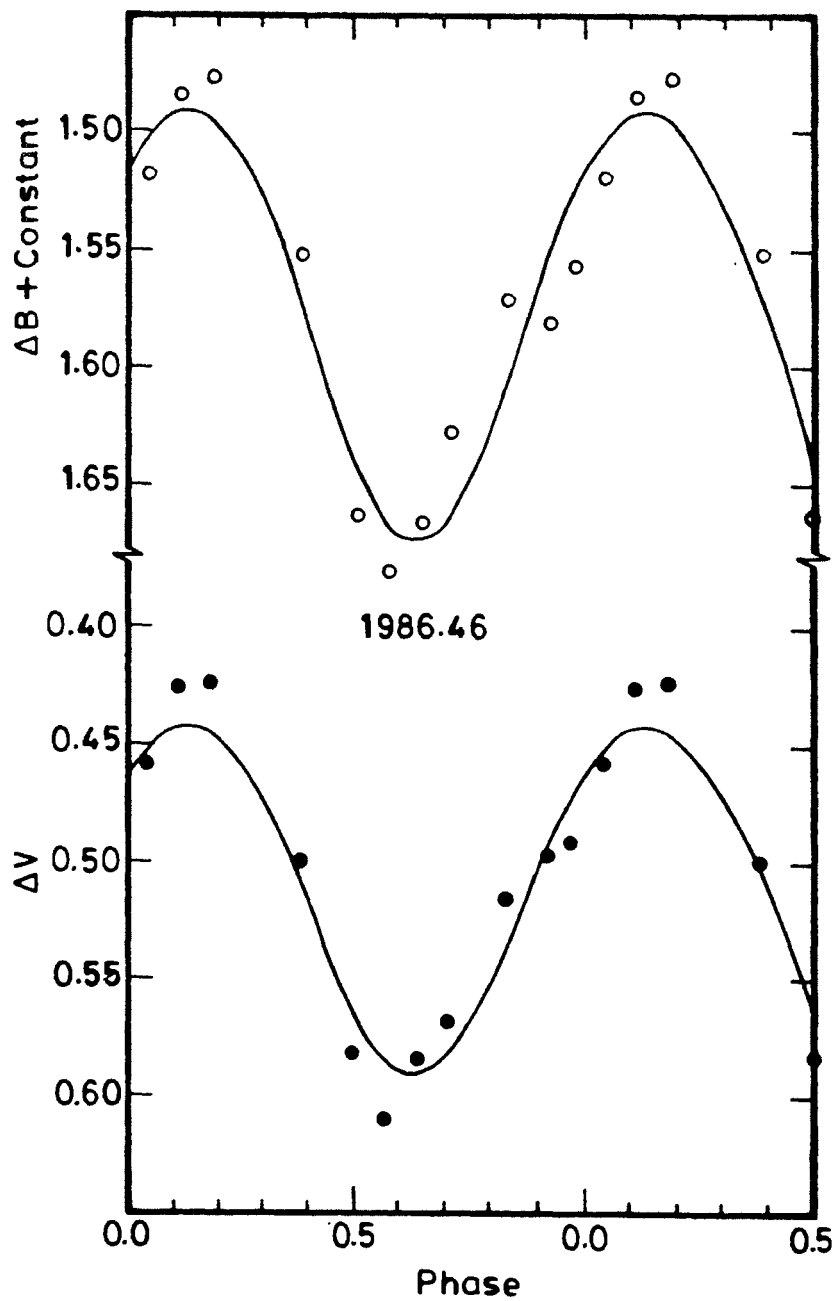

Figure 14. The 1986.46 light curve of DM UMa (Heckert et al. 1988). The descriptions are as in Fig. 8.

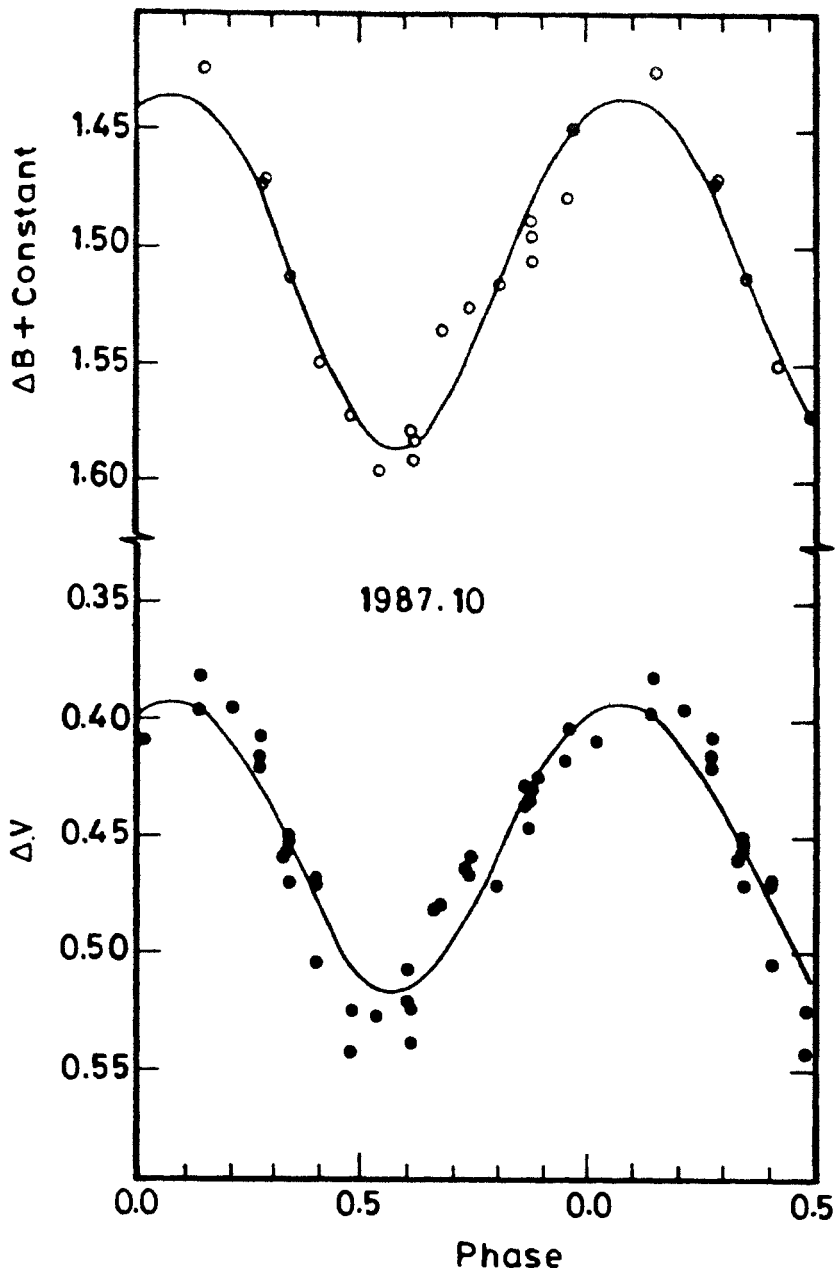

Figure 15. The 1987.10 light curve of DM UMa (present study). The descriptions are as in Fig. 8.

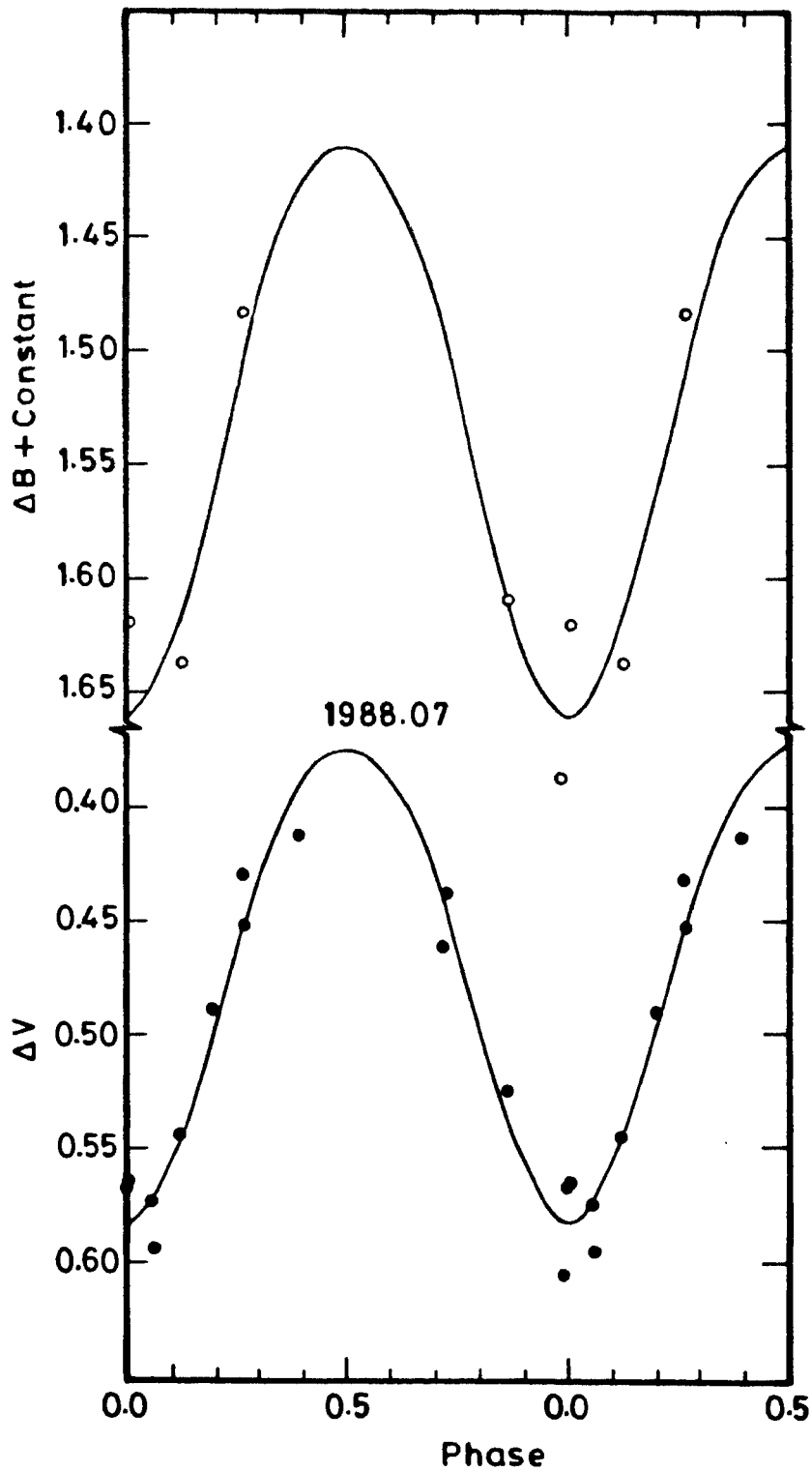

Figure 16. The 1988.07 light curve of DM UMa (present study). The descriptions are as in Fig. 8.

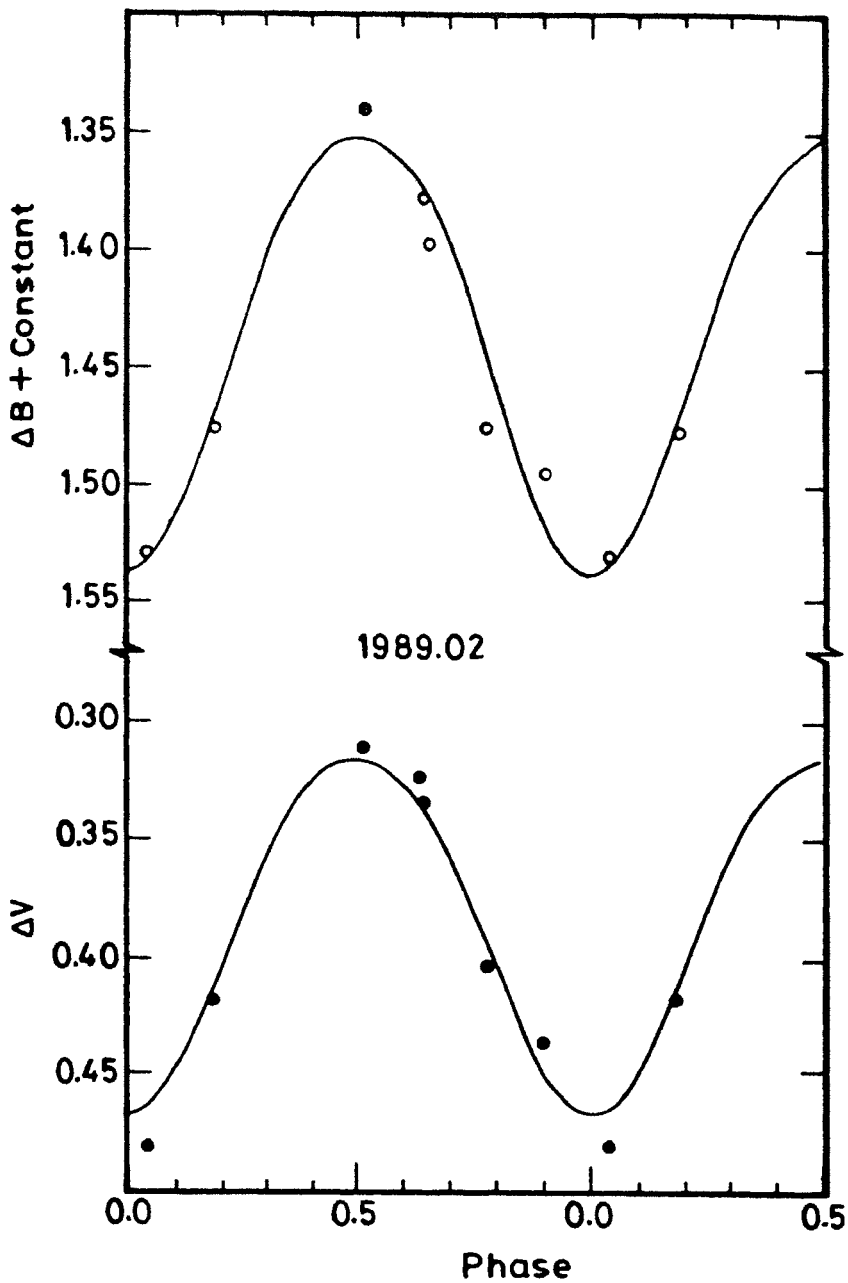

Figure 17. The 1989.02 light curve of DM UMa (present study). The descriptions are as in Fig. 8.

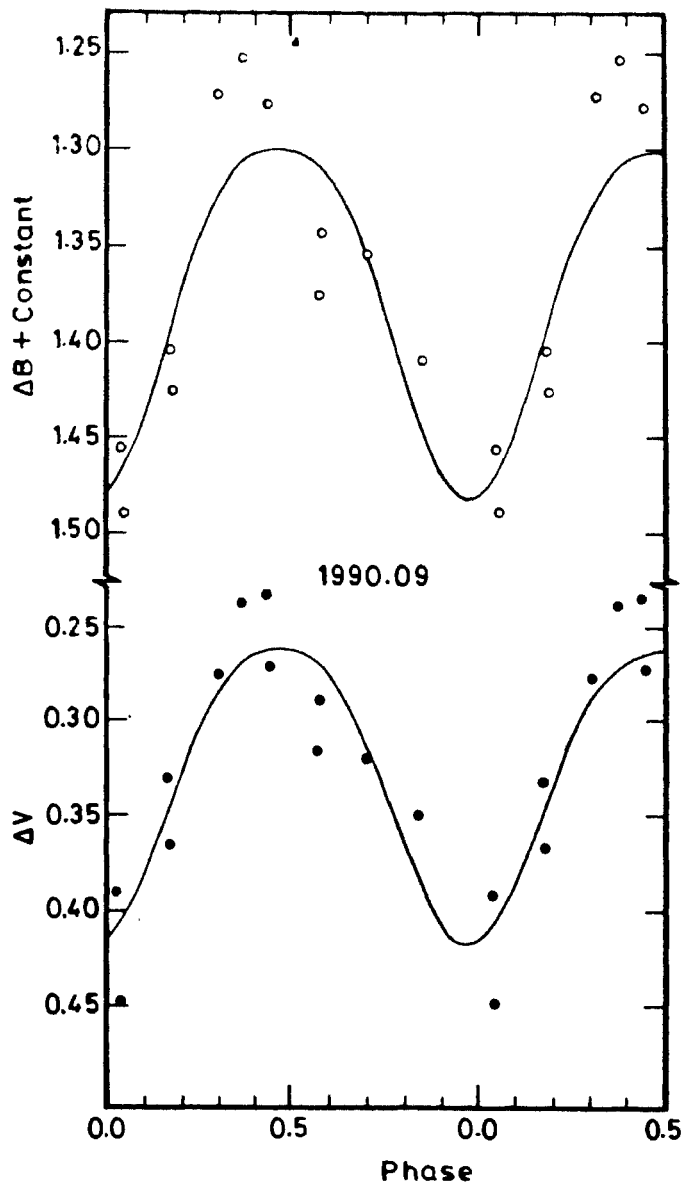

Figure 18. The 1990.09 light curve of DM UMa (present study). The descriptions are as in Fig. 8.

are these values.

As mentioned earlier, DM UMa is a non-eclipsing binary, and hence the orbital inclination is unknown. An uncertainty in the inclination will be reflected directly on the polar distance of the spot. For the present analysis we have used $i = 40°$, the probable value suggested by the mass function and the luminosity ratio (Crampton et al. 1979; Kimble et al. 1981).

The magnitude of the unspotted star is the other parameter that is uncertain and the assumed value of which has a similar direct effect on the polar distance in models that allow high latitude spots. The problems associated with the assumption of the unspotted magnitudes have already been discussed in detail by Poe & Eaton (1985). If the actual unspotted magnitude is higher than that assumed in the treatment of the model then the derived spot area and temperature would be of differential nature. Our calculations show that an increase of unspotted brightness by about 0.1 mag would decrease the spot temperature by about 200 K. DM UMa has been observed every year since the 1979 discovery of its light variation. The value ΔV=0.135 mag with respect to the comparison star BD +60°1301, observed by us during 1990−91, is the brightest magnitude observed so far. The analysis was started much before the beginning of the 1990−91 observations. Hence the brighter magnitude ΔV=0.23 observed during the previous season was assumed to represent the V magnitude of unspotted star and the corresponding B=1.26 mag to represent the unspotted B magnitude. The assumed unspotted magnitude does not change significantly the derived spot parameters except the temperature which would be affected by about 200 K. The effective temperature of the undisturbed photosphere was taken as $T_* =$ 4700 K, which according to Johnson (1966) approximately corresponds to K1 III−K2 IV spectral type and the assumed unspotted $B - V$=1.03 mag. The nature of the secondary component of DM UMa is unknown; it is probably a late-type dwarf (Kimble et al. 1981), and we neglected the contribution of the secondary in the B and V spectral regions.

Table 6 summarizes the results of the least square analysis; it gives the mean epoch of observation; the polar distance; longitude and temperature of spots; area of spots as a fraction of the total surface area of the star; the

Table 6. The spot parameters derived for the light curves of DM UMa

Mean epoch	Polar dist. (degrees)	Longitude (degrees)	Radius (degrees)	Temp. (K)	Fractional area	S. d. of fit (mag.)	No. of obs. V	No. of obs. B	Ref.
1979.42	24.6±0.7	177±1	32.0±0.6	3230±190	0.076±0.003	0.023	21	21	1
1980.17	13.8±0.6	160±2	32.7±0.7	3190±200	0.079±0.003	0.027	32	21	2
1981.22	71.8±8.5	71±1	31.7±2.0	3560±90	0.075±0.009	0.013	30	17	2
	25.2±4.6	265±3	25.8±1.0	3560±90	0.050±0.004				
1982.21	2.0±1.2	172±39	27.9±0.3	3400 (assumed)	0.058±0.001	0.035	33	...	2
1983.35	27.0±1.8	123±3	27.0±0.3	3400 (assumed)	0.054±0.001	0.020	8	6	2
1984.37	12.6±0.4	93±1	34.1±0.3	2800±240	0.086±0.001	0.018	24	22	2
1985.06	8.7±0.6	55±4	34.1±0.9	3380±190	0.086±0.005	0.019	11	9	3
1986.46	11.0±0.6	226±3	36.4±1.5	3640±160	0.098±0.008	0.022	11	11	4
1987.10	11.5±0.4	207±2	31.9±0.8	3610±100	0.075±0.004	0.016	36	18	3
1988.07	17.9±1.1	0±3	32.7±1.4	3490±210	0.079±0.007	0.022	13	5	3
1989.02	19.9±1.4	3±3	28.1±2.3	3720±250	0.059±0.009	0.015	7	7	3
1990.09	32.7±3.3	348±5	21.9±2.8	3400±920	0.036±0.009	0.035	12	11	3

Ref.: (1) Kimble, Kahn and Bowyer 1981. (2) Mohin *et al.* 1985. (3) Present study. (4) Heckert *et al.* 1988.

standard deviation of fit; the number of observations in V and B bands; and the reference from where the data were taken. In the case of observations with mean epoch 1982.21 only V band data are available. At epoch 1983.35 the available data are few in number. Therefore in these two cases we have assumed the temperature to be the mean of temperatures derived in other cases.

It is found (Table 6) that a high latitude single spot could reproduce all the light curves except that obtained during early 1981 where two spots are found to be necessary to account for the light variation. In all the cases considered we have calculated the standard deviation of the fit $\sigma = \sqrt{\frac{(O-C)^2}{n-L}}$, where n is the total number of observations in B and V bands and L is the total number of parameters solved for. It is found to be of the order of the scatter seen in the data, which is largely due to the temporal changes that occur in the light curves within a few orbital cycles, probably as a result of changes in the configuration of spots. The present model assumes that the spots are circular in shape; *i.e.*, a spot or spot group of irregular shape (which is more likely) is effectively replaced by an 'equivalent' spot of circular shape. This assumption seems to account for all the light variation seen; the slightly larger standard deviation of fit obtained in some cases may be due to the departure from this approximation.

Calculations were made with the same linear limb-darkening law for both the spots and undisturbed photospheric region. The linear coefficients used, A = 0.78 for the V band and A = 0.92 for the B band, were derived from interpolations of the values tabulated by Manduca et al. (1977) for the solar composition. They have shown that the darkening is remarkably insensitive to surface gravity in B and V bands. Fig. 10 also shows the computed curves with different quadratic limb-darkening laws for the spotted and unspotted regions and for the same set of spot parameters: ($A_* = 0.77$, $B_* = 0.01$, $A_s = 1.08$, and $B_s = -0.24$ for the V band; and $A_* = 1.07$, $B_* = -0.22$, $A_s = 1.36$, and $B_s = -0.50$ for the B band. These values correspond to temperatures $T_* = 4700$ K, $T_s = 3500$ K, *log* g = 1.5, and [A/H] = 0.0, and were derived from the tables of Manduca et al. (1977). It is clear that the differences between the two cases of limb-darkening are insignificant, well

within the observational uncertainties; the least square solutions show only marginal differences in the resulting spot parameters and negligible difference in the standard deviations of fit to the data.

Out of the 12 observing seasons considered, we could derive spot temperatures for the data obtained on 10 occasions; this is the first time that such an attempt has been made from an extensive set of data for an RS CVn object. From Table 6, it is seen that the derived spot temperatures lie in the range 2800±240 K to 3720±250 K, with a mean of 3400±60 K. In view of the uncertainties in the determination, it is difficult to be sure whether the differences in the temperatures seen at different epochs are real. The derived temperature represents the effective temperature of the equivalent large spot. Hence, a difference in the effective spot temperatures observed at different times probably indicates various distributions of spot sizes and temperature at different epochs.

In Figure 19, we have plotted the observed quantities, amplitude of light variation and brightness at light curve maximum, and the derived spot parameters, fractional area, polar distance and longitude. The set of observations with the mean epoch 1982.21 shows a larger scatter and does not define the light curve well, and the least square solution indicates a single large polar spot. Because of the large errors involved, we have not plotted the corresponding longitude and polar distance. From Fig. 19 we find that from 1984 onwards the brightness at light curve maximum has increased nearly monotonically (by ~0.2 mag), whereas the amplitude has remained within a narrow range (0.16-0.23 mag) with no apparent trend. Qualitatively, this implies a disappearance of high latitude spots and a corresponding reduction in the spot area.

The results of modelling indicate the presence of spots at high-latitudes at all times; only in one case there is an indication of an additional low-latitude spot (mean epoch 1981.22, θ_P=71°. Incidentally, the spot area was the highest during this epoch). From a study of light curves of several objects using spot modelling, Rodono et al. (1986) and Zeilik et al. (1990) have already noted that high latitude spots seem to be commonplace in active spotted stars. We find from Fig. 19 that the high-latitude spots can be

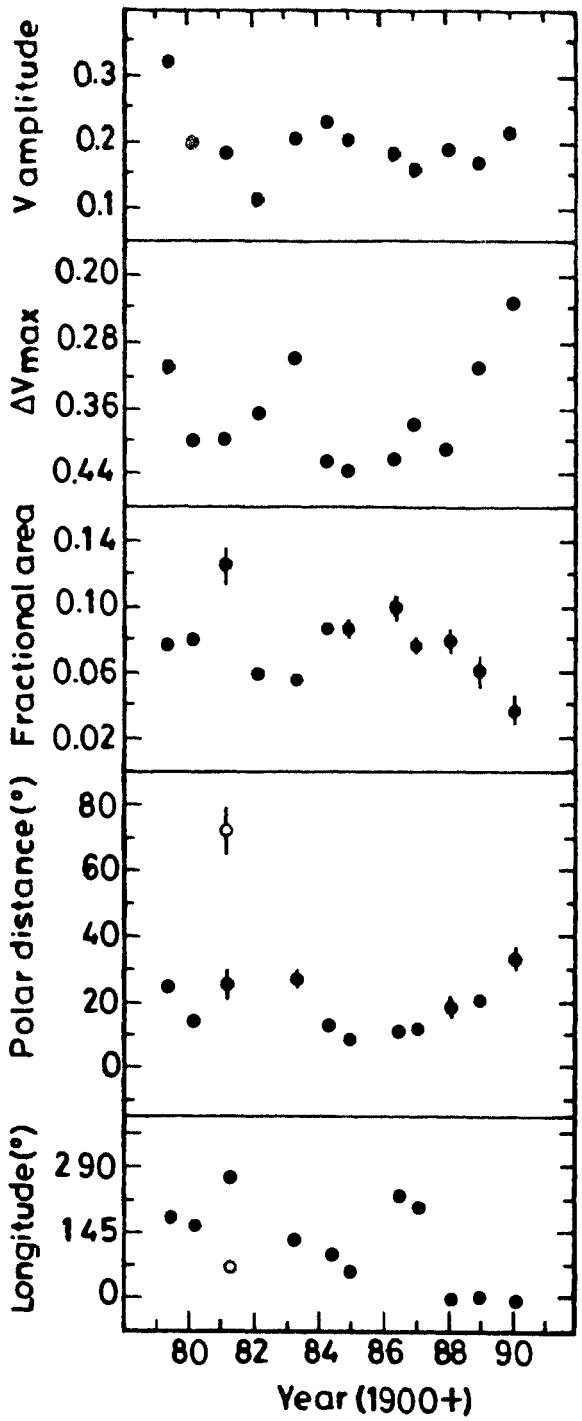

Figure 19. Plots of observed quantities—the amplitude of light variation and the brightness at light curve maximum—and the derived spot parameters —fractional area, polar distance and longitude—against the corresponding epoch of observation.

traced for two or three consecutive seasons, whereas there is no trace of the low-latitude spot during the earlier or later seasons. This seems to suggest that if spots are present near the equator then the centre of activity has a lower lifetime than that if the spots were present at higher latitudes. During the period 1988-90, the longitudes of the spots have remained close to ~0°, but the latitudes have drifted slightly towards the equator. We also find from Fig. 19 that there is a slow migration of spots in latitude towards the equator from 1984 onwards, and a decrease in the spot area during the same period. Note that this result is contrary to what is observed in the sun.

20. $H\alpha$ observations

DM UMa was observed at $H\alpha$ region on a total of seven nights during the 1990−91 observing season.

Table 7. $H\alpha$ data of DM UMa

Date	JD 2440000.+	Phase	EW1 Å	FWHM Å	Height	EW2 Å
28 Nov 1990	8224.4660	0.69	1.22	3.67	0.39	0.17
07 Jan 1991	8264.4229	0.03	1.95	3.37	0.64	0.82
06 Feb 1991	8294.4444	0.04	1.22	3.18	0.42	0.11
07 Feb 1991	8295.4521	0.17	1.08	3.42	0.30	0.12
08 Feb 1991	8296.3153	0.28	0.95	3.07	0.31	−0.04
08 Feb 1991	8296.4334	0.30	1.04	3.36	0.31	0.13
06 Mar 1991	8322.2451	0.75	1.38	3.16	0.55	0.08

Table 7 gives the log of observations; it contains the Julian day of observation; $H\alpha$ emission equivalent width EW1; full width at half maximum of $H\alpha$ emission, FWHM; height of the $H\alpha$ emission in terms of F_λ/F_c; photometric phase and the equivalent width EW2. The computations of EW1 and EW2 were done as described in Chapter 2.

The results of $H\alpha$ observations are plotted in Figs 20 and 21. The

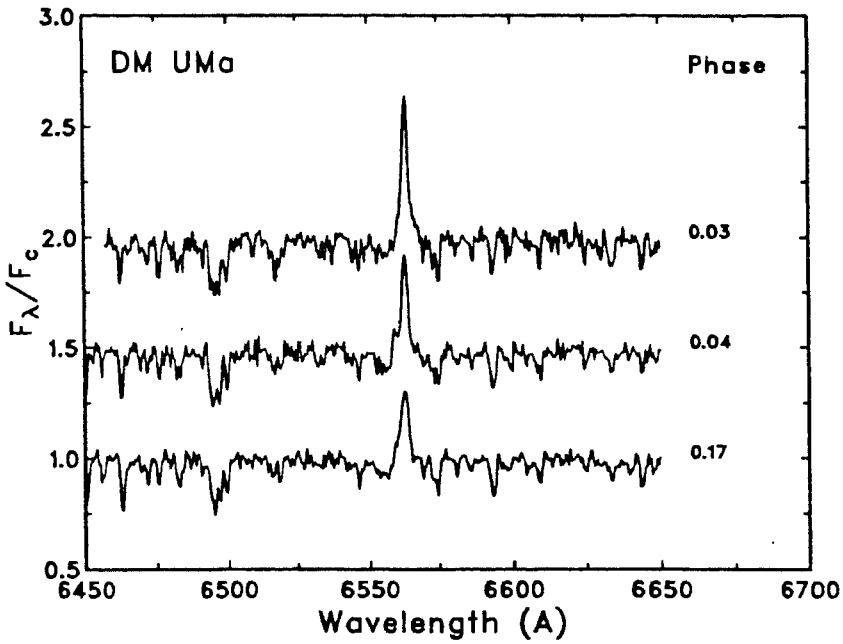

Figure 20. *Hα* spectra of DM UMa. The spectra are adjusted in wavelength to line up the absorption lines. Each spectrum is normalized to continuum and shifted by 0.5. Phases are reckoned as in Fig. 8.

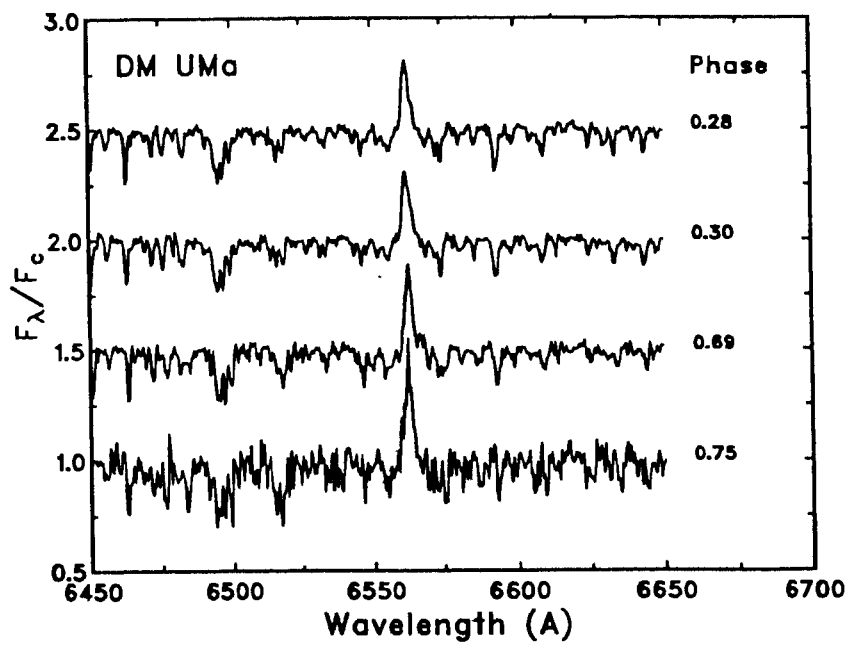

Figure 21. *Hα* spectra of DM UMa. The descriptions are as in Fig. 20.

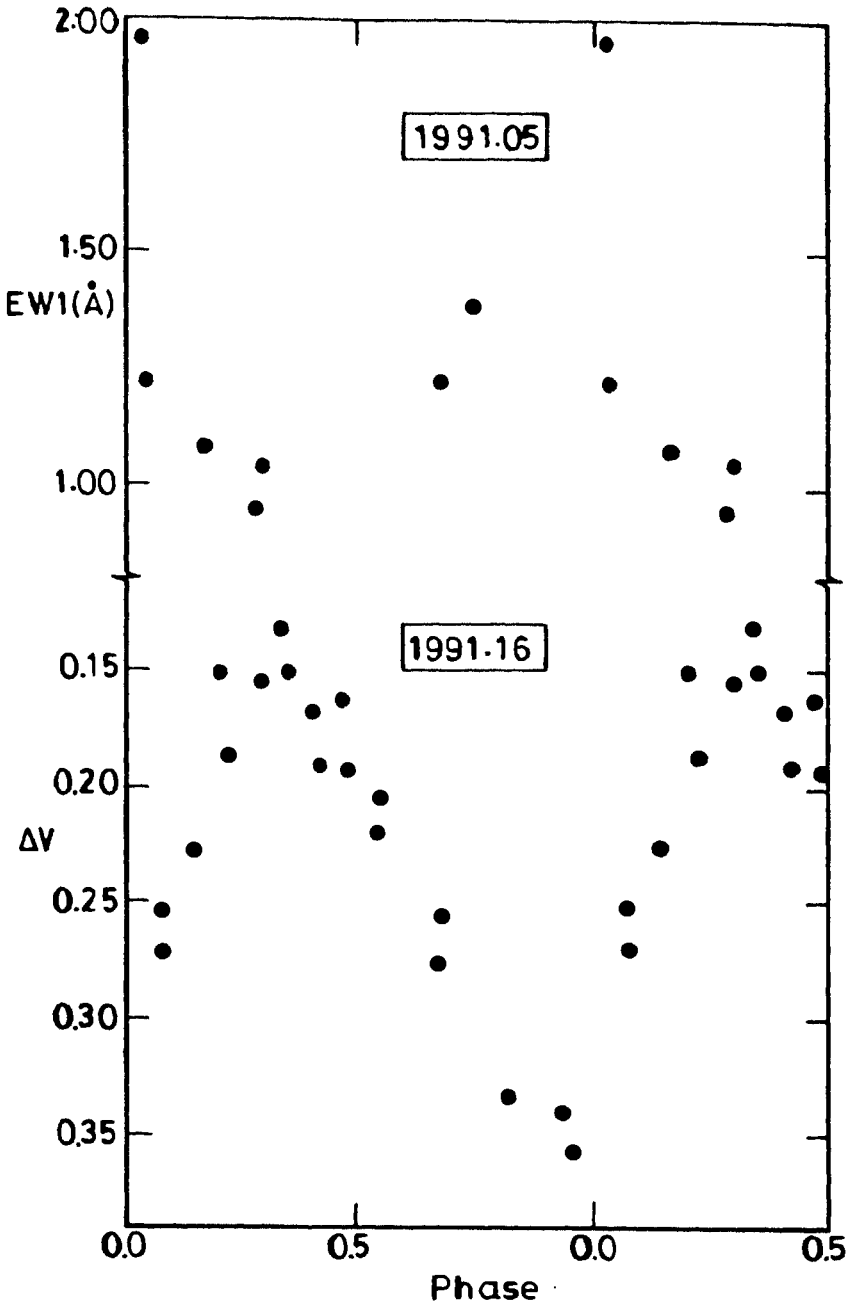

Figure 22. Top panel shows the V light curve and the bottom panel the variation of EW1. The mean epochs of observation are indicated in the figure.

nightly EW1 values range from 0.95 Å to 1.95 Å indicating that the emission in $H\alpha$ was very strong and varied by a factor of two during the period of the observation. The average values of EW1 and FWHM are $\sim$ 1.26 Å and $\sim$ 3.32 Å respectively. Similar $H\alpha$ behaviour has been reported by Crampton et al. (1979) and Nations & Ramsey (1986). Significant changes in the $H\alpha$ profile and equivalent width on time scales as short as a few hours have been reported (Tan & Liu 1985; Nations & Ramsey 1986).

We could not begin photometric work simultaneously with the spectroscopy because of poor sky conditions. Two of the $H\alpha$ spectra were obtained before the photometry was begun; the rest during the period of photometry. Fig. 22 displays both the light curve and EW1; the mean epoch of observations are indicated in the figure. It is seen from the figure that the $H\alpha$ emission strength is well correlated with the photometric phase in the sense that the emission is more intense near the light curve minimum.

The $H\alpha$ observations obtained on 7 Jan and 6 Feb 1991 fall nearly at the same phase. But the equivalent width obtained on the former occasion is significantly larger than that obtained on the latter occasion. Both these observations fall close to the photmetric minimum. It is very likely that the larger equivalent width observed on 7 January 1991 is related to a flare event. This interpretation is favoured because of its coincidence with the light minimum when the spotted region is facing the observer.

5

II PEGASI

21. Historical introduction

II Peg (= HD 224085 = BD $+27^{\circ}$ 4642) is a non-eclipsing binary consisting of a visible K2 IV primary and a spectroscopically invisible secondary. The orbital elements of.II Peg were first determined by Sanford (1921) and later by Halliday (1952). Chugainov's (1977) radial velocity measurements showed a systematic shift of about $0^{p}.15$ with respect to the elements of Halliday. Accordingly Raveendran, Mohin & Mekkaden (1981) re-analysed Halliday's data and obtained a refined period of 6.724464 days. In a spectroscopic study of II Peg, Vogt (1981) obtained several radial velocity measurements, and combining them with the previously published values independently derived new orbital elements for the system. Using both spectroscopic and photometric data obtained by him, Vogt argued that during the time of his observations the star showed predominantly one large spot or spot group which at certain phases essentially passed completely out of view. A series of high-resolution $H\alpha$ profiles obtained by him showed that the shape of $H\alpha$ emission profile was consistent with rotational phase, but its strength showed rotational modulation. In addition, a low-dispersion spectrum obtained by Vogt close to a light minimum showed strong TiO and VO features when compared to a spectrum taken close to a light maximum, giving evidence of

the presence of starspots.

Many spectroscopic studies have indicated that II Peg has strong *Ca II H* and *K*, and *Hα* emissions. The solar flare diagnostic line λ 5876 of He I has also been detected in emission (Buzasi, Huenemoerder & Ramsey 1991). Simultaneous photometry and spectroscopy indicated a strong correlation between the light variation and the strengths of *TiO* bands (Bopp & Noah 1980; Huenemoerder & Ramsey 1987; Buzasi, Huenemoerder & Ramsey 1991).

Though the light variability of this star was first noted by Eggen (1968), it was Chugainov (1976) who obtained the first photometric light curve and derived the 6.75 day photometric period. Chugainov tentatively classified the star as a BY Draconis−type variable due to its flare activity, variable amplitude in *V* and the time-scales of the changes in the highly asymmetric light curves. A more detailed study of the system was done a little later by Rucinsky (1977) who argued that this star resembles more closely an *RS CVn* though it exhibits many of the characteristics of the post−T Tauri star FK Ser. Hartmann, Londono & Phillips (1979) have found from the Harvard archival plate collection that II Peg was essentially constant in mean light level over the years 1900−40.

Interest in this system increased when Spangler, Owen & Hulse (1977) in a radio survey of close binaries discovered that it is a radio variable with the longest time-scale of variation among the radio binaries known then. The observed absolute radio luminosity is comparable to that of the well known RS CVn systems such as AR Lac, SZ Psc and V711 Tau (Owen & Gibson 1978). It has been detected as a strong source of both soft and hard X-ray flares (Walter et al. 1980; Schwartz et al. 1980).

The *IUE* observations revealed that it has strong and variable *UV* emission lines (Linsky 1984; Byrne et al. 1984). The most important evidence for the rotational modulation of plages in the case of RS CVn stars was provided by the *IUE* observations of II Peg which showed a clear enhancement of chromospheric and transition regions lines centered about the light curve minimum (Rodono et al. 1987). Moreover this star gave an indirect evidence for the presence of starspots, analogous to sunspots, by displaying flares and plages in the ultraviolet region which are anticorrelated with the light curve,

i.e., the UV fluxes are highest when the optical brightness is lowest (Marstad et al. 1982; Andrews et al. 1988). Near-simultaneous ground-based high resolution optical spetroscopy, *IUE* observations and photometry provided evidences for the changes in the distribution of brightness in the photosphere, chromosphere and transition region (Byrne et al. 1989). They have argued that these changes are interlinked and possibly a result of rotation.

22. *BV* photometry

II Peg was observed on a total of 57 nights during the five observing seasons 1986−87 (17 nights), 1987−88 (10 nights), 1988−89 (6 nights), 1989−90 (16 nights), and 1990−91 (8 nights). HD 223094 (K2) and HD 224895 (K0) were observed along with the variable as comparison stars. The observations were made differentially with respect to HD 223094 and were transformed to the Johnson's *UBV* system. The average magnitude and colour of the comparison star HD 223094 determined by us are 6.957 ± 0.013 and 1.621 ± 0.006, respectively. These values are in good agreement with those given by Nicolet (1978). The magnitudes and colours of II Peg thus determined are listed in Table 8. The typical uncertainty in the measurements of the differential magnitudes and colours is $\sim$ 0.01 mag. Each value given in Table 8 is a mean of three to four independent measurements. The Julian days of observation given in Table 8 are converted to orbital phases using the following ephemeris given by Raveendran, Mohin & Mekkaden (1981):

$$\text{JD (hel.)} = 2443030.396 + 6^d.724464\ \text{E},$$

where the zero phase corresponds to the conjunction with the visible K2 IV primary in front and the period is the spectroscopic orbital period.

23. Light curves

The observations obtained during the seasons 1986−87, 1988−90, and 1989−90 are plotted in Figs 23−25. The mean epochs of observations are indicated in each figure. The observations obtained during 1986−87 season (Fig. 23) show that the shape of the light curve has undergone remarkable changes from that of the earlier season's light curve. The amplitude is 0.4

Table 8. Magnitudes and colours of II Peg

J.D. (Hel) 2440000.+	ΔV	$\Delta(B-V)$	J.D. (Hel) 2440000.+	ΔV	$\Delta(B-V)$
		1986–87 Observing Season			
6801.1340	7.515		6821.1020	7.601	
6802.1180	7.349	1.034	6823.1248	7.374	
6803.1145	7.326	1.032	6824.0946	7.427	
6804.0958	7.403	1.061	6825.0858	7.462	
6816.1134	7.342		6828.0824	7.510	
6817.1032	7.384		6830.0885	7.326	
6818.0958	7.423		6831.0852	7.394	
6819.0995	7.554	1.084	6832.0916	7.462	
6820.1115	7.722				
		1987–88 Observing Season			
7175.0861	7.491		7184.1076	7.370	1.041
7176.0875	7.509		7185.0941	7.412	1.036
7178.1078	7.417	1.037	7201.0829	7.450	
7179.0985	7.480		7202.0829	7.496	
7183.0847	7.466		7203.0970	7.461	
		1988–89 Observing Season			
7556.0771	7.581		7559.0814	7.419	
7557.0881	7.751	1.084	7560.0828	7.313	
7558.0847	7.731		7561.0833	7.346	

Table 8 continued

J.D. (Hel) 2440000.+	ΔV	$\Delta(B-V)$	J.D. (Hel) 2440000.+	ΔV	$\Delta(B-V)$
		1989–90 Observing Season			
7852.2499	7.527	1.058	7895.1142	7.700	1.052
7853.1379	7.709	1.069	7896.0834	7.564	1.052
7854.0917	7.746	1.076	7912.1025	7.431	1.050
7855.1629	7.661	1.074	7913.0887	7.581	1.056
7856.0897	7.472	1.044	7916.0809	7.610	1.080
7867.0901	7.726	1.087	7917.0839	7.417	1.038
7877.1769	7.350	1.063	7918.0830	7.378	1.023
7878.1659	7.391	1.040	7919.0799	7.463	1.051
		1990–91 Observing Season			
8280.0803	7.476	1.033	8299.0830	7.603	
8281.0769	7.445	1.059	8300.0846	7.545	1.042
8297.0848	7.484	1.091	8301.0936	7.459	1.098
8298.0834	7.526	1.058	8302.0874	7.523	1.079

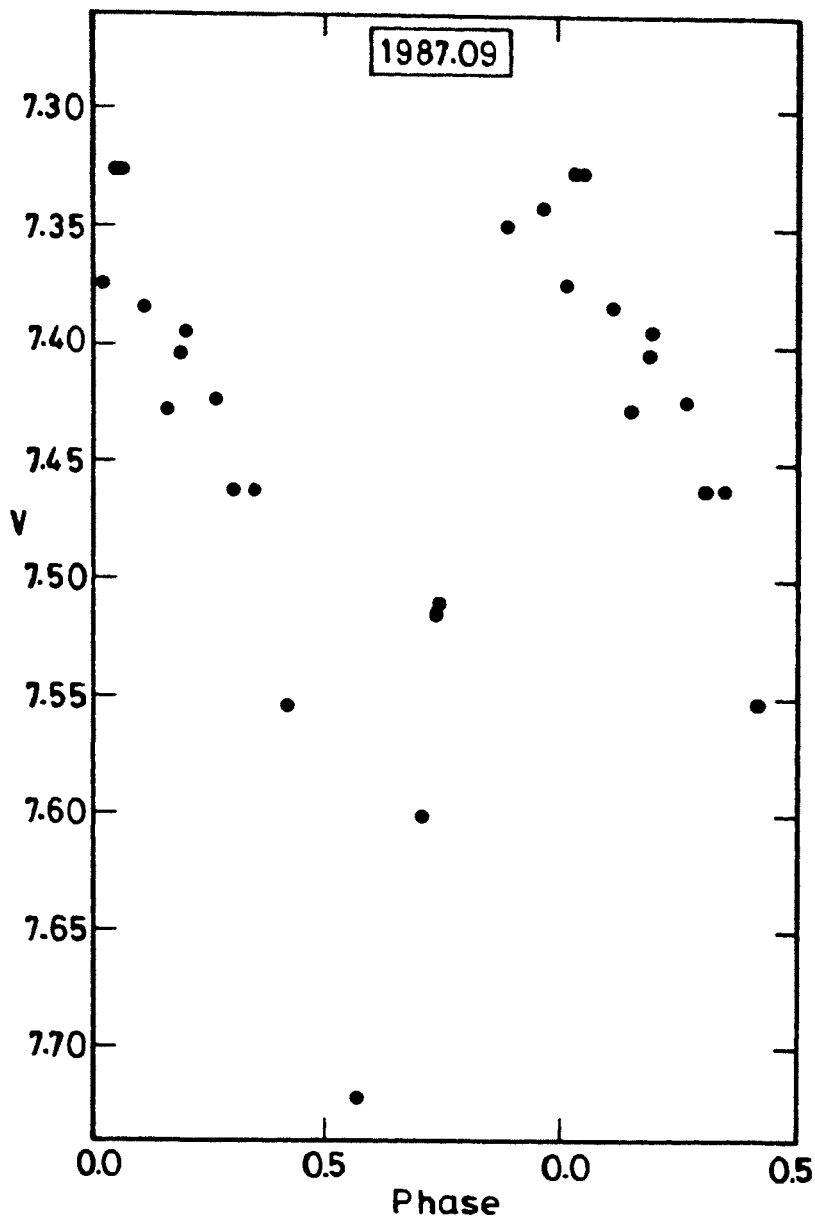

Figure 23. The 1987.09 light curve of II Peg. Phases are reckoned from JD (Hel.) 2443030.396 using the period $6^d.724464$.

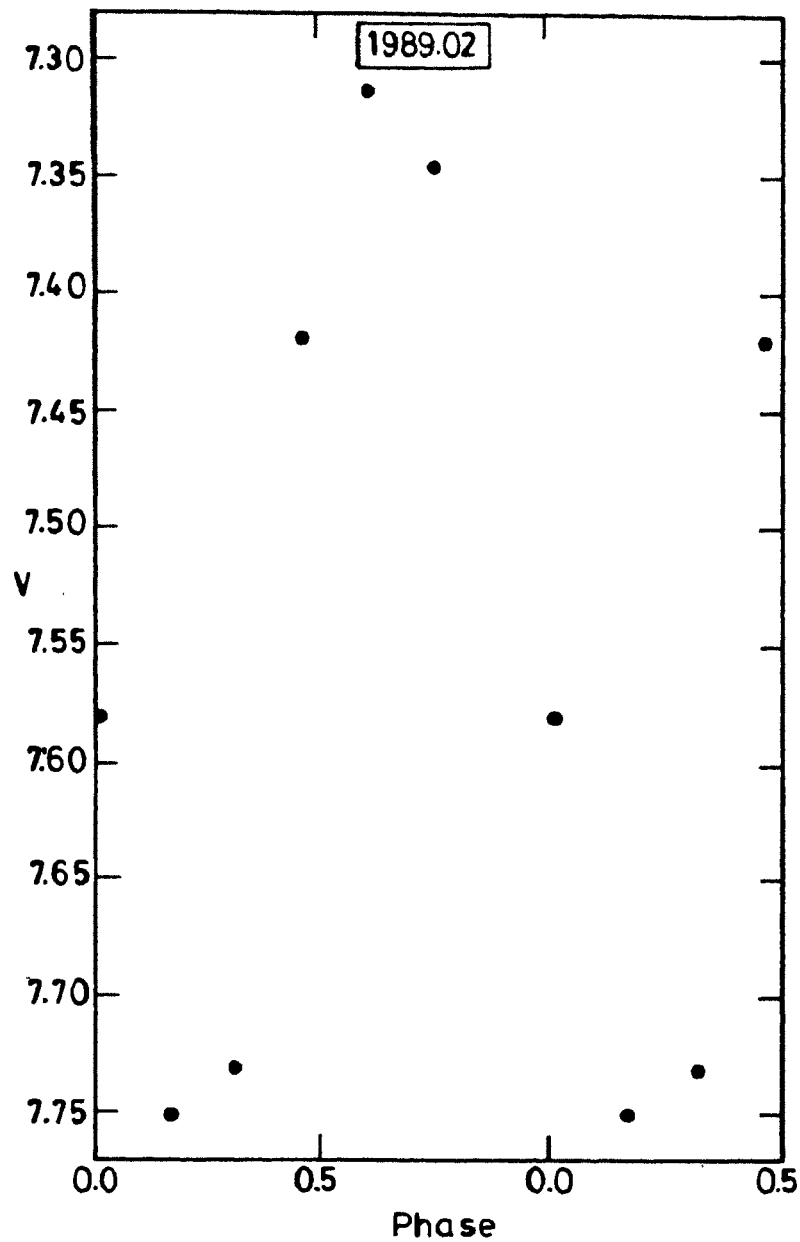

Figure 24. The 1989.02 light curve of II Peg. Phases are reckoned as in Fig. 23.

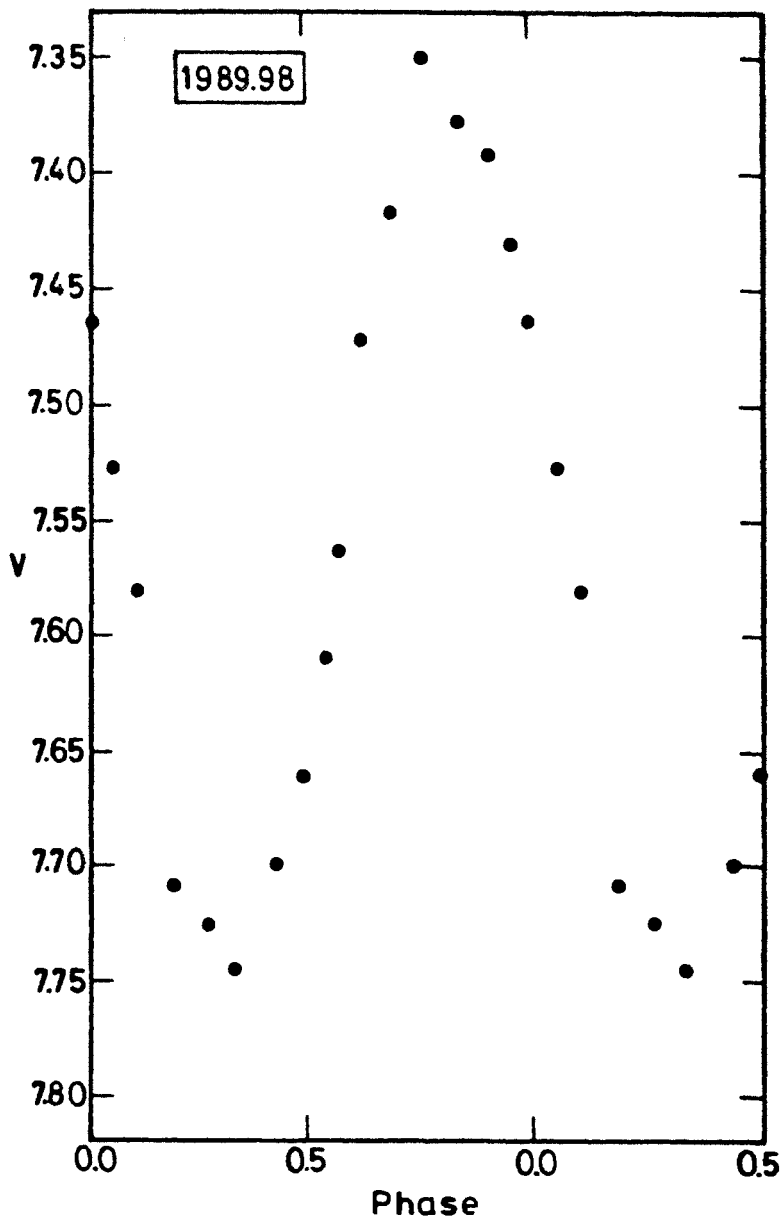

Figure 25. The 1989.98 light curve of II Peg. Phases are reckoned as in Fig. 23.

mag, and the minimum ($V = 7.722$) and maximum ($V = 7.326$) occur at $0^p.50$ and $0^p.00$ respectively. A similar large amplitude for II Peg had occurred earlier during 1977–78 (Vogt 1979). The amplitudes of the light curve just before and after 1986–87 season were only around 0.20 mag.

Fig. 24 shows the observations made during the 1988–89 season. Though the data are limited, the light curve is clearly defined close to both the minimum and maximum which occur around $0^p.25$ and $0^p.65$. The amplitude is around 0.44 mag. The light curve obtained by Casas et al. (1989) immediately after our observations registered the highest so far observed amplitude of 0.50 mag. Doyle et al. (1988) also have reported a similar value for the amplitude around 1986.78, but the observational uncertainty in their case is of the order of 0.04 mag. Casas et al. (1989) have also reported that the system's maximum brightness during their observations was 7.250 mag which is close to the value of 7.20 mag in 1974 (Chugainov 1976).

In Fig. 25 we have plotted the observations obtained during 1989–90 season. The amplitude of light variation is around 0.39 mag; the light maximum and minimum occur at $0^p.80$ and $0^p.35$, respectively. Fig. 26 is the plot of $B - V$ given in Table 8 against the corresponding observed visual magnitude. There is apparently no correlation between the colour $B - V$ and the visual brightness of II Peg; but there is a scatter with a total range of about 0.10 mag and this is much larger than the expected observational uncertainty.

The photometric properties derived from the present observations together with those compiled from various sources are given in Table 9. The quantities given in the table are mostly evaluated from graphical plots of the observations. The ephemeris of Raveendran, Mohin & Mekkaden (1981) was used throughout for the analysis.

24. Brightness at light maximum and minimum

Fig. 27 is a plot of V_{max} and V_{min} from Table 9 against the corresponding amplitude. An inspection of Fig. 27 clearly reveals that at larger amplitudes the brightness at minimum decreases and the brightness at maximum increases. Chugainov's observations however do not conform to this

Table 9. Photometric characteristics of II Peg

Epoch	Amplitude	V_{max}	V_{min}	Phase Min	References
1974.05	0.10	7.284	7.424	0.15	Chugainov (1976)
1974.65	0.32	7.200	7.500	0.15	Chugainov (1976)
1976.80	0.26	7.350	7.595	0.07	Rucinski (1977)
1977.65	0.42	7.350	7.773	0.90	Vogt (1979)
1979.82	0.17	7.430	7.598	0.65	Nations & Ramsey (1981)
				0.25	
1980.00	0.15	7.425	7.600	0.75	Raveendran et al. (1981)
				0.25	
1980.70	0.17	7.530	7.650	0.65	Bohusz & Udalski (1981)
				0.08	
1980.73	0.17			0.05	Hall & Henry (1983)
1980.97	0.22	7.440	7.660	0.00	Mohin et al. (1986)
				0.65	
1981.75	0.27			0.83	Rodono et al. (1983)
1981.76	0.22			0.77	Lines et al. (1983)
1981.83	0.20			0.69	Zeilik et al. (1982)
1982.05	0.29	7.360	7.656	0.70	Mohin et al. (1986)
1982.10	0.24			0.72	Henry (1983)
1983.10	0.11			0.77	Andrews et al. (1988)
1983.63	0.09			0.66	Evren (1988)
				0.10	
1983.76	0.05			0.74	Evren (1988)
				0.14	
1984.60	0.16			0.34	Evren (1988)

Table 9. continued

Epoch	Amplitude	V_{max}	V_{min}	Phase Min	References
1984.63	0.12	7.483	7.623	0.35	Byrne et al. (1989)
				0.65	
1984.65	0.12	7.460	7.606		Kaluzny (1984)
1984.68	0.15			0.55	Arevalo et al. (1985)
1985.00	0.23			0.76	Strassmeier et al. (1989)
1985.01	0.20	7.390	7.590	0.70	Mohin et al. (1986)
				0.35	
1985.87	0.23			0.57	Boyd et al. (1987)
				0.24	
1985.88	0.21			0.24	Wacker & Guinan (1986)
				0.72	
1986.00	0.29			0.29	Strassmeier et al. (1989)
				0.71	
1986.77	0.47	7.322	7.791	0.65	Cutispoto et al. (1987)
1986.78	0.50	7.220	7.800	0.60	Doyle et al. (1988)
1986.80	0.45	7.325	7.775	0.58	Byrne et al. (1986)
1986.90	0.40	7.290	7.690	0.63	Mekkaden (1987)
1986.96	0.40			0.57	Boyd et al. (1987)
				0.24	
1987.09	0.40	7.326	7.722	0.50	Present study
1987.92	0.15			0.23	Cano et al. (1987)

Table 9. continued

Epoch	Amplitude	V_{max}	V_{min}	Phase Min	References
1987.79	0.27				Evren (1990)
1988.65	0.30			0.32	Evren (1990)
1988.78	0.41			0.65	Pajdosz et al. (1989)
1988.91	0.43			0.22	Cutispoto et al. (1989)
1989.02	0.44	7.310	7.750	0.25	Present study
1989.07	0.50	7.250	7.750	0.24	Casas et al. (1989)
1989.31	0.46			0.27	Evren (1990)
1989.50	0.43			0.38	Cutispoto et al. (1989)
1989.61	0.42			0.32	Evren (1990)
1989.98	0.39	7.350	7.740	0.35	Present Study
1991.06			7.603	0.50	Present Study

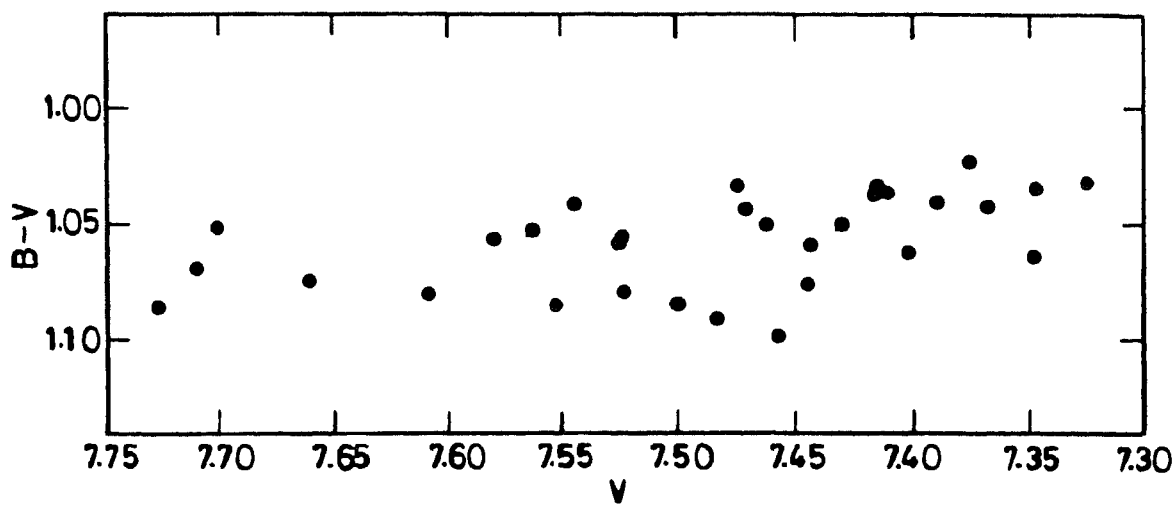

Figure 26. Plot of $B - V$ against the corresponding V

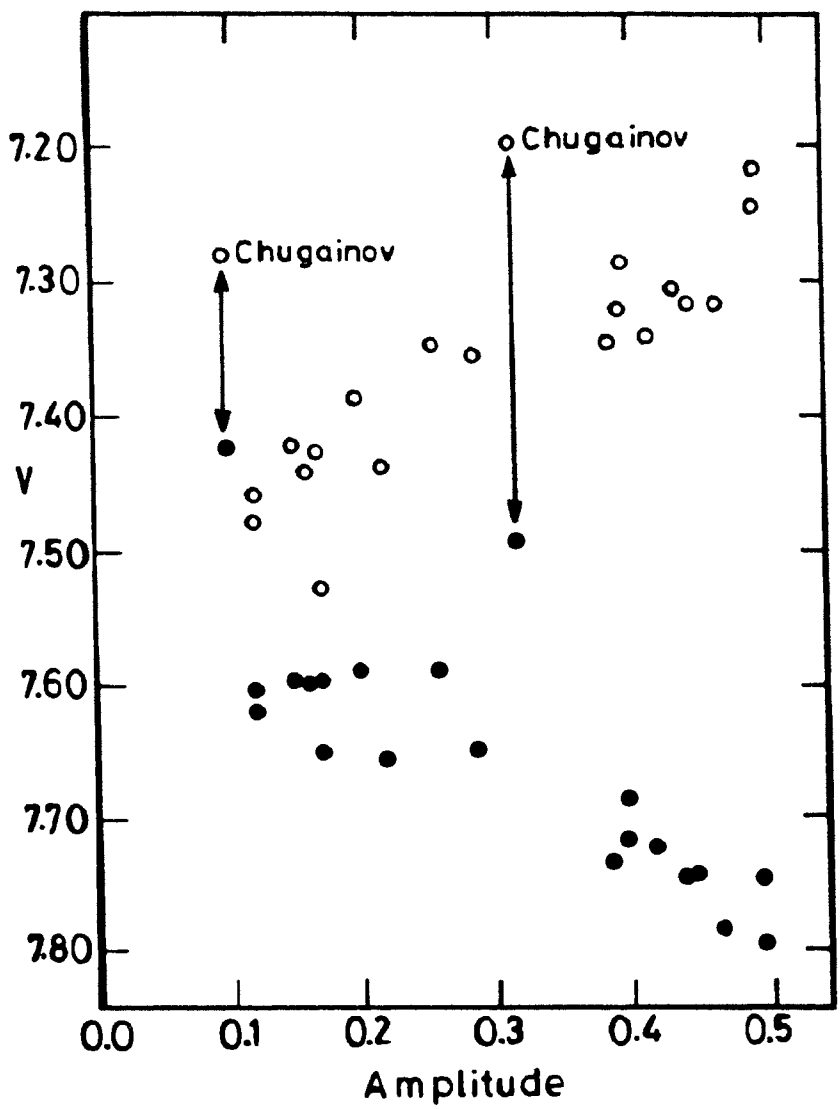

Figure 27. Plot of the brightness at light maximum (open circles) and light minimum (filled circles) against the V amplitude.

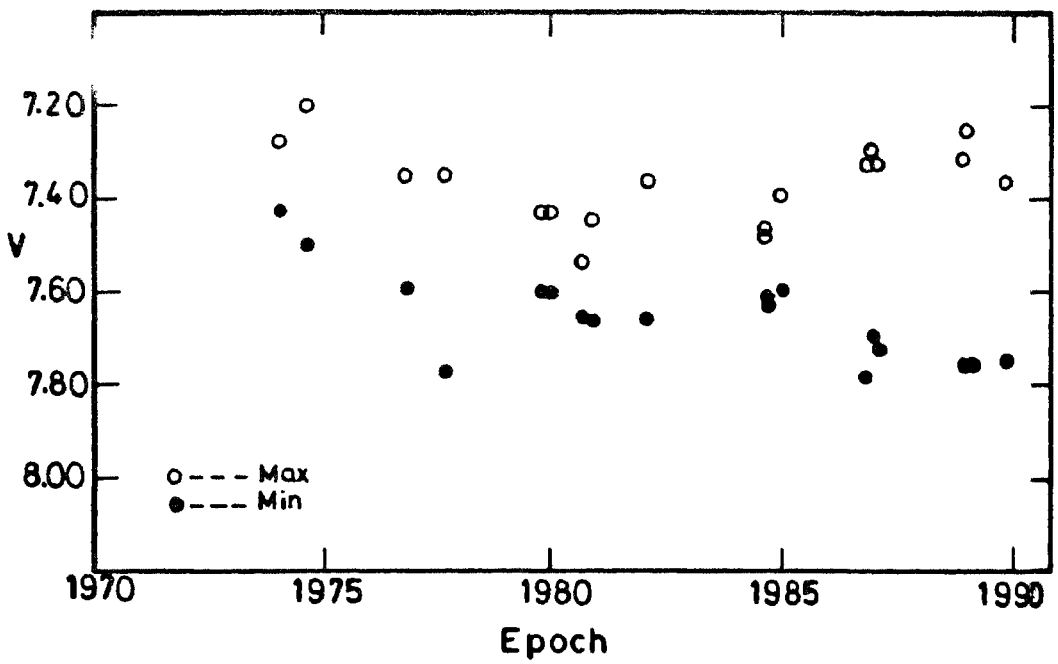

Figure 28. Plot of the brightness at light maximum (open circles) and light minimum (filled circles) against the mean epoch of observation.

trend. As argued by Vogt (1981) it may probably be due to a difference in the zero-points of magnitude between Chugainov's and the others' observations. The behaviour of II Peg as seen in Fig. 27 is similar to that seen in the case of UX Ari and V711 Tau, two other active RS CVn stars (Chapter 7 and Chapter 8).

To find out the time variations in the brightness at maximum and minimum of light curves all the available V_{max} and V_{min} given in Table 9 are plotted in Fig. 28 against the corresponding epoch of observations. As can be seen from the figure significant changes occur in the mean light level of the system from season to season. The maximum light level V_{max} has maintained a value less than or equal to 7.35 mag during 1976–85. However, V_{max} shows a secular increase from 1986 onwards; the highest value of V_{max} obtained by Casas et al. (1989) during 1989 was 7.25 mag.

25. Phase of light minimum and amplitude

To find out the evolution of starspots or starspot regions we have plotted the phase of light minimum (ϕ_{min}) and V amplitude of light variation given in Table 9 against the corresponding mean epoch of observation in Figs 29 and 30 respectively.

An inspection of Fig. 29 clearly shows that on most occasions during the period 1974–91 there were two prominent spots or spot groups present as indicated by two light minima in the light curves. We could identify a total of six spots or spot groups from the migration of the ϕ_{min}. Their life times (as indicated by the time interval during which a spot or spot group could be traced from the values of ϕ_{min}) range from two to seven years. The difference in their photmetric periods from the orbital period indicates a range of -0.0037 to +0.0042 for ΔP/P. Here Δ is in the sense photometric minus orbital period. A study of the available photometry from 1974–81 by Rodono et al. (1983) have indicated that the two main features of the light curve, namely, the phase of light maximum and minimum migrate towards decreasing orbital phases at different rates (0.23 and 0.03 period per year respectively), with the minimum being almost synchronous with the orbital motion. They have argued that the difference in the migration rates

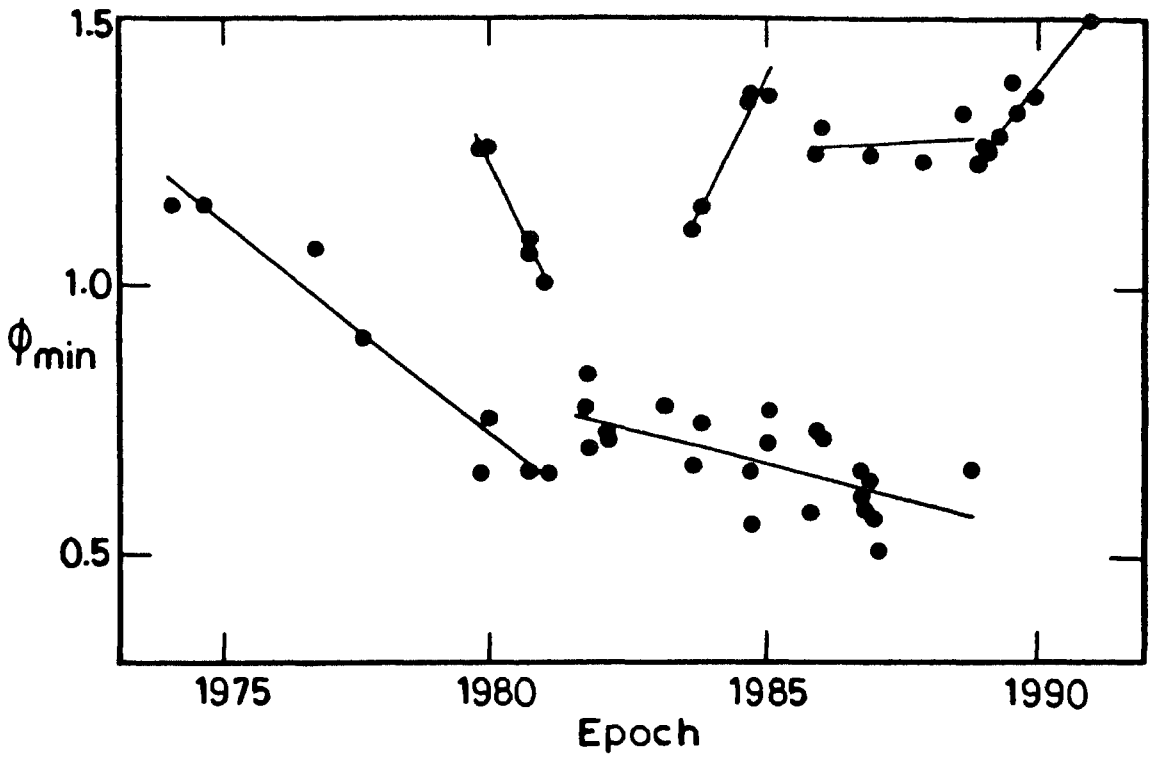

Figure 29. Plot of the phase of light minimum versus mean epoch of observation.

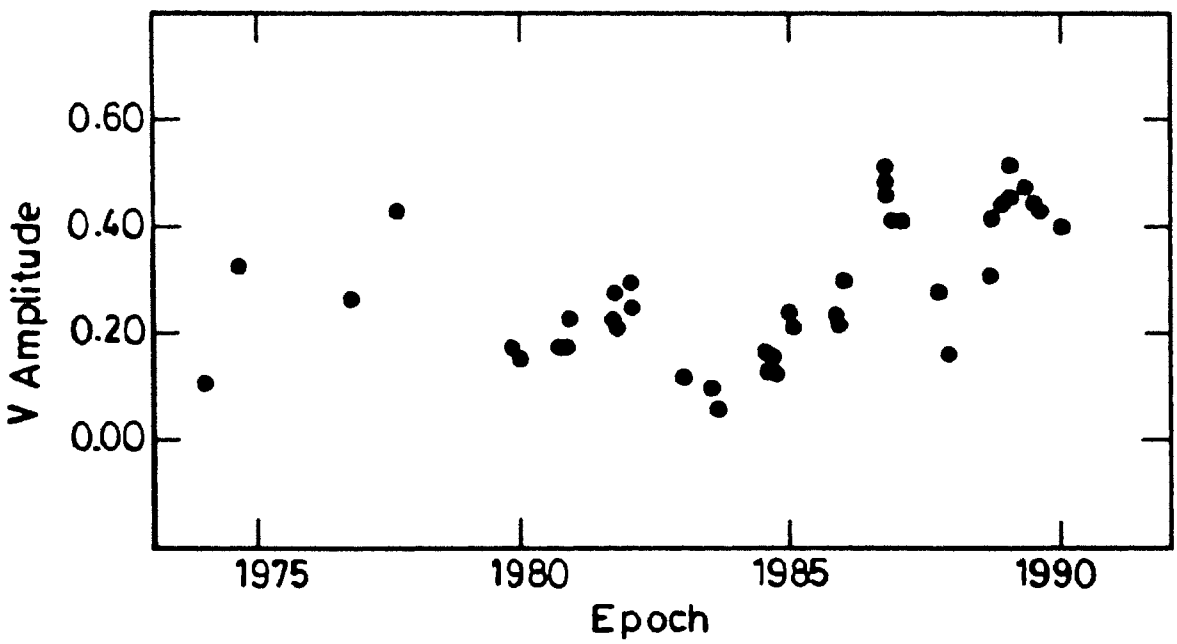

Figure 30. Plot of V amplitude against the mean epoch of observation.

produce the observed changes in the light curve, *i.e.*, from almost sinusoidal, to asymmetric, to double-peaked to almost flat. But from Fig. 29 which covers a more extended period it is obivious that the migration of the phase of light minimum has both direct and retrograde motions.

Fig. 30 shows that the amplitude of light curve is highly variable. In a recent analysis Evren (1990) has claimed that the amplitude variation is cyclic and the period is roughly four years. However, it is clear from the figure that II Peg had minimum amplitudes in 1980, 1984, 1988, whereas the maximum amplitudes occurred in 1978, 1982, 1987 and 1989 which are not separated by four years.

In a recent analysis of starspot lifetimes considering 40 spots or spot groups on 17 different stars, Hall (1990) has argued that smaller spots (radius $< 20°$) die before they can be disrupted by differential rotation, but larger spots are disrupted by differential rotation. He has proposed the following two scenarios: (i) a large spot originates in a deep layer which may be rigidly rotating, is magnetically disconnected after a while, and is disrupted by differential rotation characteristic of the surface, or (ii) a large spot is not disconnected magnetically but the deeper layers from which it originates has approximately the same differential rotation law which applies to the surface layers. In the case of II Peg the discontinuities in the migration which are interpreted as the disappearence (or weakening) of the existing spot or spot group and the appearence (or strengthening) of a new spot or spot group (Mekkaden, Raveendran & Mohin 1982; Hall 1990) indicate lifetimes in the range 2–7 years. According to Hall's scenario this implies the formation of both large and small spots on the surface of II Peg.

26. Spot modelling

As discussed earlier (Chapter 3) the factor that most affects the modelling is the unspotted V magnitude of the star. Different values for the unspotted magnitude have been used in the modelling of the light curves of II Peg (Vogt 1981; Poe & Eaton 1985; Rodono et al. 1986). The highest value of $V_{max} = 7.20$ mag reported in the literature was obtained by Chugainov (1976) in 1974. While modelling the light curve obtained by him,

Vogt (1981) found that satisfactory results could not be obtained with this value for the unspotted magnitude. So he argued that Chugainov's data suffer from a zero point error when compared to others' data and that the unspotted V magnitude is close to $V = 7.35$ mag. Vogt's argument need not be a sufficient reason to condemn Chugainov's observation because Casas et al.'s (1989) value of 7.25 mag is close to Chugainov's value of 7.20 (see Fig. 28). So in the present analysis Chugainov's values of $V = 7.20$ mag and $B = 8.22$ mag are assumed to represent the unspotted photosphere. Using the method described in Chapter 3 we have modelled the observations obtained during 1989−90 as an example. These observations are chosen because during this season sufficient data were obtained in both B and V bands so as to include temperature also as an unknown in the least square analysis.

Table 10. The spot parameters derived for the light curves of II Peg for 1989−90 season

	Inc. $(i) = 45^o$	Inc. $(i) = 75^o$
Polar distance (degrees)	161.4±0.7	164.0±0.7
Longitude (degrees)	118±1	119±1
Radius (degrees)	118.0±1.0	95.0±1.4
Temperature (K)	3780±55	3750±80
Fractional area	0.735±0.008	0.541±0.012
S. d. of fit (mag)	0.019	0.022

II Peg is a single-lined spectroscopic binary and hence the orbital inclination i is unknown. Spot parameters are derived using $i = 45^o$ and $i = 75^o$. The effective temperature of the undisturbed photosphere is assumed to be 4600 K. Calculations are carried out with the same quadratic limb-darkening law for both the spots and undisturbed photospheric region. The coefficients used are the following: A = 0.785 and B = 0 for V band, and A = 1.080 and B = −0.230 for B band. The above values are derived from

interpolations using the table given by Manduca, Bell & Gustafsson (1977) for the solar composition. The computed best fit V and B light curves are shown in Figs 31 and 32 along with the observed values. Results of the least square analysis are given in Table 10. The standard deviations of the fit in the two cases are nearly identical. There is a close agreement in the values derived for the polar distances, longitudes and temperatures in the two cases. However, there is a large difference in the value of the derived spot radii. In both cases a substantial fraction of the spots lie in the invisible portion of the stellar surface, the fraction being large for $i = 45°$. The results indicate a very large fractional area for the spots (as high as 75 % for $i = 45°$). Doyle et al. (1988) have suggested a more complicated triangular distribution of spots to account for the photometric variation.

27. $H\alpha$ observations

$H\alpha$ region spectra of II Peg were obtained on a total of 12 nights during the 1990–91 observing season. Table 11 gives the log of observations; it contains the Julian day of observation; the $H\alpha$ emission equivalent width EW1; full width at half maximum of the $H\alpha$ emission (FWHM); height of the $H\alpha$ emission in terms of F_λ/F_c; the photometric phase reckoned from the ephemeris of Raveendran, Mohin & Mekkaden (1981); and the equivalent width EW2. The computations of EW1 and EW2 were done as described in Chapter 2. The results of $H\alpha$ observations are plotted in Figs 33–36.

The average values of EW1 and FWHM are $\sim$ 0.91 Å and $\sim$ 2.40 Å respectively. The nightly EW1 values range from 0.61 Å to 1.93 Å. Bopp & Noah's (1980) observations obtained during 1978 show a large scatter in equivalent width (EW) (range $\approx$ 0.2Å to $\approx$ 2.0 Å) with a tendency to cluster in phase. Ramsey & Nations (1984) have reported $H\alpha$ EW values ranging from −0.07 Å to 1.94 Å obtained at two different resolutions ($\approx$ 1 Å and 0.5 Å) during 1981. Observations during July 1984 indicate EW values from 0.69 Å to 1.39 Å (Byrne et al. 1989). While spectra obtained on five consecutive nights during November–December 1984 showed a monotonically decreasing EW values from 1.22 Å to 0.64 Å , a single spectra obtained after three weeks showed the EW to be 0.86 Å (Liu & Tan 1987). The observations given in

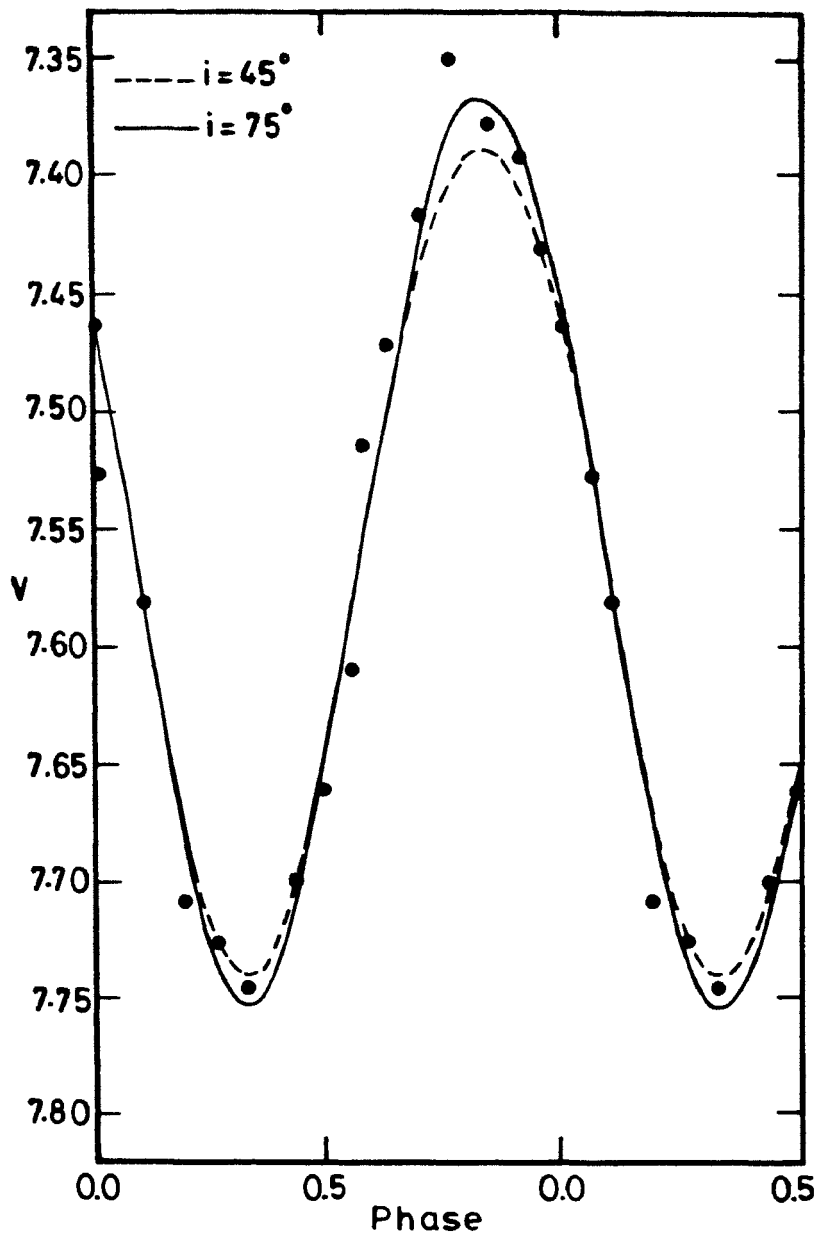

Figure 31. The 1989.98 V light curve of II Peg along with the corresponding best fit computed curves for the assumed orbital inclinations $i = 45°$ (broken) and $i = 75°$ (continuous). Phases are reckoned as in Fig. 23.

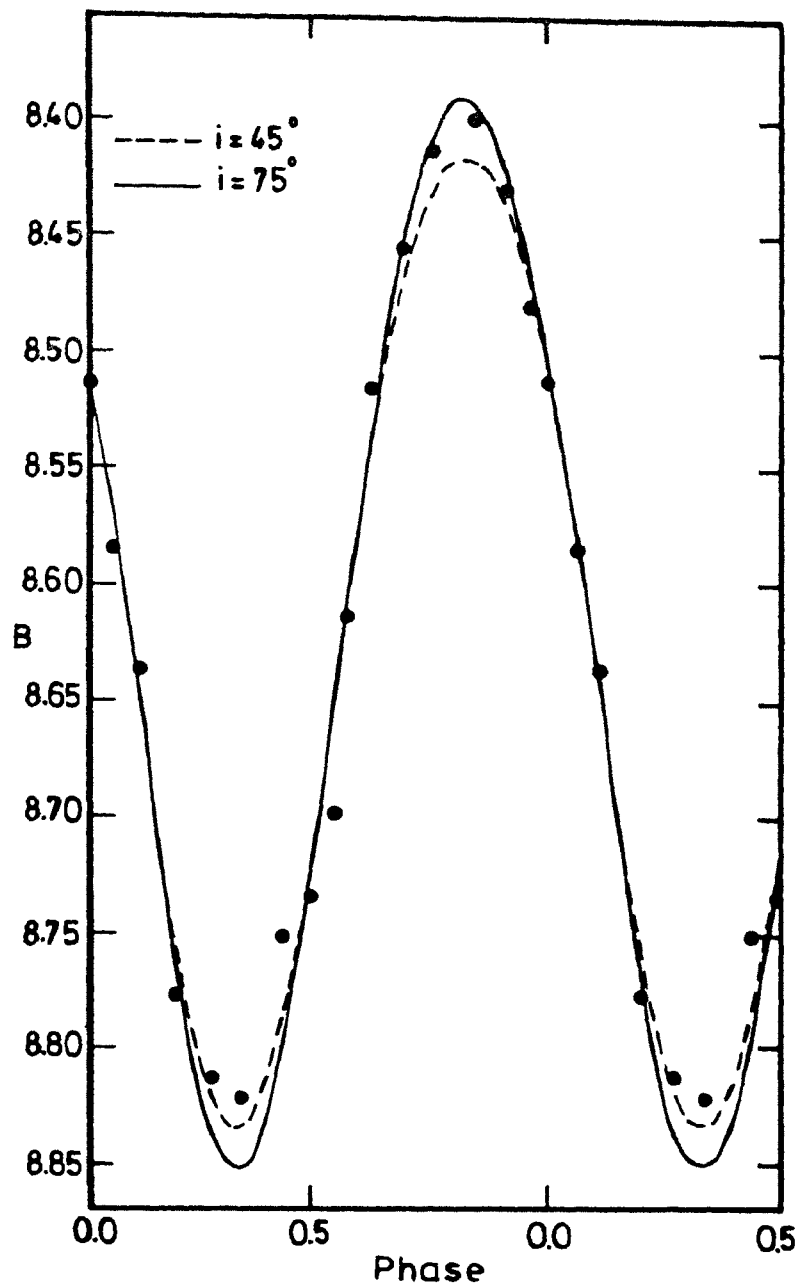

Figure 32. The 1989.98 B light curve of II Peg along with the corresponding best fit computed curves for the assumed orbital inclinations $i = 45°$ (broken) and $i = 75°$ (continuous). Phases are reckoned as in Fig. 23.

Table 4 and plotted in Figs 10−13 show clearly that the star was monitored at almost all the orbital phases.

Table 11. $H\alpha$ data of II Peg

Date	JD (Hel.) 2440000.+	Phase	EW1 Å	FWHM Å	Height	EW2 Å
08 Oct 1990	8173.2549	0.799	0.80	2.68	0.33	−0.19
08 Oct 1990	8173.3365	0.811	0.61	2.27	0.28	−0.55
10 Oct 1990	8175.3431	0.109	1.40	3.02	0.54	+0.23
11 Oct 1990	8176.2889	0.250	0.77	2.09	0.36	−0.44
11 Oct 1990	8176.3323	0.256	0.66	1.83	0.35	−0.90
22 Nov 1990	8218.1413	0.474	1.93	3.62	0.53	+1.05
22 Nov 1990	8218.2198	0.485	1.62	3.31	0.50	+0.49
23 Nov 1990	8219.0945	0.615	0.93	2.99	0.32	−0.08
28 Nov 1990	8224.1602	0.369	1.25	2.75	0.46	+0.19
29 Nov 1990	8225.1694	0.519	0.88	2.11	0.40	−0.44
30 Nov 1990	8226.1934	0.671	0.61	1.83	0.32	−1.07
07 Jan 1991	8264.1375	0.314	0.70	2.13	0.33	−0.71
08 Jan 1991	8265.1278	0.461	0.57	2.04	0.27	−0.70
07 Feb 1991	8295.1049	0.919	0.45	1.60	0.29	−0.98
08 Feb 1991	8296.0785	0.064	0.49	1.77	0.27	−0.71

An inspection of the Figs 33−36 indicates that II Peg shows a very strong and asymmetrical $H\alpha$ emission line. All earlier investigators have remarked on the variability of the $H\alpha$ profile in II Peg. The figures confirm the observations of Vogt (1981) who reported that *the notch* in the profile occurs precisely at the nominal $H\alpha$ rest wavelength with respect to the absorption lines and the centroid of the emission lies blueward. The emission is always fixed in wavelength with respect to the absorption lines and occurs

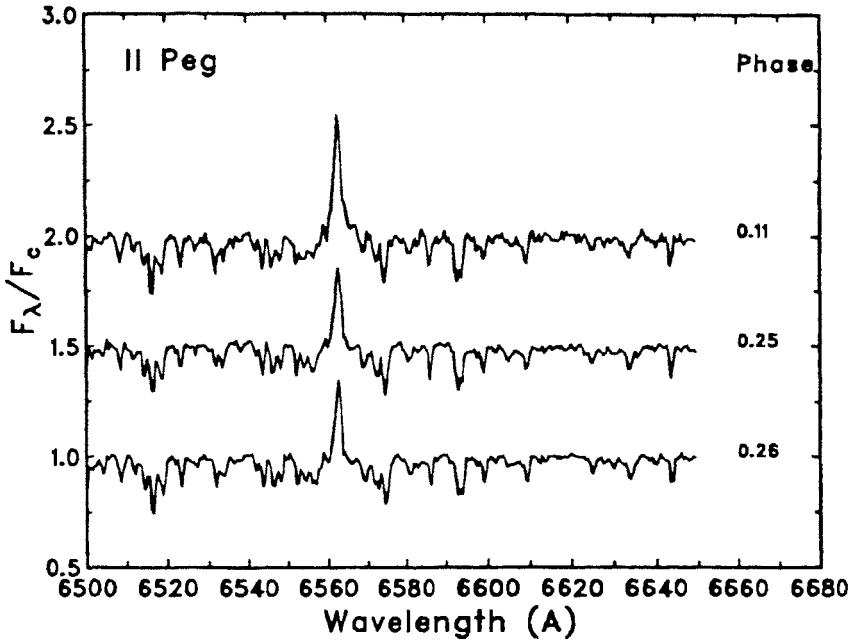

Figure 33. $H\alpha$ spectra of II Peg. The spectra are adjusted in wavelength to line up the absorption lines. Each spectrum is normalized to continuum and shifted by 0.5. Phases are reckoned as in Fig. 23.

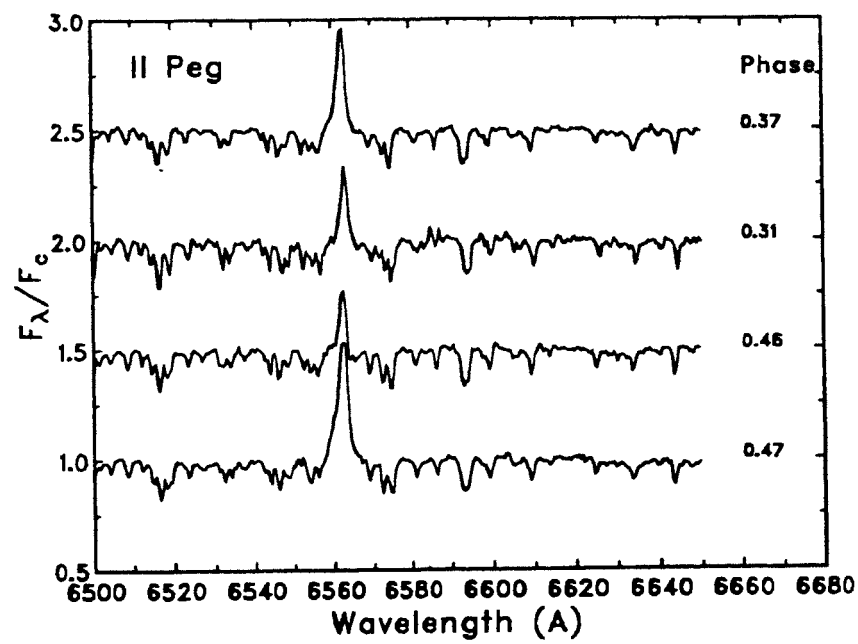

Figure 34. $H\alpha$ spectra of II Peg. The descriptions are as in Fig. 33.

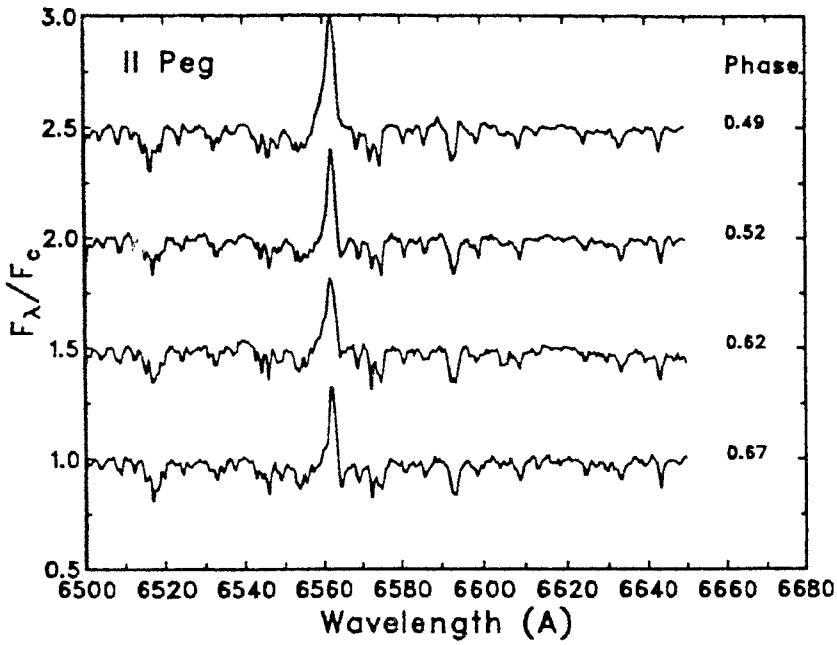

Figure 35. $H\alpha$ spectra of II Peg. The descriptions are as in Fig. 33.

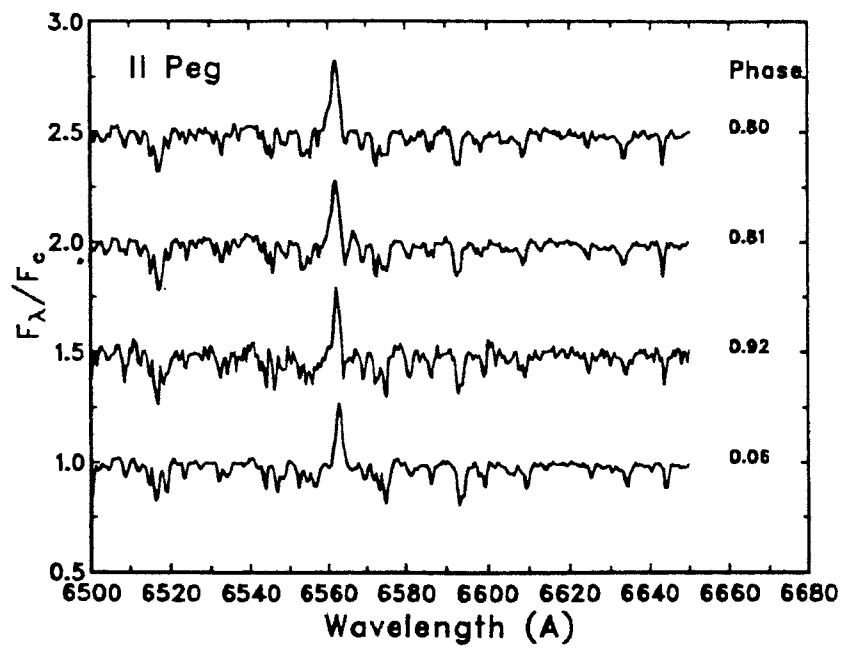

Figure 36. $H\alpha$ spectra of II Peg. The descriptions are as in Fig. 33.

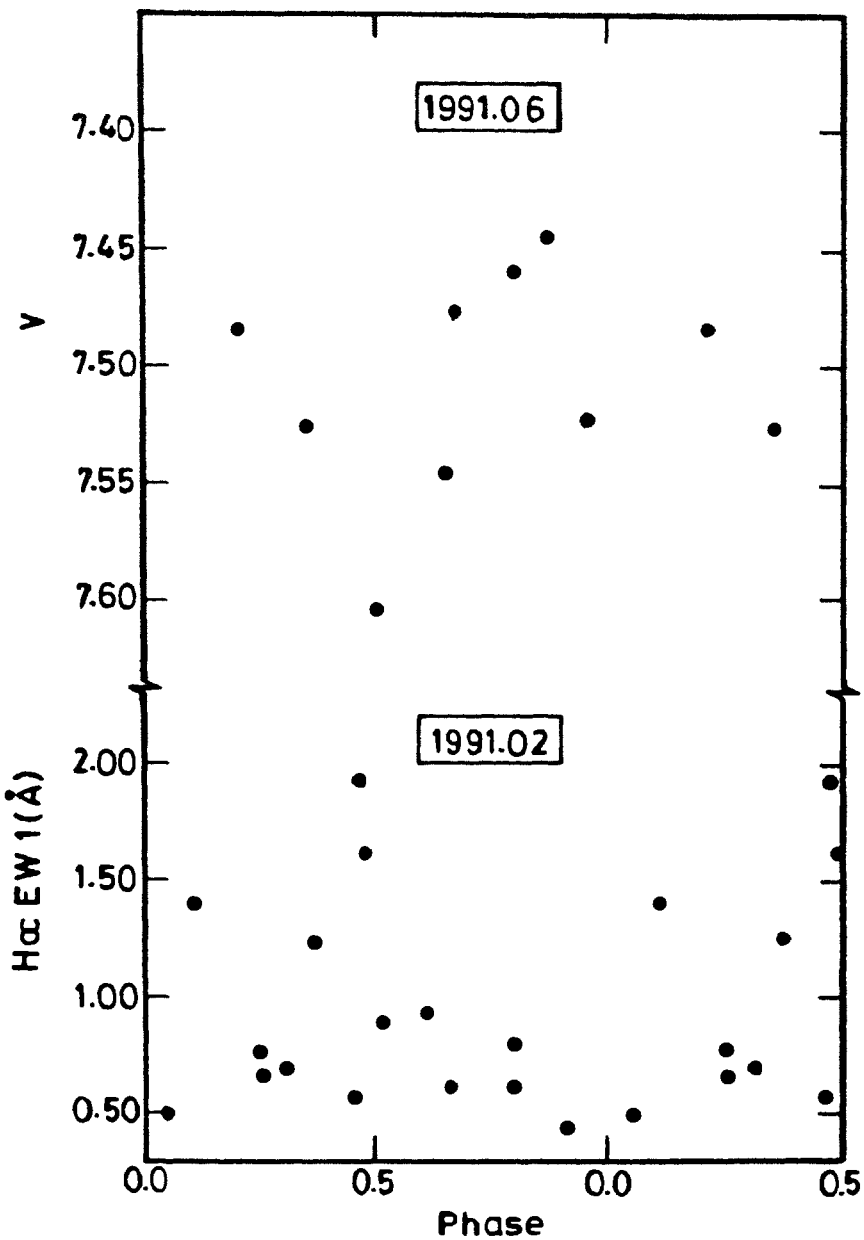

Figure 37. Top panel shows the V light curve and the bottom panel the variation of EW1. Phases are reckoned as in Fig. 23. The mean epochs of observation are indicated in the figure.

at the expected position of $H\alpha$. This clearly demonstrates that the emission is associated with the visible K2 IV primary without any contamination.

Spectroscopic studies by Bopp & Noah (1980) have shown that the $H\alpha$ emission strength is well correlated with the photometric phase in the sense that the emission is more intense near the light curve minimum. They have also noted several sudden *flare-like* enhancements of $H\alpha$ with decay times up to several days. An attempt was made by us to have near-simultaneous photometry and spectroscopy. Due to the unfavourable sky conditions we could begin the photometry of the star only three months after the beginning of the spectroscopic observations. Though the phase coverge is incomplete the light curve is well-defined near the light minimum. The $H\alpha$ EW1 in Table 11 is plotted in Fig. 37 along with the V light curve obtained. It is evident from the figure that the emission is variable and there is a strong anticorrelation. It is interesting to see that all values of EW1 except four are below 0.90 Å. Out of these four two values fall on the same ordinate with a difference of 0.3 Å. These two values were obtained on the same night namely on 1990 Nov 22. Recently, Buzasi, Ramsey & Huenemoerder (1991) have concluded that II Peg appears to flare approximately once in every five hours. Their conclusion is based on rapidly changing $He\ D_3$, $H\alpha$ and $H\beta$ emissions obtained on a single night. Moreover Fig. 37 indicates that the star appears to have a tendency for flaring up during the photometric minimum, *i.e*, when the spotted region is visible to the observer.

6

V711 TAURI

28. Historical introduction

The star HD 22468 (= HR 1099), more commonly known by its variable star nomenclature V711 Tau, is a bright star with V $\sim$ 5.7 mag.

The first spectroscopic study of V711 Tau has indicated that it has double absorption lines (Adams, Joy & Sanford 1924). The extraordinary strengths of *Ca II H* and *K* reversals and the moderately strong $H\alpha$ emission line having a width of 5-6 Å in its spectrum were first reported by Wilson (1963, 1964). Apart being a spectroscopic binary, V711 Tau is also the primary of a physically associated visual binary ADS 2644 whose companion classified as a K3 V star is 6 arc sec away (Jeffers & van den Bos 1963). The intrinsic light variability of V711 Tau was first reported by Cousins (1963).

Bopp & Fekel (1976) identified V711 Tau as an RS CVn type star and determined the physical parameters of the system. It is a non-eclipsing, double-lined spectroscopic binary (K1 IV + G5 V) with an orbital period $\sim$ 2.84 days. Fekel (1983) has found substantial differences in the rotational velocities and line strengths of the two components using Reticon observations with high signal to noise ratio. He has also found a correlation between the asymmetries in the absorption lines of the more massive, active, cool star and the photometric variations, and has derived improved physical parameters of

the system.

V711 Tau is known as a strong and variable radio source (Owen, Jones, & Gibson 1976) and also as a source of strong radio bursts (see the series of papers in *Astronomical Journal* **83**, No. 12, 1978). In addition to the radio emission, V711 Tau is found to emit both soft and hard X-rays (Walter, Charles & Bowyer 1978; White, Sanford & Weiler 1978).

Chromospheric and transition region emission lines, implying stellar surface fluxes of up to several hundred times the typical solar values, have been detected in the ultraviolet with *IUE* (Linsky 1984 and references therein). The ultraviolet observations indicate the presence of compact active regions.

Vogt & Penrod (1983) applied the Doppler Imaging Technique for the first time to V711 Tau in order to determine the position of photospheric spots and bright chromospheric regions by exploiting its high rotational velocity and fairly certain orbital inclination ($v \sin i \approx 40$ km s^{-1} and $i \approx 33^o$, Fekel 1983). Later Gondoin (1986) applied the same technique to photospheric absorption lines (*Fe I*) and chromospheric emission lines (*Ca II IR* and $H\alpha$) and found that on the surface of the primary both photospheric spots and bright solar-like chromospheric plages overlap. He also found that the location and extent of the active centres suggest the existence of strong magnetic flux at relatively high latitudes $\sim 60^o$.

Ramsey & Nations (1980) have spectroscopically established the existence of starspots, using 8860Å *TiO* band observations. Spectroscopic studies by several investigators (Simon & Linsky 1980; Fraquelli 1984; Nations & Ramsey 1986; Buzasi, Ramsey & Huenemoerder 1991) have indicated that V711 Tau shows evidences of strong, variable, and short-term $H\alpha$ activity. Recent spectroscopic analysis indicates that V711 Tau displays evidences of mass transfer (Buzasi, Ramsey & Huenemoerder 1991).

Zeeman-Doppler Imaging has given evidence of the presence of localized magnetic fields, thus providing spatial information regarding the seats of stellar activity centres in RS CVn stars (Donati et al. 1990).

Photometric observations of V711 Tau have been carried out by many observers (see the references given in Table 13). Perhaps V711 Tau is one of the few RS CVn stars that have got extensive and uninterrupted photometric

history since 1976. Photometry of V711 Tau has been discussed by many authors, notably by Dorren et al. (1981), Mekkaden, Raveendran & Mohin (1982), Bartolini et al. (1983), Rodono et al. (1986), and Strassmeier et al. (1989).

29. BV photometry

V711 Tau was observed on a total of 120 nights during the seven observing seasons 1984–85 (10 nights), 1985–86 (8 nights), 1986–87 (30 nights), 1987–88 (25 nights), 1988–89 (10 nights), 1989–90 (14 nights), and 1990–91 (23 nights). The visual companion ADS 2644B (K3 V) was included in all the measurements. The observations were made differentially with respect to the comparison star 10 Tau (= HR 1101, F9 V, V = 4.28 mag, $B-V$ = 0.58 mag) and were transformed to the Johnson's UBV system. Table 12 gives the differential magnitudes and colours for V711 Tau in the sense variable minus 10 Tau. The typical uncertainty in the measurements of the differential magnitudes and colours is $\sim$ 0.01 mag. The unpublished individual observations obtained during 1981–82 season (Mohin et al. 1982) are also given in Table 12. Each value in Table 12 is a mean of three to four independent measurements.

Recently Fekel (1983) has given the following spectroscopic ephemeris:

$$\text{JD (hel.)} = 2442763.952 + 2^d.83774\ \text{E}.$$

However, in the present analysis to convert the Julian days of observation into orbital phases we have used the ephemeris of Bopp & Fekel (1976):

$$\text{JD (hel.)} = 2442766.069 + 2^d.83782\ \text{E},$$

since it is this ephemeris that is used in most of the data analysis presented in literature. The zero phase corresponds to conjunction with the more active K-subgiant in front and the period is the spectroscopic orbital period.

30. Light curves

The observations obtained during the seasons 1986–87, 1987–88, 1989–90, and 1990–91 are plotted in Figs 38–41. The mean epochs of observation are indicated in each figure. The observations obtained during

Table 12. Differential magnitudes and colours of V711 Tau

J.D. (Hel) 2440000.+	ΔV	$\Delta(B-V)$	J.D. (Hel) 2440000.+	ΔV	$\Delta(B-V)$
		1981–82 Observing Season			
4973.1826	1.447	.385	5017.1169	1.497	.368
4984.2340	1.468	.377	5018.1019	1.467	.387
4985.2009	1.527	.373	5018.1405	1.439	.372
4986.2120	1.527	.381	5019.1302	1.440	.368
4987.2038	1.433	.403	5021.1255	1.424	.367
4990.2144	1.425	.364	5022.1279	1.463	.397
4991.2170	1.500	.382	5024.1122	1.391	.375
4992.2390	1.508	—	5025.1368	1.466	.387
4999.1822	1.463	.359	5026.1333	1.467	.394
5000.1582	1.491	.352	5027.1392	1.412	.375
5002.1701	1.471	.403	5028.1323	1.490	.352
5004.2045	1.441	.354	5029.1194	1.497	—
5005.0875	1.485	.394			
5014.1271	1.513	.380			
5015.1411	1.508	.356			
		1984–85 Observing Season			
6051.2615	1.353	.386	6083.2310	1.377	—
6052.2524	1.457	.355	6087.1817	1.491	.331
6054.2362	1.431	.369	6088.3705	1.393	.341
6055.2800	1.498	.355	6090.1939	1.504	.348
6056.2346	1.540	.352	6094.0984	1.366	.359

Table 12. continued

J.D. (Hel) 2440000.+	ΔV	$\Delta(B-V)$	J.D. (Hel) 2440000.+	ΔV	$\Delta(B-V)$
		1985–86 Observing Season			
6468.0966	1.491	.343	6474.1072	1.489	.345
6468.1126	1.496	.328	6475.1108	1.432	.351
6471.1723	1.473	—	6476.1209	1.498	—
6471.1789	1.450	—	6506.1008	1.427	—
6472.0868	1.455	.332	6506.1122	1.440	—
6472.1080	1.440	.345			
		1986–87 Observing Season			
6800.2295	1.506	—	6824.2344	1.452	—
6801.2028	1.495	—	6825.1949	1.470	.331
6801.2361	1.490	.333	6825.2220	1.456	—
6801.2529	1.496	.336	6827.1826	1.444	—
6802.2481	1.471	.322	6828.1271	1.484	—
6803.2501	1.497	.313	6829.1268	1.470	—
6803.2674	1.496	.310	6830.1739	1.442	.323
6804.1770	1.476	.328	6831.2020	1.488	—
6816.1941	1.437	—	6832.1510	1.479	.330
6817.2065	1.500	—	6832.1700	1.478	.322
6818.1829	1.480	—	6833.1203	1.427	—
6819.1811	1.437	.330	6835.0898	1.471	.325
6820.1861	1.488	.337	6836.0927	1.429	.327
6821.1555	1.501	—	6847.1174	1.439	.333
6823.2257	1.464	.322	6850.1375	1.437	.324

Table 12. continued

J.D. (Hel) 2440000.+	ΔV	$\Delta(B-V)$	J.D. (Hel) 2440000.+	ΔV	$\Delta(B-V)$
		1986–87 continued			
6851.1340	1.504	.331	6861.1166	1.453	—
6852.1361	1.476	.325	6862.1370	1.494	—
6860.0944	1.473	.326			
		1987–88 Observing Season			
7157.0878	1.529	.351	7203.1573	1.530	.339
7176.1877	1.501	.350	7204.1308	1.492	.350
7178.2149	1.486	.337	7205.1220	1.522	.373
7179.2051	1.508	.350	7206.1028	1.518	.350
7183.1171	1.527	.357	7207.0914	1.494	.350
7184.2170	1.481	.360	7208.1213	1.519	.350
7185.1299	1.518	.340	7217.0983	1.523	.353
7196.1695	1.515	.353	7220.0927	1.526	.350
7197.1599	1.538	.343	7230.1128	1.489	.350
7198.0985	1.497	.350	7231.1316	1.533	.332
7200.1361	1.532	.342	7232.1385	1.481	.344
7201.1487	1.497	.339	7233.1345	1.499	.391
7202.1040	1.515	.344			

Table 12. continued

J.D. (Hel) 2440000.+	ΔV	$\Delta(B-V)$	J.D. (Hel) 2440000.+	ΔV	$\Delta(B-V)$
		1988–89 Observing Season			
7530.2771	1.485	—	7560.1645	1.515	.328
7556.1457	1.526	.323	7561.1728	1.466	.340
7557.1590	1.508	.323	7564.1615	1.474	.328
7558.1461	1.485	.332	7572.0993	1.521	.331
7559.1668	1.546	.324	7573.1363	1.519	.333
		1989–90 Observing Season			
7852.3223	1.479	.332	7912.2406	1.450	.326
7853.2548	1.428	.322	7913.1199	1.401	.337
7854.2557	1.511	.325	7914.1637	1.521	—
7855.2955	1.465	.331	7915.1755	1.432	.329
7856.2702	1.428	.327	7916.1580	1.437	.324
7867.3277	1.419	.334	7917.1477	1.497	.330
7878.2829	1.442	.315	7918.1506	1.445	.329
		1990–91 Observing Season			
8279.1963	1.485	—	8299.1111	1.488	.328
8280.1142	1.531	.319	8300.1172	1.533	.348
8296.2181	1.482	.339	8301.1420	1.531	.347
8297.1464	1.521	.339	8302.1198	1.484	.350
8298.1352	1.559	.332	8303.1152	1.546	.343

Table 12. continued

J.D. (Hel) 2440000.+	ΔV	$\Delta(B-V)$	J.D. (Hel) 2440000.+	ΔV	$\Delta(B-V)$
		1990−91 continued			
8305.1473	1.487	.337	8330.1098	1.506	.305
8306.1394	1.534	.344	8331.0869	1.513	.340
8325.1406	1.517	.297	8332.0892	1.540	.330
8326.1363	1.557	.323	8333.0876	1.498	.336
8327.1236	1.504	.333	8334.0863	1.512	.325
8328.1167	1.519	.328	8335.0937	1.536	.364
8329.1308	1.555	.315			

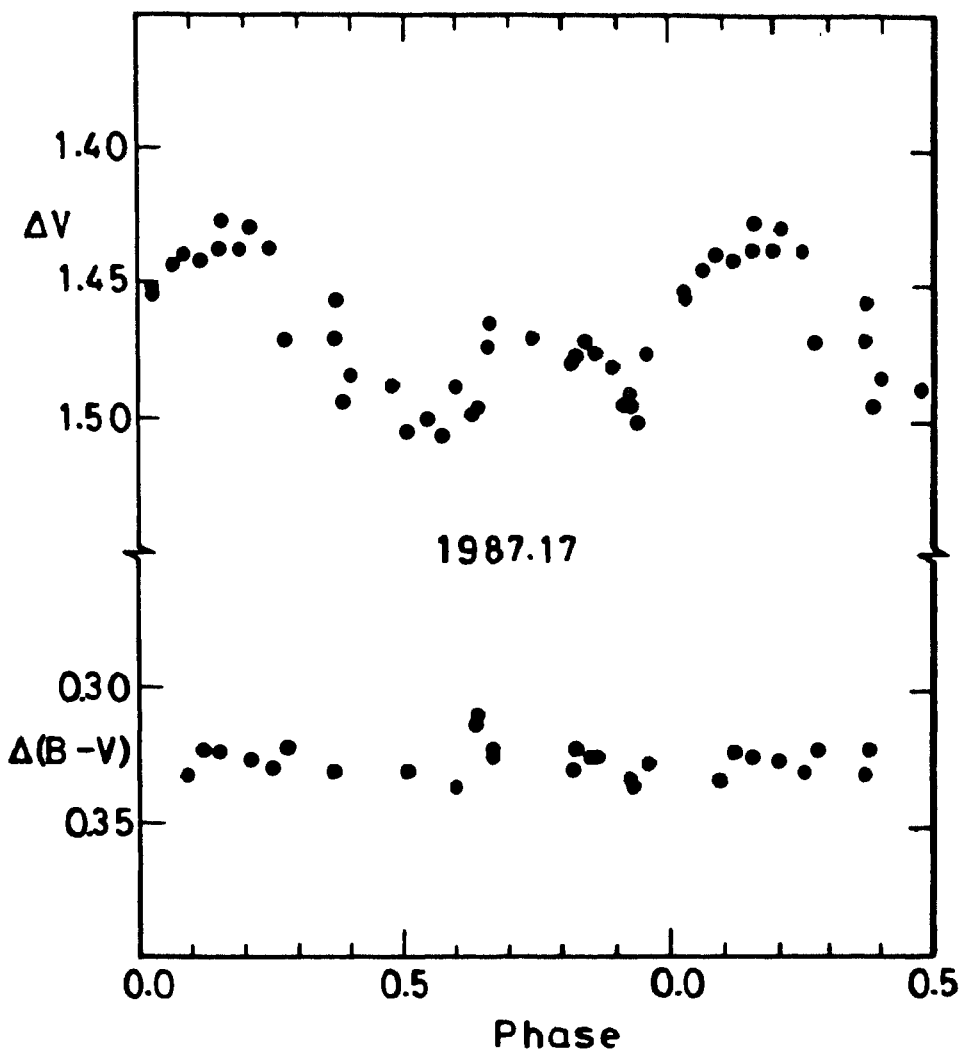

Figure 38. The 1987.17 V and $B-V$ curves of V711 Tau. Phases are reckoned from JD (Hel.) 2442766.069 using the period $2^d.83782$.

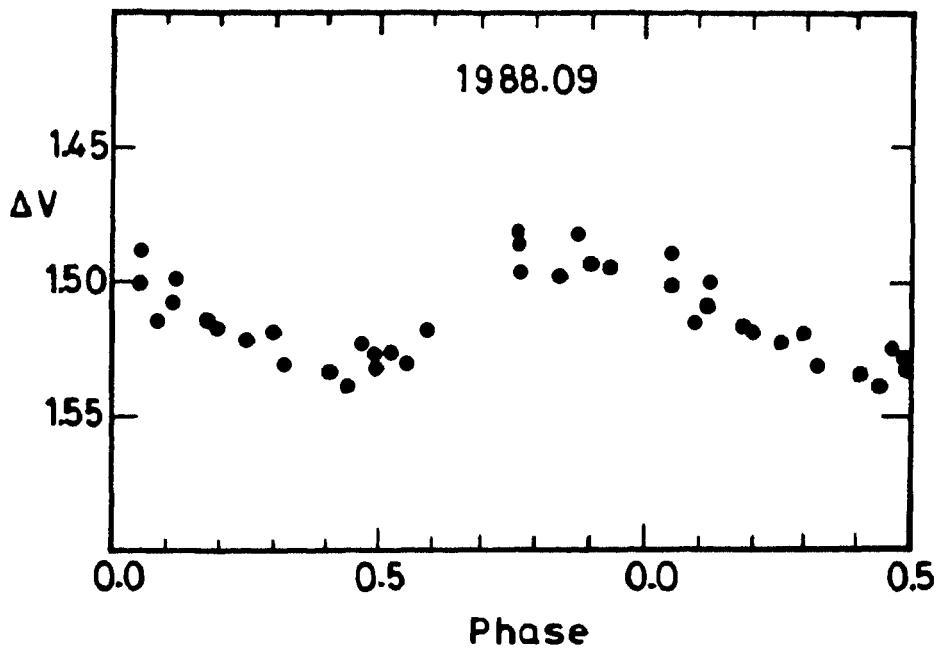

Figure 39. The 1988.09 light curve of V711 Tau. Phases are reckoned as in Fig. 38.

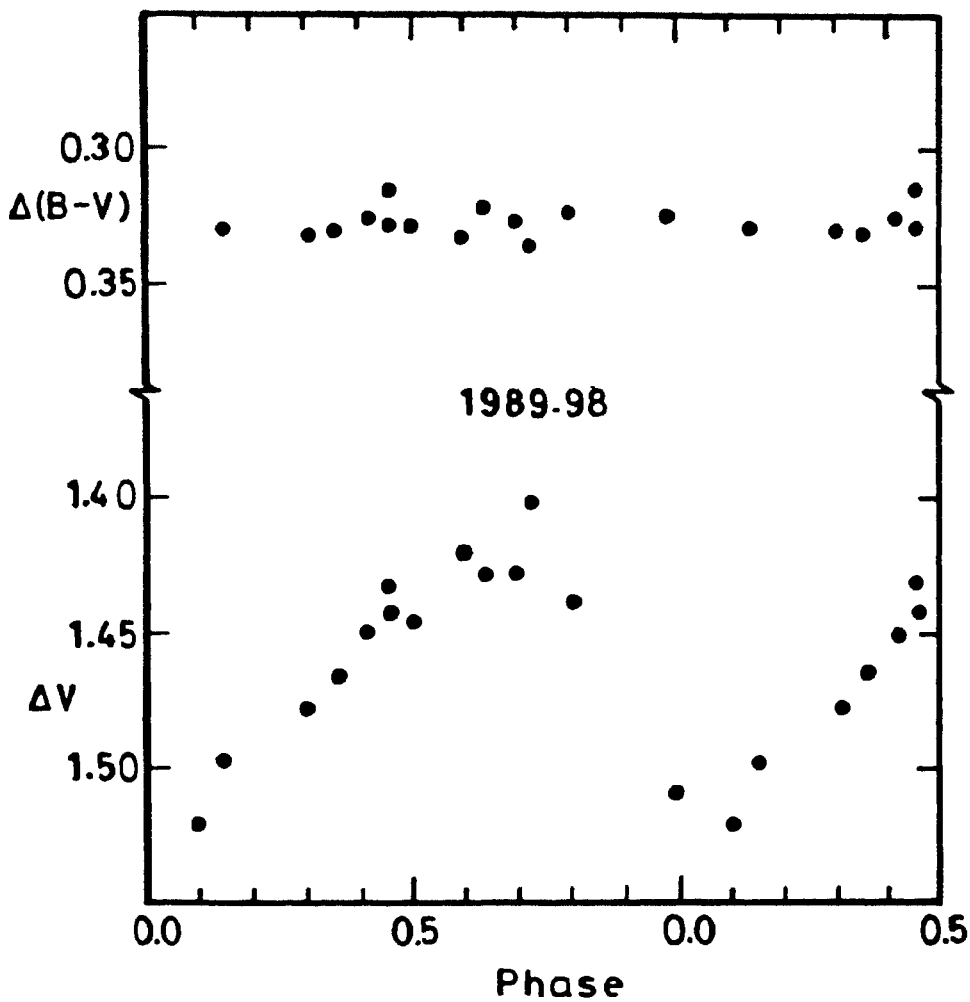

Figure 40. The 1989.98 V and $B - V$ curves of V711 Tau. Phases are reckoned as in Fig. 38.

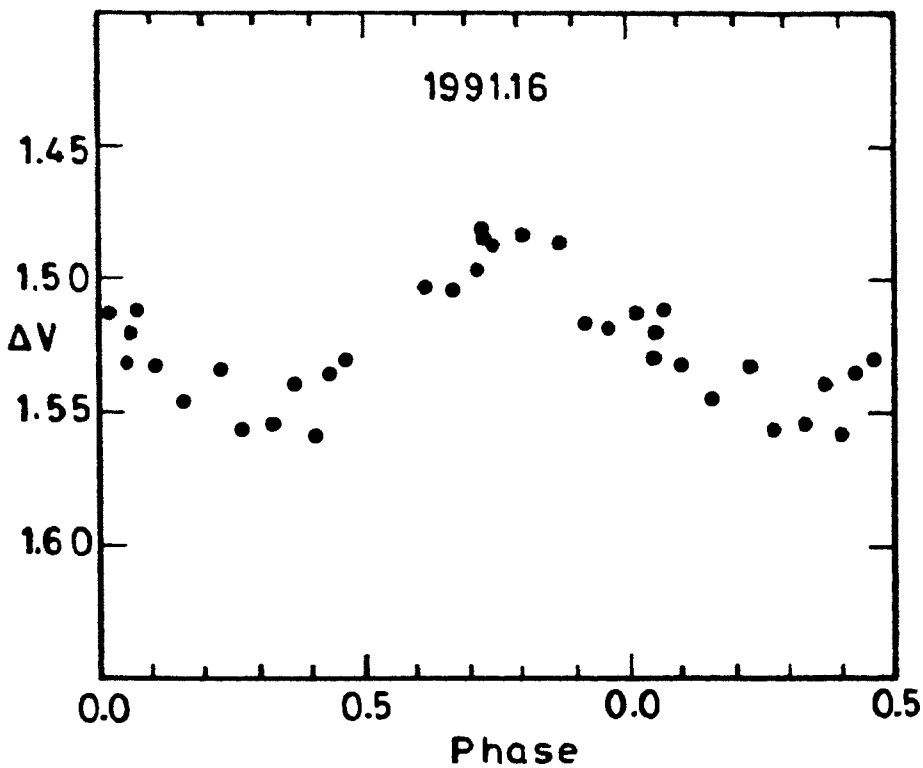

Figure 41. The 1991.16 light curve of V711 Tau. Phases are reckoned as in Fig. 38.

1986−87 season (Fig. 38) show that the shape of the light curve has undergone remarkable changes from an almost sinusoidal shape as found during the previous season by Strassmeier et al. (1989). The light curve given in Fig. 38 is double-peaked with the minima occuring at $\sim 0^p.50$ and $\sim 0^p.90$. The amplitude is ~ 0.08 mag, and ΔV_{max} is nearly the same as that of 1985−86 season, where as ΔV_{min} is brighter by ~ 0.10 mag.

The 1987−88 season's observations show that the light curve (Fig. 39) has become nearly sinusoidal and the amplitude has further reduced to $\sim$ 0.05 mag and that the minimum occurs $\sim 0^p.43$. There is a decrease of ~ 0.05 mag in the mean light level when compared to that of the previous season.

In Fig. 40 we have plotted the observations obtained during 1989−90 season. The figure shows that the star's mean V magnitude has increased by ~ 0.05 mag from that of the previous season and the amplitude of light variation has increased to ~ 0.12 mag. The light curve is asymmetric with a slow rise and sudden fall. Both the maximum and minimum of the light curve are very clearly defined and occur at $\sim 0^p.68$ and $\sim 0^p.07$ respectively.

The light curve obtained during the 1990−91 season is plotted in Fig. 41. It is similar to the light curve of 1987−88 season in mean light level. However, the values of ΔV_{max} and ΔV_{min} are ~ 1.484 mag and ~ 1.60 mag respectively, and occur at phases $0^p.79$ and $0^p.33$.

Figs 38 and 40 which also contain the corresponding $B - V$ colours clearly illustrate that there is no significant correlation of the colour with the light variation.

The photometric properties derived from the present observations together with those compiled from various sources are listed in Table 13. For a few light curves which show a reasonably sinusoidal nature the phases of the light minima were determined by fitting the truncated Fourier series,

$$L = A_0 + A_1 cos\theta + A_2 cos2\theta + B_1 sin\theta + B_2 sin2\theta,$$

where θ is the photometric phase, and A_0, A_1, A_2, B_1 and B_2 are the Fourier coefficients. For other light curves the light minima were taken from the respective graphs. The amplitude of the light variation given in Table 13 is the difference between the values of ΔV_{max} and ΔV_{min}, the brightness at

Table 13. Photometric characteristics of V711 Tau

Epoch	Amplitude	ΔV_{max}	ΔV_{min}	Phase Min	References
1975.85	0.095	1.525	1.620	0.59±0.15	Bopp et al. (1977)
1975.95	0.115	1.490	1.605	0.63±0.05	Bopp et al. (1977)
1976.02	0.135	1.465	1.595	0.63±0.05	Bopp et al. (1977)
1976.13	0.090	1.495	1.585	0.54±0.07	Bopp et al. (1977)
1976.76	0.115	1.495	1.610	0.57±0.07	Landis et al. (1978)
1976.91	0.120	1.500	1.620	0.63±0.05	Landis et al. (1978)
1977.14	0.115	1.495	1.610	0.55±0.11	Parthasarathy et al. (1981)
1977.72	0.110	1.500	1.610	0.60±0.07	Bartolini et al. (1978)
1978.00	0.085	1.505	1.590	0.70±0.10	Bartolini et al. (1978)
1978.18	0.072	1.520	1.592	0.72±0.08	Chambliss et al. (1978)
1978.91	0.190	1.460	1.650	0.89	Bartolini et al (1983)
1979.08	0.200	1.440	1.640	0.90±0.01	Sarma & Ausekar (1980)
1979.11	0.210	1.440	1.650	0.91±0.01	Bartolini et al (1983)
1979.15	0.210	1.415	1.625	0.91±0.06	Chambliss & Detterline (1979)
1979.88	0.140	1.450	1.590	0.95±0.01	Bartolini et al. (1983)
1979.91	0.140	1.460	1.600	0.94±0.01	Bartolini et al. (1983)
1979.94	0.140	1.450	1.590	0.99±0.01	Bartolini et al. (1983)
1979.96	0.120	1.490	1.610	0.96±0.01	Bartolini et al. (1983)
1979.98	0.170	1.430	1.600	0.92±0.07	Mekkaden et al. (1982)
1980.00	0.160	1.470	1.630	0.97±0.01	Sarma & Ausekar (1981)

Table 13. continued

Epoch	Amplitude	ΔV_{max}	ΔV_{min}	Phase Min	References
1980.13	0.120	1.450	1.570	0.93±0.02	Bartolini et al. (1983)
1980.14	0.155	1.440	1.595	0.86±0.07	Mekkaden et al. (1982)
1980.73	0.050	1.500	1.550	0.06	Bartolini et al. (1983)
				0.53	
1980.82	0.060	1.490	1.550	0.05	Bartolini et al. (1983)
				0.50	
1980.97	0.075	1.490	1.565	0.05	Bartolini et al. (1983)
				0.50	
1981.04	0.040	1.520	1.560	0.10	Bartolini et al. (1983)
				0.48	
1981.05	0.053	1.542	1.595	0.02±0.08	Mekkaden et al. (1982)
				0.53±0.07	
1981.15	0.085	1.530	1.615	0.12±0.08	Mekkaden et al. (1982)
				0.43±0.05	
1981.19	0.090	1.490	1.580	0.42	Bartolini et al. (1983)
1981.73	0.104	1.510	1.614	0.35±0.05	Rodono et al. (1986)
1981.78	0.100	1.500	1.600	0.30±0.05	Rodono et al. (1986)
1981.91	0.086	1.504	1.590	0.25±0.10	Rodono et al. (1986)
1982.08	0.136	1.391	1.527	0.38±0.04	Mohin et al. (1982)
1983.04	0.055	1.485	1.540	0.33±0.01	Andrews et al. (1988)

Table 13. continued

Epoch	Amplitude	ΔV_{max}	ΔV_{min}	Phase Min	References
1984.00	0.136	1.373	1.509	0.36	Strassmeier et al. (1989)
1985.00	0.167	1.364	1.531	0.33	Strassmeier et al. (1989)
1986.00	0.167	1.423	1.590	0.41	Strassmeier et al. (1989)
1986.80	0.100	1.440	1.540	0.50±0.01	Mekkaden (1987)
				0.80±0.10	
1987.17	0.079	1.427	1.506	0.50±0.06	Present Study
				0.89±0.06	
1988.09	0.052	1.481	1.533	0.43±0.02	Present Study
1989.11	—	—	—	0.47±0.05	Present Study
				0.03±0.05	
1989.98	0.120	1.401	1.521	0.07±0.01	Present Study
1991.16	0.075	1.484	1.559	0.33±0.01	Present Study

light maximum and minimum.

31. Mean light level

In Fig. 42 we have plotted the mean light level of the system calculated from

$$\text{mean } \Delta V = (\Delta V_{max} + \Delta V_{min}) \ / \ 2$$

against the corresponding mean epoch of observations. It is interesting to see from the diagram that the mean light level of the system during the period 1975−82 was fainter by $\sim$ 0.05 mag than that during the period 1982−91. It can be seen that this significant change in the mean light level of the system occurred during a very short period. Observations obtained around the epoch 1981.91 show a mean brightness of $\sim$ 1.55 mag, whereas those obtained around the epoch 1982.08 indicate a mean brightness $\sim$ 1.47 mag (Mohin et al. 1982; Rodono et al. 1986). Here we note that the mean quiescent *uv* emission level of V711 Tau observed around the epoch 1983 was higher than that observed at ealier epochs. For example the 1983 *CIV* emission line flux was 30 % brighter than 1978 (Andrews et al. 1988). The mean light level during 1982−91 shows a rather erratic variation when compared to that seen during 1975−82. The change in the mean light level probably arises from a global reduction in the area of spots or from the diappearence of spots from the polar region.

32. Brightness at light maximum and minimum

From an analysis of the brightness at light maximum and light minimum, based on the then available data, Mekkaden, Raveendran & Mohin (1982) found that the brightness of V711 Tau at light minimum is nearly constant and that an increase in the amplitude is directly related to an increase in the brightness at light maximum. From this they argued that the hemisphere of the active component visible at light minimum is always saturated with spots and that an increase in amplitude of light variation is a consequence of the disappearance of spots from the hemisphere visible at light maximum. Later from more extended observational data Bartolini et al. (1983) found

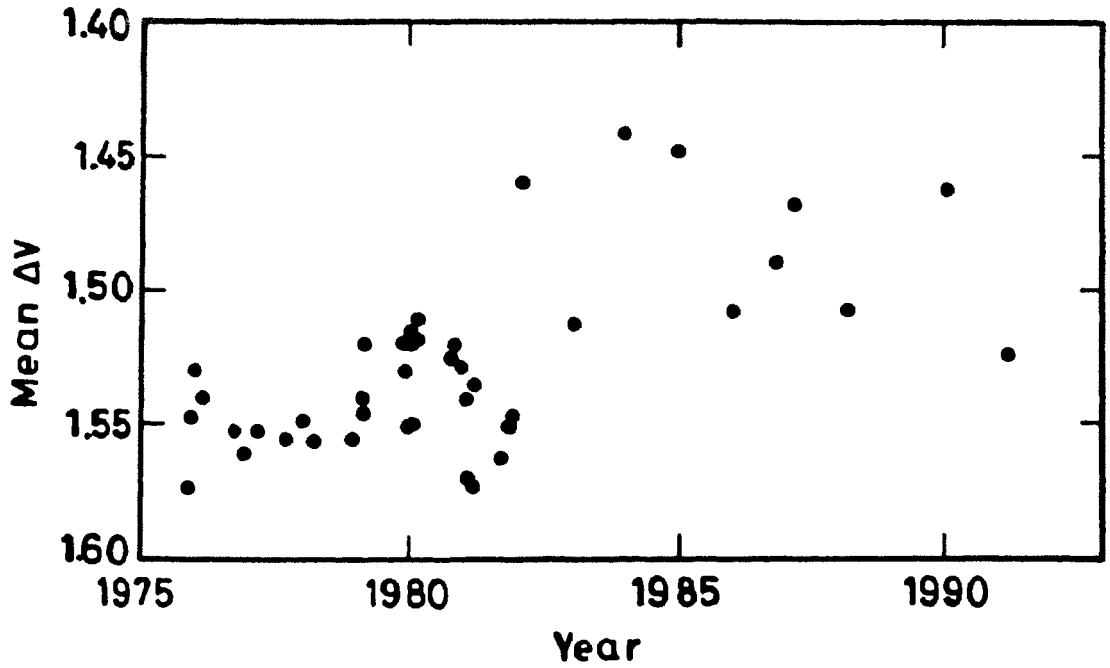

Figure 42. Plot of mean ΔV against the corresponding mean epoch of observation.

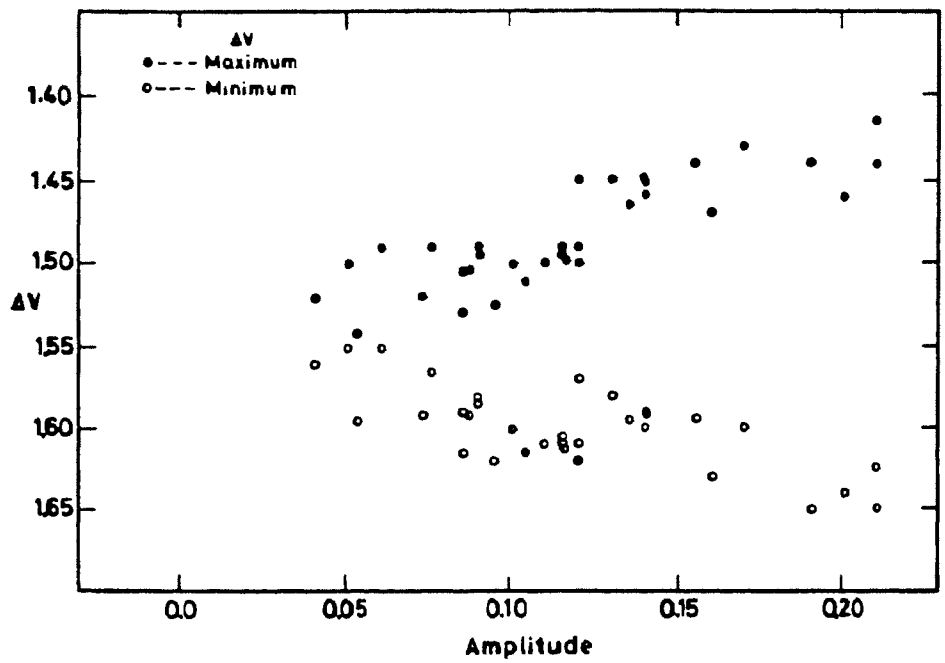

Figure 43. Plot of the brightness at light maximum (filled circles) and light minimum (open circles) against the V amplitude during the period 1975–81.

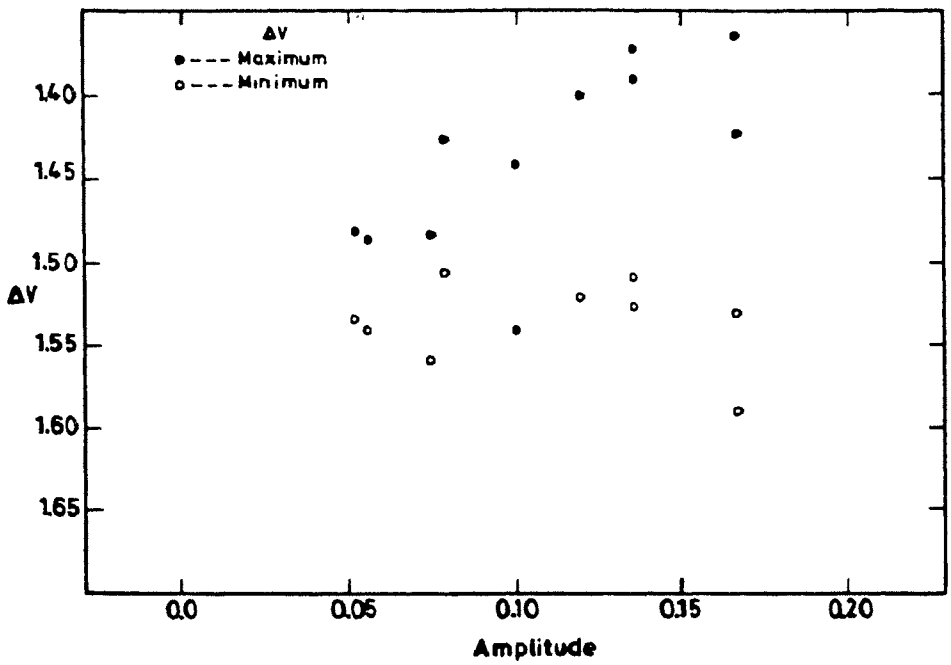

Figure 44. Plot of the brightness at light maximum (filled circles) and light minimum (open circles) against the V amplitude during the period 1982–91.

that in V711 Tau the brightness at both light maximum and light minimum is variable.

In the light of the results presented in Fig. 42, we have divided the data in two groups representing two different periods, one covering from 1975−81 and the other from 1982−91, and in Figs 43 and 44 we have plotted the ΔV_{max} and ΔV_{min} against the corresponding amplitudes for the two periods.

An inspection of Fig. 43 reveals that at larger amplitudes the brightness at minimum decreases and the brightness at maximum increases and both of them converge to $\Delta V \sim 1.55$ mag at very low amplitudes as seen in the case of UX Ari (Chapter 7). This indicates, qualitatively, the following: (i) At lower amplitudes spots are evenly distributed in longitudes and are predominantly present at higher latitudes and hence are seen through out the rotational period. (ii) At higher amplitudes spots are more concentrated about some longitude and are predominantly at lower latitudes and hence disappear from the field of view during the rotational period. More over Fig. 43 indicates that probably there is no substantial change in the total spotted area on the surface of the star during the period 1975−81 since the gain or loss in ΔV_{max} is more or less compensated by the same amount in ΔV_{min} when the amplitude increases or decreases.

We meet probably a similar situation from Fig. 44. The dataset for 1982−91 is limited, making it difficult to draw firm conclusions. The increase in ΔV_{max} with increase in amplitude of the light curve is very obvious, whereas the variation in ΔV_{min} with the amplitude is not that apparent; in fact ΔV_{min} appears more or less constant with a mean value of $\sim \Delta V = 1.52$. The 1986 observations of Strassmeier et al. (1989) stand alone. Most likely, the situation here is similar to what Mekkaden, Raveendran, & Mohin (1982) faced in their analysis from a limited data series.

33. Phase of light minimum and amplitude

The evolution of starspots in RS CVn systems is usually analysed from the temporal behaviour of the phase of light minimum (ϕ_{min}) and amplitude of light variation. We have plotted the ϕ_{min} and V amplitude given in Table

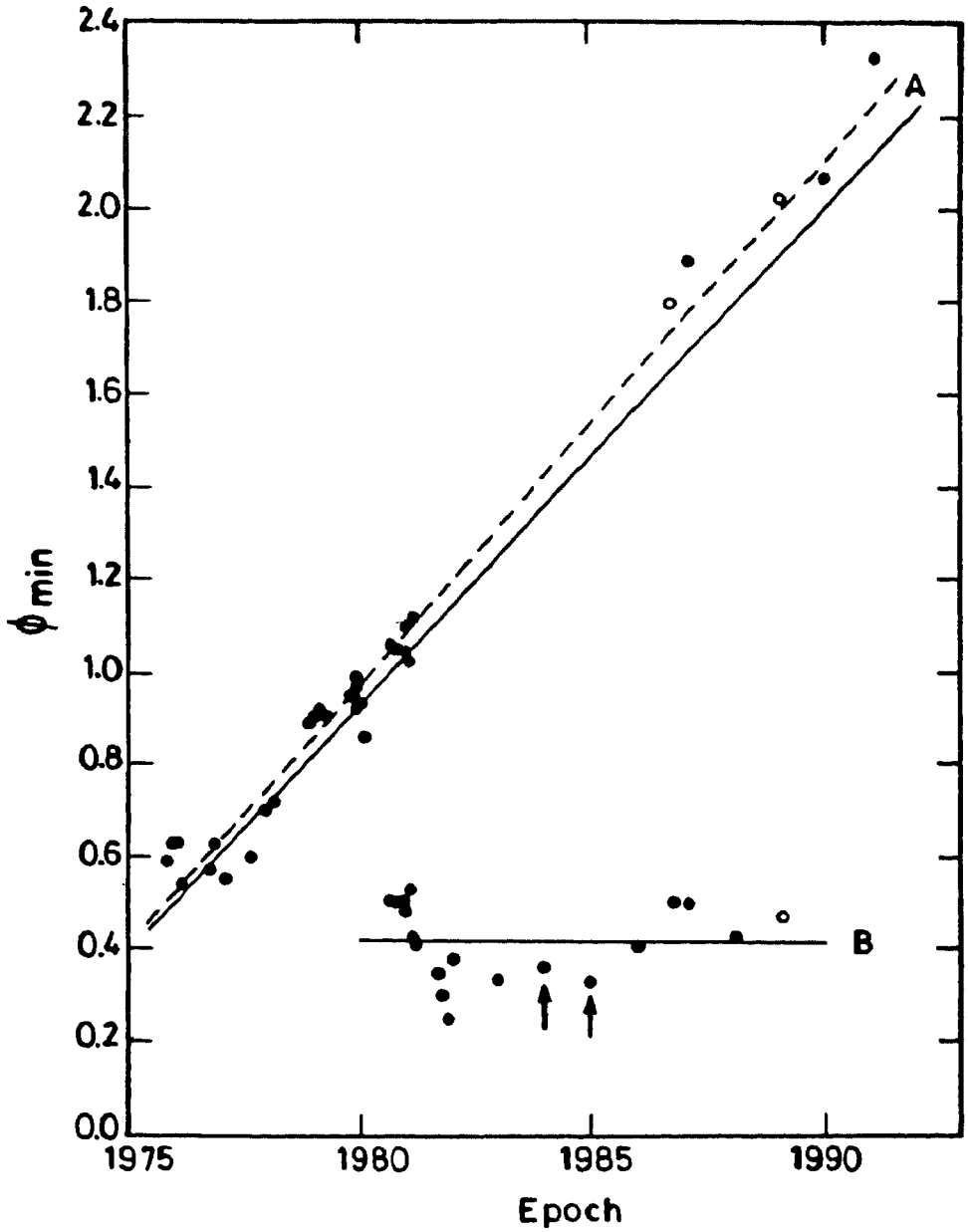

Figure 45. Plot of the phase of light minimum versus mean epoch of observation.

13 against the corresponding mean epoch of observation in Figs 45 and 46 respectively. The phases of shallow minima are indicated by open circles in Fig. 45.

The minimum (group A) observed in 1975 can be traced to about 1981 nearly continuously. Just before this minimum disappeared (or became less prominent) almost in the opposite longitude another centre of activity (group B) was formed which could be traced upto about 1985 unambiguously. On most occasions during the period 1986–90 two light minima could be identified in the light curves. It appears that one group of minima is a continuation of the minimum (group B) seen from 1981 onwards, and the other group lies close to the positions expected if the minimum (group A) observed from 1975 had continued. Group B has a slope close to zero indicating that the corresponding photometric period is very close to the assumed orbital period. The migration of the other minima is a result of the difference in the photometric and orbital periods. The migration of the minima seen during 1975–80 indicates a rotation period of 2.84007 ± 0.00009 days (continuous line), and when we include the minima seen after 1986 also we arrive at a photometric period of 2.84036 ± 0.00005 days (dotted line). The shallow minima are not included in the least square solutions.

The minima observed around 1984–85 which occur $\sim 0^p.4$ and plotted as part of group B (indicated by arrows in Fig. 45) could be part of the group A minima as well. The presence of single minima in the light curve does not necessarily imply that there is only one centre of activity. It indicates the longitude of the predominant spot group. The light curve obtained during 1986–87 shows two minima, one $\sim 0^p.5$ and the other $\sim 0^p.8$, whereas the next season's light curve shows only one minimum centred $\sim 0^p.43$. The brightness at the light maximum of the later light curve is nearly the same as the brightness at the light minimum at $0^p.8$ of the former light curve.

The two groups of minima lie on two independent near-straight lines, implying that spots are confined predominantly to two different latitude belts. It is likely that the centre of activity corresponding to the minimum first observed in 1975 (group A), probably with varying extent of spots has continued to exist at least till the last observing season. This indicates a life

span of more than 15 years for the centre of activity. If it had ceased to exist in between, say after about 1982, then the appearence of light minima after 1986 close to the positions expected from an extrapolation of earlier positions would mean the reappearence at the initial longitude of occurrence implying a preferred longitude also.

From the results of Doppler Imaging Techniques applied to UX Ari, Vogt & Hatzes (1991) have argued that the equtorial regions in the active component are synchronized to the orbital motion and that higher latitudes rotate faster than the equatorial regions, contrary to what is observed in the sun. The photometric period for group B is close to the orbital period indicating near synchronization at the latitude corresponding to that spot group. For the other group the period is larger than the orbital period indicating a slower rotation. If the results obtained for UX Ari hold in the case of V711 Tau, we would expect the photometric period to be either equal to or less than the orbital period. In the case of V711 Tau the photometric results do not indicate that there are latitudes which rotate faster than the synchronous latitudes, and that if equatorial regions are synchronized higher latitude regions rotate slower than the equatorial regions.

Amplitude of the light curve is an important parameter which reflects the longitudinal distribution of spots. The changes in the amplitude can result either from (i) a change in the size of the spot and its temperature, or (ii) due to a longitudinal redistribution of the spots on the stellar surface, or (iii) due to the occurrence of spots predominantly at higher latitudes. An inspection of Fig. 46 reveals that the light curve amplitudes are highly variable and show a cyclic behaviour with a period of about 3 years. It is also found that substantial changes in the amplitude can occur in as short as a few orbital cycles. The change from larger to smaller amplitude is followed at times with the appearence of two minima. Largest amplitudes so far observed was during 1979 when the system's ΔV_{min} was also at its minimum value reported to date. The highest ΔV_{max} observed so far is 1.364 mag (during the 1985–86 period). The ΔV_{max} observed during 1979 was 1.44 mag considerably fainter than the highest ΔV_{max} observed so far indicating that spots were seen through out the light phase and never disappeared from

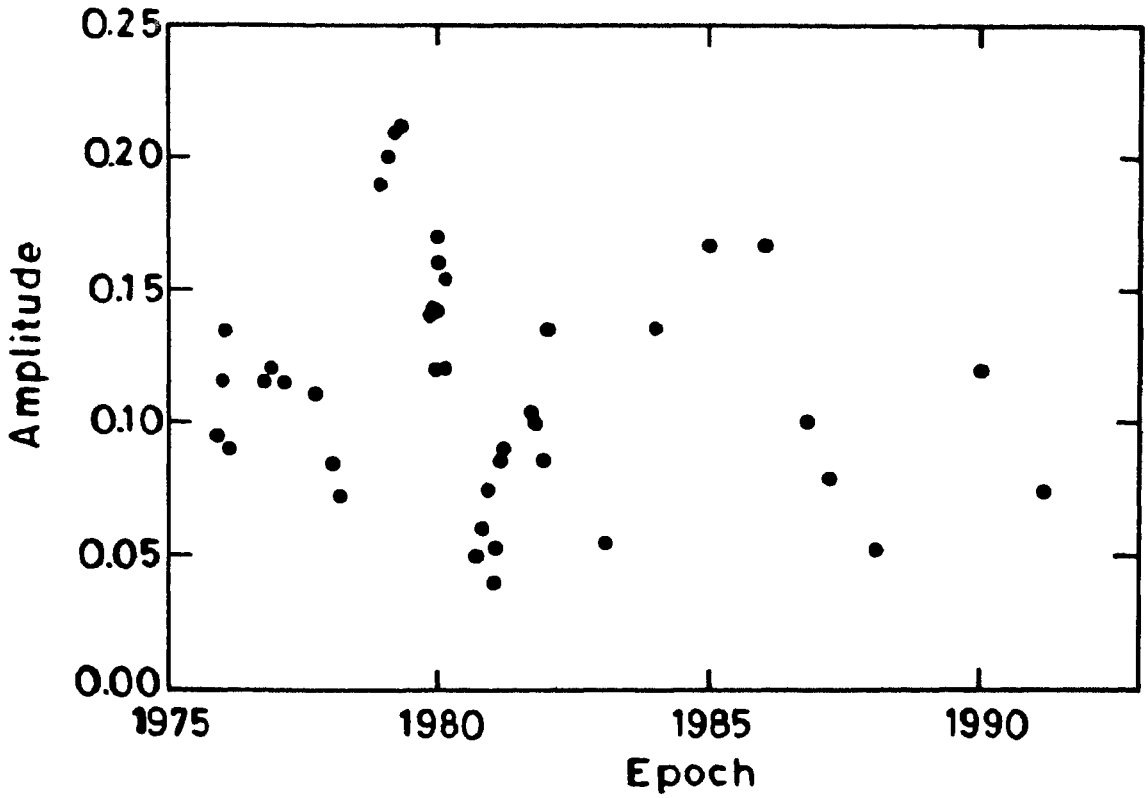

Figure 46. Plot of V amplitude against the mean epoch of observation.

the view even at the epochs of the highest amplitudes so far observed.

34. $H\alpha$ observations

$H\alpha$ region spectra of V711 Tau were obtained on a total of 14 nights during the 1990−91 observing season. Table 14 gives the log of observations; it contains Julian day of observation along with $H\alpha$ emission equivalent width (EW1), full width at half maximum of $H\alpha$ emission (FWHM), height of the $H\alpha$ emission in terms of F_λ/F_c, photometric phase reckoned from the ephemeris of Bopp & Fekel (1976), and the equivalent width EW2. The computations of EW1 and EW2 were done as described in Chapter 2.

The results of $H\alpha$ observations are plotted in Figs 47−50, which show that the emission is variable and there is no correlation either with the photometric or with the orbital phases. The average values of EW1 and FWHM are $\approx$ 0.87 Å and $\approx$ 3.66 Å respectively and are comparable to the mean values obtained by Bopp & Talcott (1978) from the observations spanning a rather long period, 1975−78. They found that the variation in equivalent width is $\approx$ 50% over intervals of several days and were probably not related to flare events. The mean equivalent width obtained by them is $\approx$ 0.8 Å.

The equivalent width of $H\alpha$ emission appears to be uncorrelated with either the amplitude, or ΔV_{max}, or ΔV_{min} of the light curves. The light curve during 1975−78 is quite normal with an amplitude about 0.10 mag, with ΔV_{max} about 1.50 mag and ΔV_{min} about 1.60 mag, where as 1990−91 light curve shows a smaller amplitude of 0.075 mag with ΔV_{max} and ΔV_{min} of 1.484 and 1.559 mag respectively. The average values of the $H\alpha$ emission EW and FWHM obtained by Nations & Ramsey (1986) during 1981 (Mar, Sept, Oct, and Nov) shows 1.2 Å and 3.9 Å respectively. The light curve obtained during this period shows an amplitude about 0.10 mag with ΔV_{max} about 1.50 mag and ΔV_{min} about 1.60. The mean light level of the system during 1990−91 observing season is brighter by about 0.03 mag than that of 1975−78 and 1981 seasons.

If the extensive starspot activity on the surface of the active component is analogues to what is observed in the sun, then a strong correlation is expected between the chromospheric activity and the light variability. If

Table 14. *Hα* data of V711 Tau

Date	JD 2440000.+	Phase	EW1 Å	FWHM Å	Height	EW2 Å
10 Oct 1990	8175.4521	0.176	0.90	4.51	0.21	−0.22
11 Oct 1990	8176.4944	0.543	0.71	3.04	0.23	−0.74
23 Nov 1990	8219.3264	0.636	1.09	3.47	0.28	+0.17
28 Nov 1990	8224.3451	0.405	0.82	2.96	0.27	−0.27
28 Nov 1990	8224.3854	0.419	0.77	2.99	0.27	−0.50
29 Nov 1990	8225.3333	0.753	1.00	3.24	0.27	−0.19
30 Nov 1990	8226.3486	0.111	1.03	5.36	0.21	+0.03
30 Nov 1990	8226.3833	0.123	1.01	5.37	0.20	−0.03
07 Jan 1991	8264.2167	0.455	1.03	4.36	0.21	−0.08
07 Jan 1991	8264.2715	0.474	0.93	4.29	0.22	−0.31
08 Jan 1991	8265.1917	0.798	0.96	3.35	0.28	+0.07
08 Jan 1991	8265.2840	0.831	0.83	2.91	0.29	−0.46
06 Feb 1991	8294.2153	0.026	0.25	2.88	0.12	−0.99
06 Feb 1991	8294.2389	0.034	0.28	3.14	0.11	−0.77
07 Feb 1991	8295.1882	0.369	1.22	3.98	0.30	+0.24
07 Feb 1991	8295.2118	0.377	1.16	3.96	0.30	+0.14
08 Feb 1991	8296.1847	0.720	0.81	3.80	0.24	−0.21
06 Mar 1991	8322.1361	0.865	0.72	2.68	0.26	−0.88
08 Mar 1991	8324.1306	0.567	0.91	3.18	0.27	−0.85

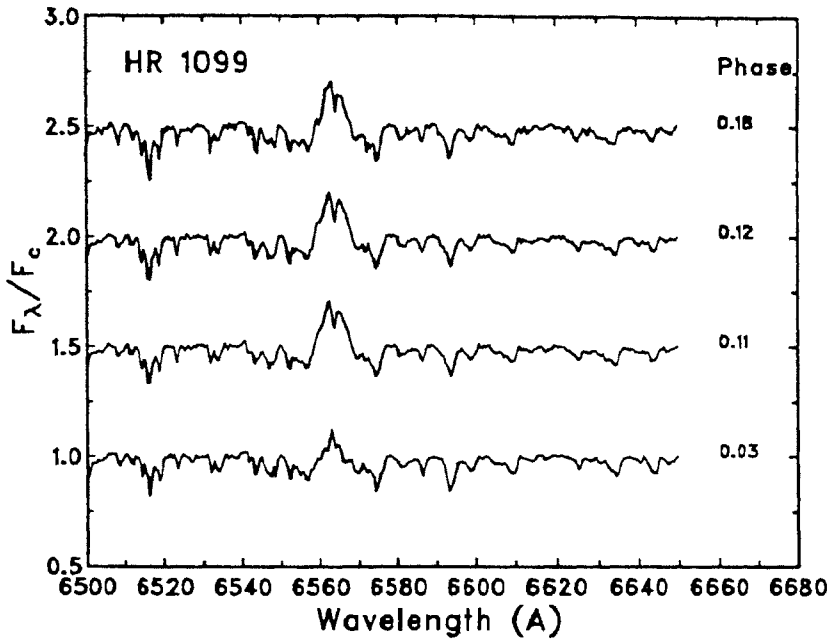

Figure 47. $H\alpha$ spectra of V711 Tau. The spectra are adjusted on the rest wavelength of $H\alpha$. Each spectrum is normalized to continuum and shifted by 0.5. Phases are reckoned as in Fig. 38.

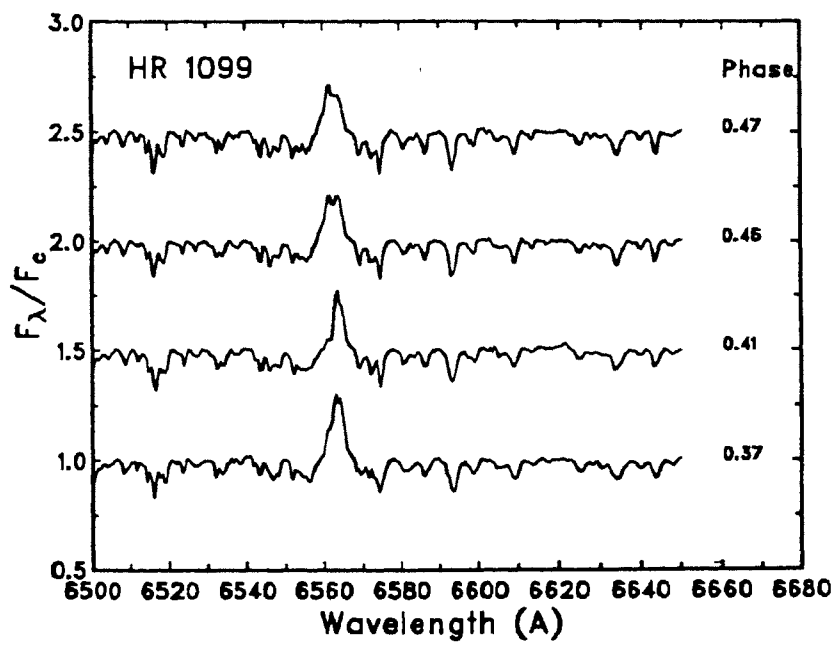

Figure 48. $H\alpha$ spectra of V711 Tau. The descriptions are as in Fig. 47.

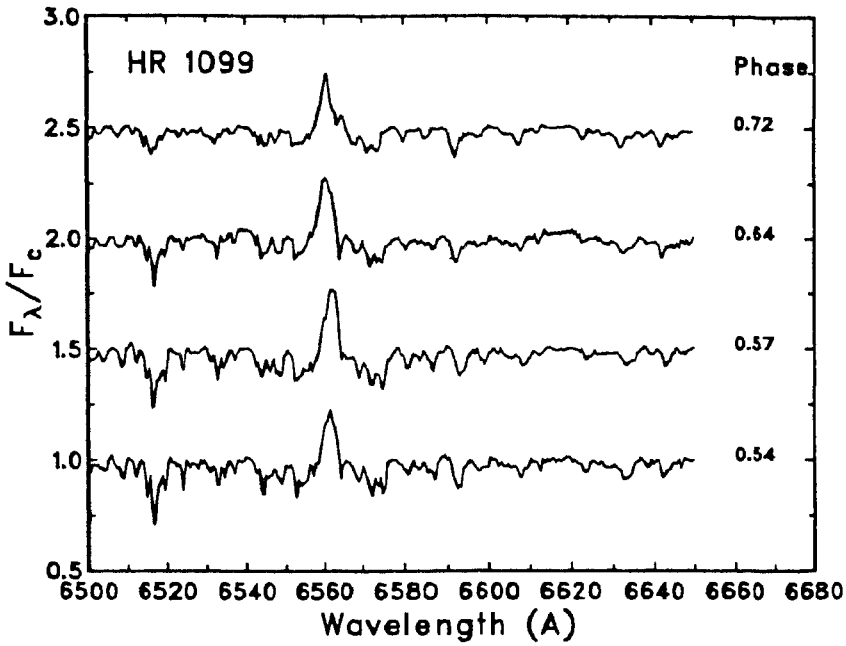

Figure 49. *Hα* spectra of V711 Tau. The descriptions are as in Fig. 47.

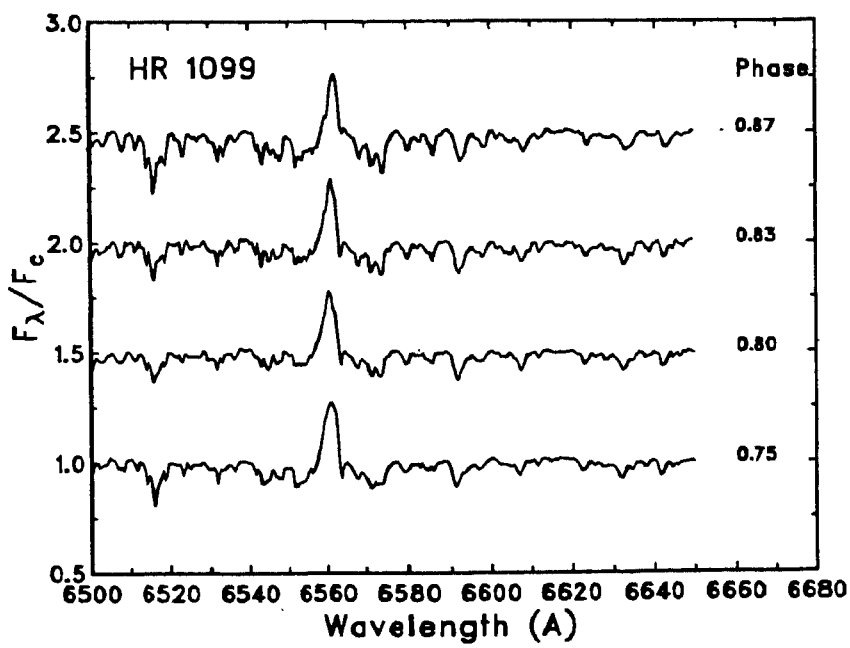

Figure 50. *Hα* spectra of V711 Tau. The descriptions are as in Fig. 47.

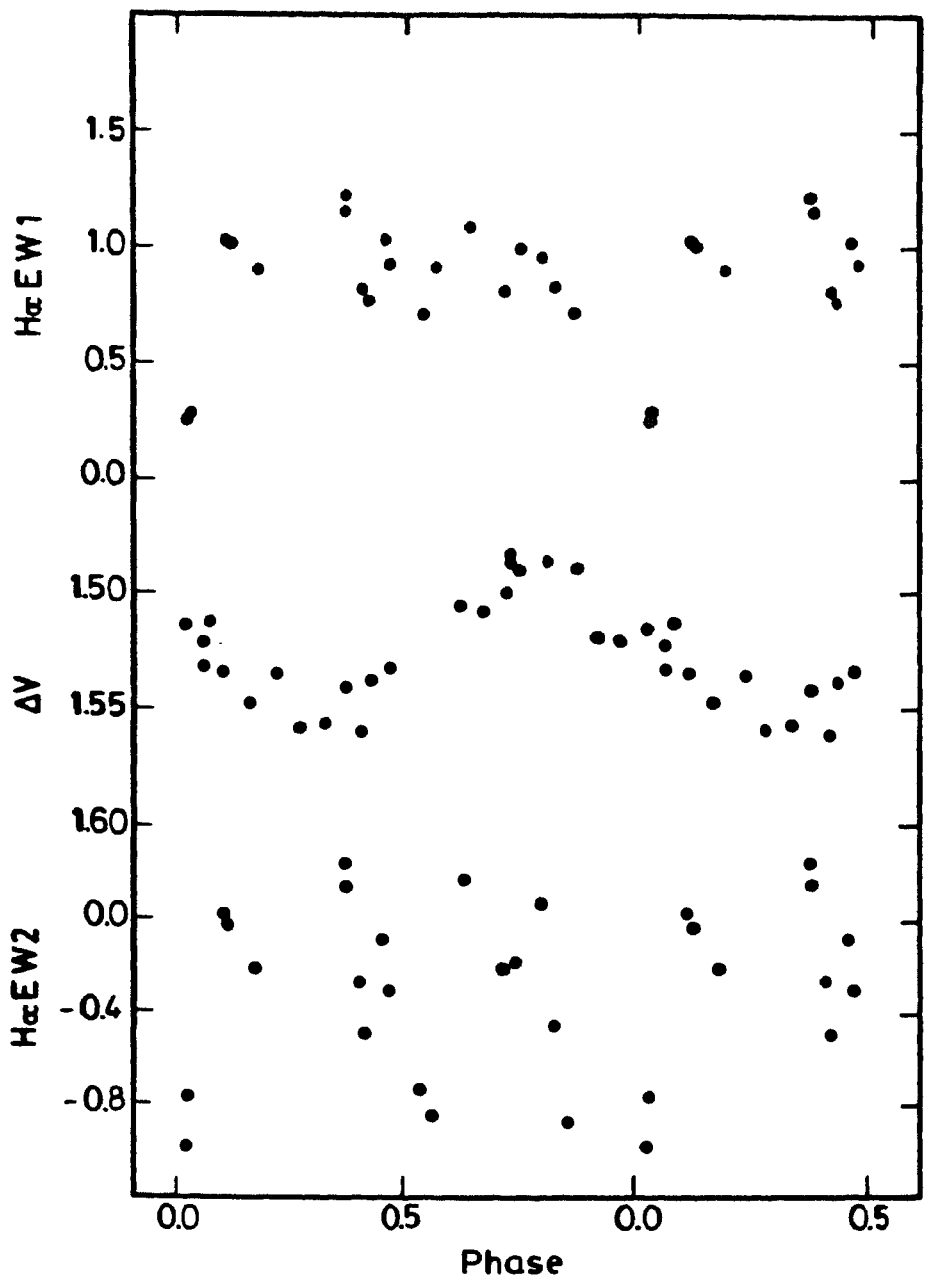

Figure 51. Top panel shows the variation of EW1, middle panel the V light curve and the bottom panel the variation of EW2. Phases are reckoned as in Fig. 38.

$H\alpha$ emission is highly localized on the cooler and active star in the system, then it should show some modulation with the rotational period of this star. The $H\alpha$ spectroscopic studies by Bopp & Talcott (1978) do not indicate any such correlation. But observations by Nations & Ramsey (1980) and Ramsey & Nations (1980) indicate some evidence of a modulation of $H\alpha$ emission equivalent width with the photometric phase. Fracquelli (1984) has argued that both stars in the system show $H\alpha$ in emission and the primary contributes $\approx$ 70% of the total emission, with the secondary star producing the remaining 30% emission. Nations & Ramsey (1986) have used the refined ephemeris of Fekel (1983) and have argued that the primary is responsible for 86% of the total emission.

It is evident from the spectra obtained on the same night that significant changes in equivalent width occur on time scales as short as a few hours (Table 14). The $H\alpha$ EW1 and EW2 listed in Table 14 are plotted in Fig. 51 along with the light curve obtained during the same period. We see from Fig. 51 that apparently there is no correlation between the light curve and the $H\alpha$ EW1 and EW2, and that there is no modulation of these with orbital phase. However EW1 observations obtained on one night (1991 Feb 6) show a sudden drop which occurs during the descending branch of the light curve. This change is not of instrumental origin, since the standard stars spectrograms obtained on that night show a scatter of only $\sim$ 5%. These observations indicate that the location of $H\alpha$ emitting region is not highly localized, but occupies a large extent of the surface area on the active component of the system. The IUE observations of V711 Tau indicate more compact active regions that are presumably magnetic in origin, analoguous to the solar-like active areas (Rodono et al. 1987; Andrews et al. 1988).

7

UX ARIETIS

35. Historical introduction

UX Ari (=HD 21242 = BD +28° 532) is another bright (V ~ 6.5) non-eclipsing double-lined spectroscopic binary. It consists of a K0 IV primary and a G5 V secondary, and has a period of 6.438 days (Carlos & Popper 1971). It is one of the 24 binary systems originally discussed by Hall (1976) defining RS CVn stars as a separate class of variables. UX Ari is similar to V711 Tau in many respects in its optical, UV, and radio properties; these are the two most frequently observed RS CVn systems at wide wavelength regions. At centimeter wavelengths both the stars exhibit strong and variable emission on time scales of minutes to several days. Radio flares in which flux density increased by an order of magnitude have also been observed (Gibson, Hjellming & Owen 1975; Owen, Jones & Gibson 1976; Spangler, Owen & Hulse 1977; Lang & Willson 1988).

HEAO 1 low-energy X-ray observations of UX Ari indicate an average X-ray luminosity of 2.1×10^{31} ergs s^{-1} with a plasma temperature of 10^7K. The X-ray emission shows rotational modulation indicating that the X-ray emitting region is small compared to the size of the star (Walter et al. 1980).

UX Ari is found to have large and erratically variable UV emission line fluxes. When compared to the sun the chromospheric line fluxes are about

25 times stronger and the transition region line fluxes are stronger by 75 to 250 times. High-resolution *Mg II* spectra indicate that the UV emission originates from the K star. The UV line fluxes do not show any correlation with orbital phase (Simon & Linsky 1980). During a flare the chromospheric and transition region emission line fluxes were found to be about 2.5 and 5.5 times brighter respectively than quiescent fluxes. Simon, Linsky & Schiffer (1980) have proposed a 'speculative scenario' of major long-lived RS CVn flares in which the component stars have very large corotating flux tubes which occasionally interact. They have also proposed that *Mg II* wings are produced by gas streaming along a flux tube from the K star to the G star.

However, from simultaneous observations of UX Ari with IUE and the Very Large Array (VLA) during a flare Lang & Willson (1988) have found that the emissions in the two wavelength regions are only weakly correlated. This indicates that the above speculative scenario is not very promising. They have argued that the flaring emission probably originates in different spatial regions at the two wavelengths and hence mass flow cannot be responsible for the observed flaring activity of UX Ari.

A survey of $H\alpha$ emission in UX Ari during 1976–77 has indicated that the equivalent width of the emission is correlated with the orbital phase. However, the phase of maximum strength is found to be different from the phases of light minimum and maximum (Bopp & Talcott 1978). Nations & Ramsey (1986) have found that the $H\alpha$ emission of the cooler K0 subgiant primary completely dominates that of the G5 V secondary. Huenemoerder, Buzasi & Ramsey (1989) concluded that there are two competing mechanisms which affect the net observed $H\alpha$ flux: (i) the chromospheric activity of the primary as shown by the emission lines of calcium and hydrogen and (ii) a phase dependent Balmer absorption at the velocity of the secondary star due to the varying aspect of the gas stream from the primary to the secondary that is presented to the observer.

From an analysis of Doppler images of UX Ari, Vogt & Hatzes (1991) have argued that the spotted primary is rotating differentially and the equator is synchronized to the orbital angular velocity, and also that the nature of differential rotation is opposite to that seen in the sun, *i.e.* the poles rotate

faster than the equator.

Extensive photometric observations of UX Ari have been obtained by several investigators (Sarma & Prakasa Rao 1984; Busso, Scaltriti & Cellino 1986; Mohin & Raveendran 1989; Strassmeier et al. 1989 and references therein).

36. BV photometry

UX Ari was observed on a total of 101 nights during the seven seasons, 1984–85 (11 nights), 1985–86 (6 nights), 1986–87 (23 nights), 1987–88 (18 nights), 1988–89 (8 nights), 1989–90 (13 nights), and 1990–91 (22 nights). The comparison stars were 62 Ari (G5 III) and HR 999 (K2 II–III). All the observations were made differentially with respect to 62 Ari and transformed to the UBV system. The mean differential magnitudes and colours of the comparison stars, in the sense 62 Ari minus HR 999, obtained during the various seasons are given in Table 15.

Table 15. The mean differential magnitudes and colours of comparison stars, in the sense 62 Ari minus HR 999.

Season	ΔV	$\Delta(B-V)$
1984–85	1.111 ± 0.005	-0.477 ± 0.004
1985–86	1.089 ± 0.002	-0.467 ± 0.003
1986–87	1.095 ± 0.001	-0.455 ± 0.002
1987–88	1.084 ± 0.002	-0.466 ± 0.002
1988–89	1.083 ± 0.002	-0.466 ± 0.002
1989–90	1.086 ± 0.002	-0.454 ± 0.002
1990–91	1.086 ± 0.002	-0.454 ± 0.002

Table 16 gives the results for UX Ari. Each value given in Table 16 is a mean of three to four independent measurements. The probable errors in the differential magnitudes and colours of the variable star for each observing season

Table 16. Differential magnitudes and colours of UX Ari

J.D. (Hel) 2440000.+	ΔV	$\Delta(B\text{-}V)$
	1984–85 Observing Season	
6052.3267	0.918±0.016	−0.213±0.011
6053.3294	0.945	−0.202
6054.2817	0.964	−0.238
6055.2335	1.107	−0.210
6055.3282	1.130	−0.236
6056.2801	1.132	−0.245
6084.1785	0.879	
6088.1282	1.113	−0.226
6089.1814	0.985	
6094.1884	1.095	−0.227
6095.0907	1.076	−0.249
6121.1317	1.020	−0.204
	1985–86 Observing Season	
6468.1933	1.072±0.004	−0.213±0.007
6472.1370	0.919	−0.190
6473.0921	0.992	−0.200
6474.0850	1.045	−0.225
6475.0896	1.061	−0.227
6476.1016	0.953	

Table 16. continued

J.D. (Hel) 2440000.+	ΔV	$\Delta(B\text{-}V)$
	1986–87 Observing Season	
6802.2046	1.051±0.005	−0.241±0.006
6803.2137	1.077	−0.237
6816.1648	1.081	
6817.1815	1.026	
6818.1454	0.910	−0.182
6819.1571	0.911	−0.197
6820.1563	0.967	−0.211
6821.1375	1.031	
6823.1707	1.046	−0.217
6824.1510	0.977	−0.216
6825.1307	0.900	−0.203
6828.1479	1.076	−0.229
6829.1453	1.083	
6830.1361	1.014	−0.201
6831.1252	0.930	
6832.1144	0.911	−0.215
6835.1157	1.092	−0.232
6836.1188	1.051	−0.230
6847.0933	1.072	−0.232
6850.1023	0.934	−0.210
6852.1004	0.962	−0.210
6861.0949	1.063	
6862.0986	1.030	−0.228

Table 16. continued

J.D. (Hel) 2440000.+	ΔV	$\Delta(B\text{-}V)$
	1987–88 Observing Season	
7157.2139	1.023±0.007	−0.214±0.007
7179.1790	0.863	
7183.1431	1.042	−0.206
7184.1757	0.926	−0.218
7185.1586	0.868	−0.200
7196.0958	1.016	−0.220
7197.0931	0.907	−0.205
7198.0806	0.857	
7200.1590	0.996	−0.214
7201.1067	1.038	−0.217
7202.1278	1.040	−0.215
7203.1220	0.936	−0.213
7204.1056	0.876	−0.208
7206.0833	0.941	
7218.0806	0.876	
7231.0970	0.890	−0.206
7232.1028	0.974	−0.210
7233.0944	1.041	−0.225

Table 16. continued

J.D. (Hel) 2440000.+	ΔV	$\Delta(B\text{-}V)$
	1988−89 Observing Season	
7556.1138	0.986±0.007	−0.220±0.007
7557.1275	0.940	−0.208
7558.1058	0.863	−0.205
7559.1608	0.808	−0.190
7560.1399	0.914	−0.209
7561.1056	1.007	−0.229
7572.1216	0.837	−0.198
7573.0971	0.922	−0.212
	1989−90 Observing Season	
7852.2956	0.946±0.008	−0.215±0.008
7853.2316	0.922	−0.208
7854.1795	0.870	−0.194
7855.2373	0.876	−0.208
7856.1988	0.946	−0.206
7867.2536	0.875	−0.190
7877.2466	0.953	−0.212
7912.1896	0.889	−0.209
7913.1786	0.894	−0.206
7915.1958	0.961	−0.214
7916.1314	0.942	−0.193
7917.1151	0.929	−0.207
7918.1197	0.916	−0.205

Table 16. continued

J.D. (Hel) 2440000.+	ΔV	$\Delta(B\text{-}V)$
	1990–91 Observing Season	
8279.1075	0.930±0.007	−0.192±0.009
8280.1855	0.987	−0.244
8297.1111	0.949	−0.220
8298.1022	0.940	−0.223
8299.1304	0.972	−0.219
8300.1419	0.981	−0.214
8301.1122	0.952	−0.205
8302.1438	0.933	−0.224
8303.1408	0.952	−0.223
8305.1130	0.956	−0.233
8306.0992	0.989	−0.233
8325.1098	0.982	−0.222
8326.0943	0.963	−0.215
8327.0859	0.927	−0.212
8328.0821	0.933	−0.197
8329.0847	0.962	−0.231
8330.0751	0.928	−0.198
8331.0985	0.969	−0.223
8332.1038	0.971	−0.219
8333.0987	0.955	−0.233
8334.0964	0.931	−0.221
8335.1036	0.919	−0.180

are also given in Table 16. The Julian days of observation were converted into orbital phases using the following ephemeris (Carlos & Popper 1971):

$$\text{JD (hel.)} = 2440133.75 + 6^d.43791\ \text{E},$$

in which zero phase corresponds to conjunction with the cooler component in front and the period is the spectroscopic orbital period.

37. Light curves

The observations listed in Table 16 for the observing seasons 1986–87, 1987–88, 1988–89, 1989–90, and 1990–91 are plotted in Figs 52–56. The light curve obtained during 1986–87 observing season (Fig. 52) is nearly sinusoidal in shape and has an amplitude of about 0.19 mag; the maximum and minimum occur at $\sim 0^p.40$ and $\sim 0^p.90$. The modulation in $B-V$ is evident from the figure, with the system being redder when brighter and bluer when fainter.

The 1987–88 light curve (Fig. 53) differs significantly from that of the previous season in brightness at light maximum and minimum; however, the amplitude is nearly the same. As in the previous case, the $B-V$ colour shows a phase-dependence, but with a slightly smaller amplitude.

The light curve obtained during the season 1988–89 is asymmetric with $\Delta V_{max} = 0.815$ occuring $\sim 0^p.40$ (Fig. 54). This is the maximum brightness so far reported in the literature. However, the amplitude of the light variation is 0.19 mag, which is the same as that of the previous two seasons. The trend in $B-V$ indicates that the system is redder as its brightness increases. The light curve obtained during 1989–90 season (Fig. 55) is totally different in every aspect. The highly asymmetric light curve has an amplitude of 0.09 mag with the ΔV_{max} and ΔV_{min} of 0.875 mag 0.960 mag respectively.

The light curve for 1990–91 (Fig. 56) shows two minima occuring at $0^p.96$ and $0^p.43$ with an amplitude of about 0.06 mag. The simultaneous presence of two minima in the light curve is not common in the case of UX Ari. There was some evidence of a secondary minimum also close to 1985 (Busso, Scaltriti & Cellino 1986; Strassmeier et al. 1989). The brightness at maximum and minimum are 0.925 mag and 0.985 mag respectively.

The photometric properties derived from our observations together with

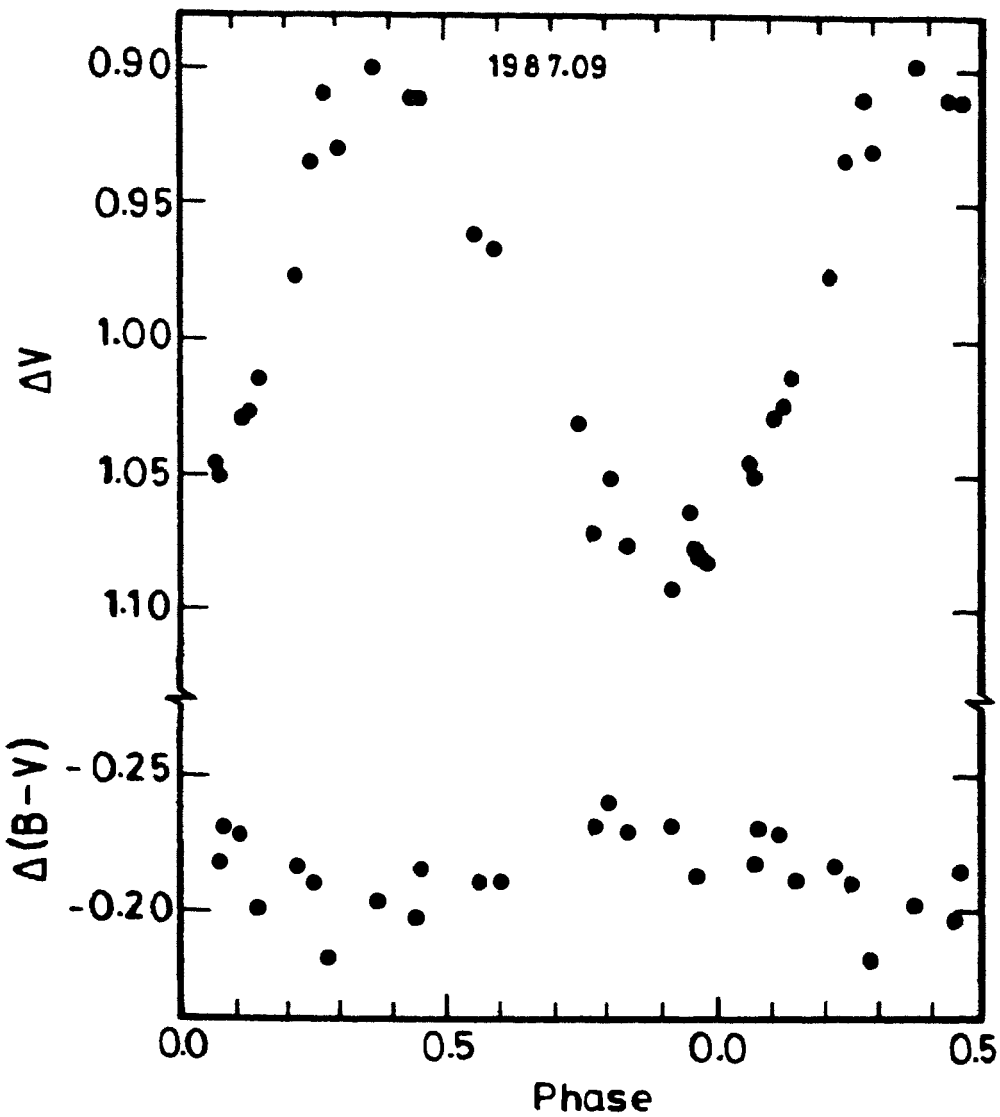

Figure 52. The 1987.09 V and $B-V$ curves of UX Ari. Phases are reckoned from JD (Hel.) 2440133.75 using the period $6^d.43791$.

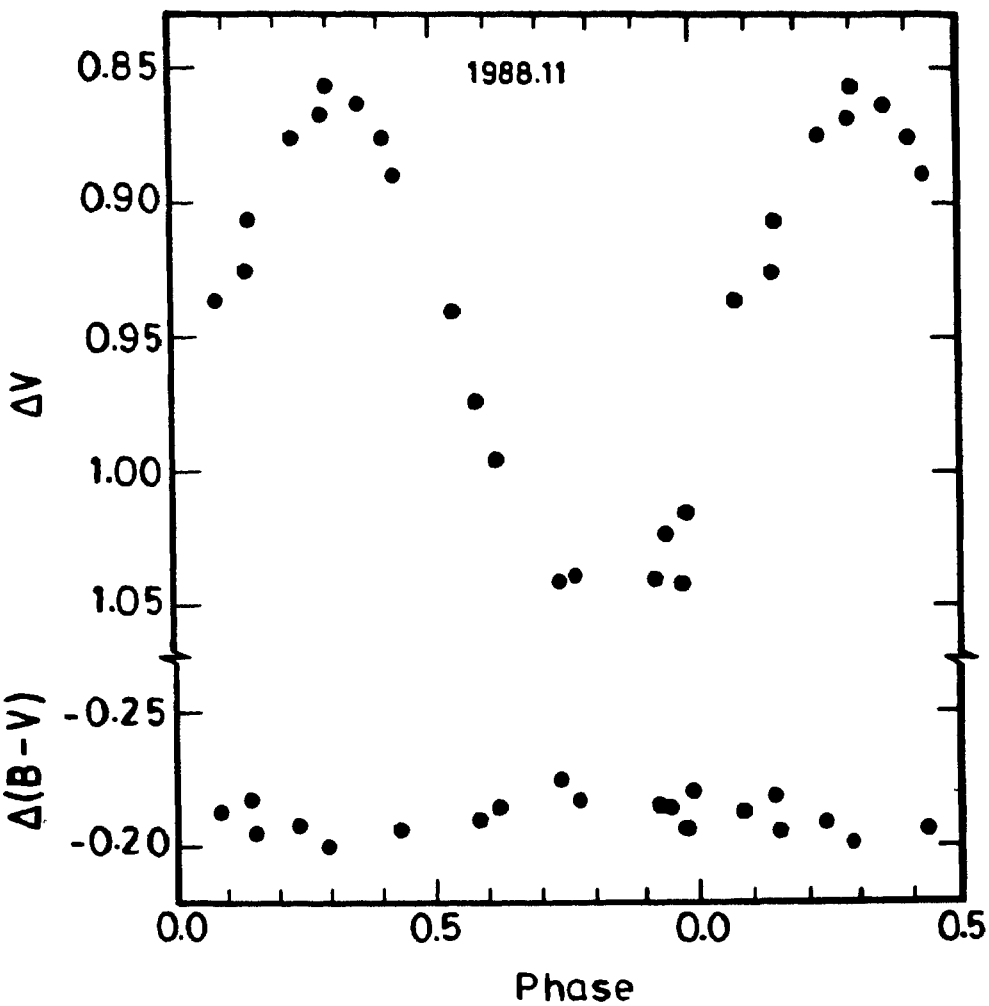

Figure 53. The 1988.11 V and $B-V$ curves of UX Ari. Phases are reckoned as in Fig. 52.

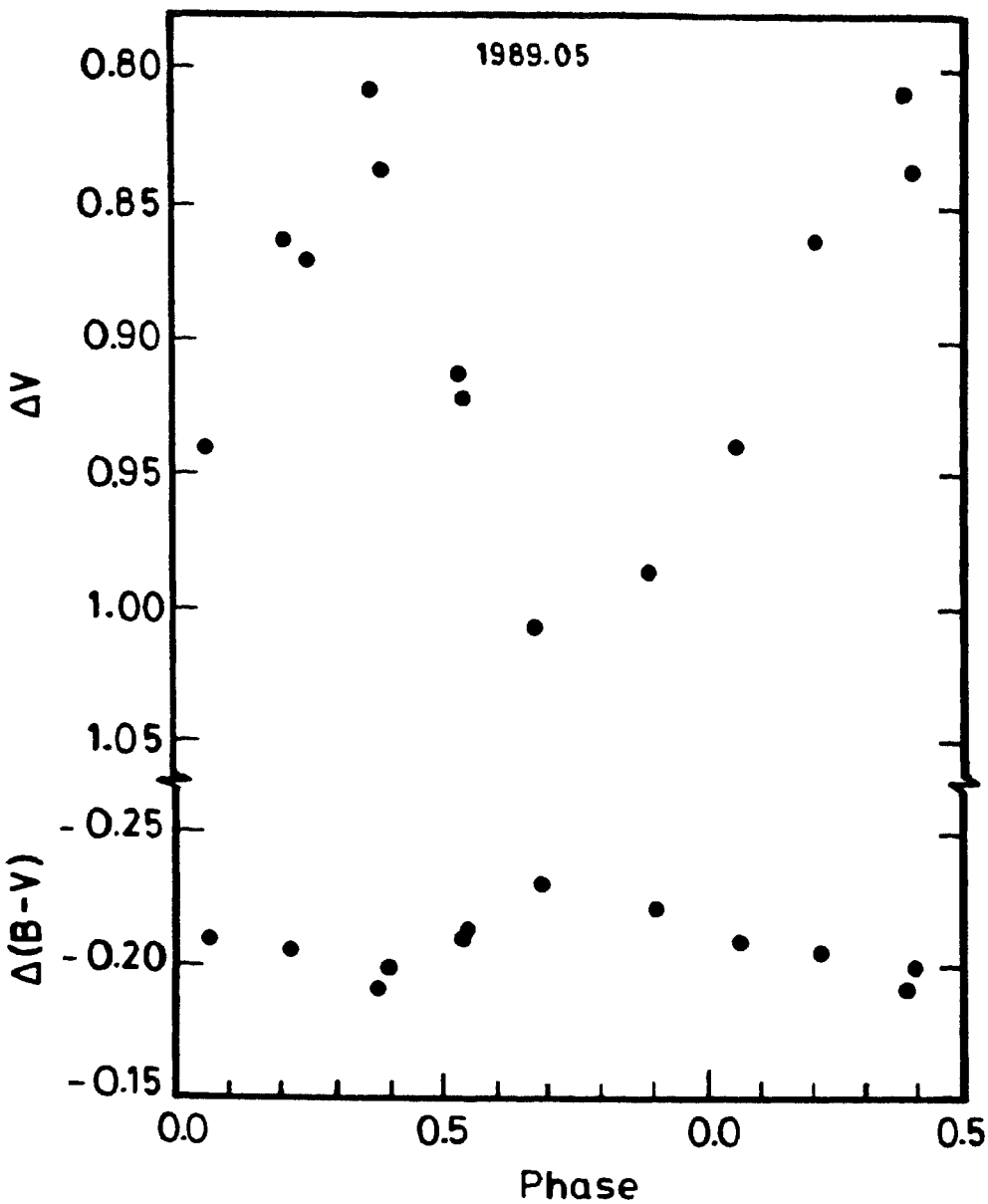

Figure 54. The 1989.05 V and $B-V$ curves of UX Ari. Phases are reckoned as in Fig. 52.

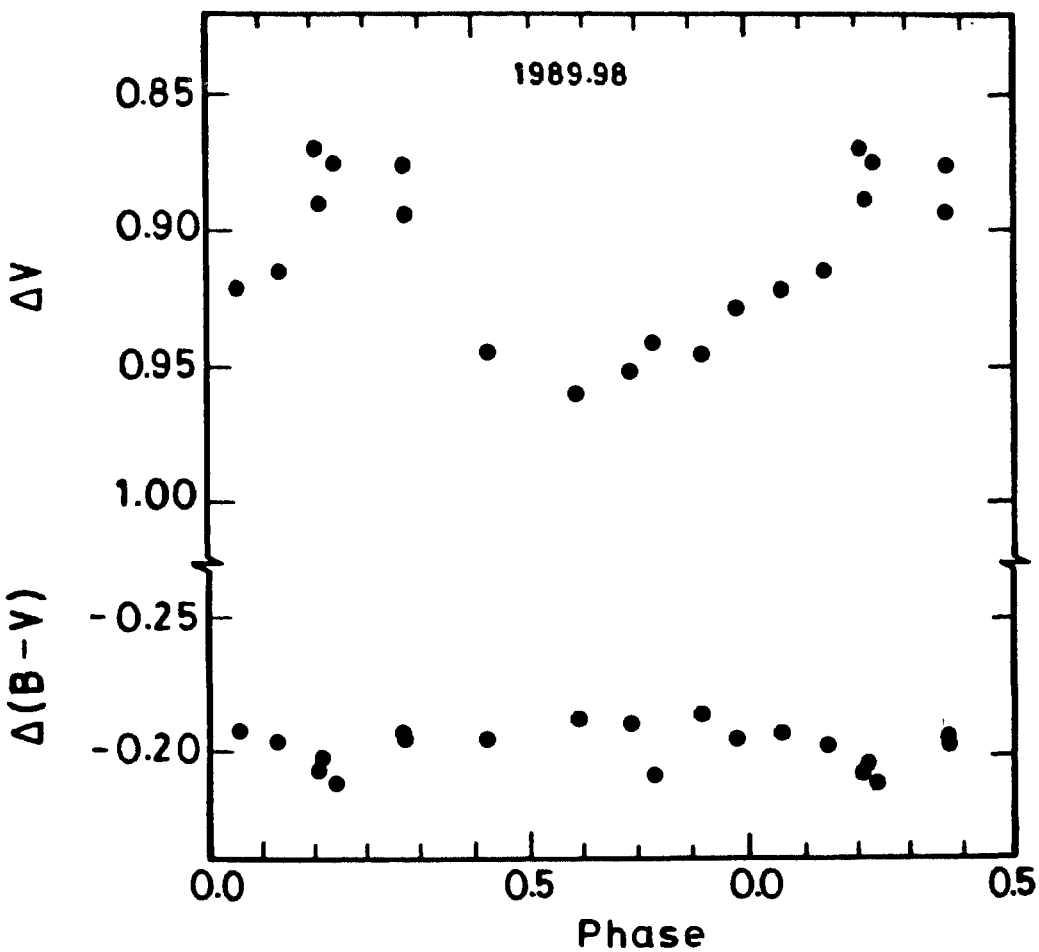

Figure 55. The 1989.98 V and $B-V$ curves of UX Ari. Phases are reckoned as in Fig. 52.

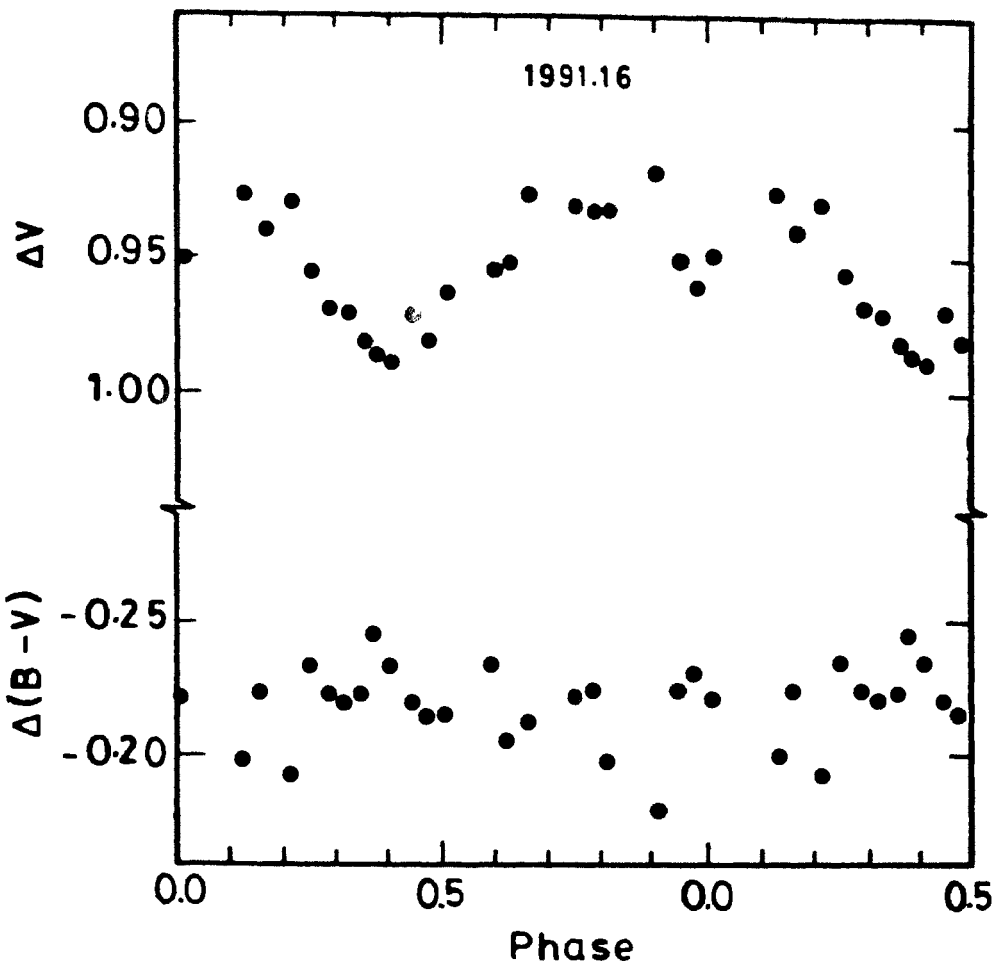

Figure 56. The 1991.16 V and $B-V$ curves of UX Ari. Phases are reckoned as in Fig. 52.

those compiled from various sources are given in Table 17. The phases of the light minima from the present data were determined by fitting a truncated Fourier series (Chapter 6). The amplitudes of the light variation were directly taken from the respective graphs.

38. Phase of light minimum and amplitude

In all well-observed RS CVn systems such as DM UMa (Chapter 4), II Peg (Chapter 5) and V711 Tau (Chapter 6) the phases of the light minima have been found to drift slowly with the orbital phases or to appear at arbitrary phases. In the case of UX Ari the behaviour of the phases of light minima has been interpreted differently by different investigators. According to Zielik et al. (1982a) the phase of light minimum has an erratic behaviour during 1972–82, whereas Sarma & Prakasa Rao (1984) have interpreted the behaviour as systematic. Applying the analogy of the sunspots Sarma & Prakasa Rao (1984) have concluded that the light minimum migrates with respect to orbital phases and the motion is direct in the beginning of a cycle and becomes retrograde after the spots migrate below the latitude that is rotating in synchronism with the orbital period of the system. They have also concluded that the amplitude of the light curve is constant during one spot cycle whose period is 5–6 years.

Busso, Scaltriti & Cellino (1986) have argued that the phase of light minimum has a cyclic behaviour with a period of about 8 years. Further, they have pointed out that a good correlation between the amplitude and the phase of light minimum exists. According to Wacker & Guinan (1987) the change in the phase of light minimum is not significant and they claim that it has remained *anchored* between $0^p.93$ and $0^p.95$ during the period 1980–86.

In Fig. 57 we have plotted the phase of light minimum and the wave amplitude given in Table 17 against the mean epoch of observation and we see from the figure that apparently there is no correlation between the two. In fact what we see is a near-sinusoidal variation in the amplitude and a secular decrease in the phase of light minimum superposed with dips of short duration during 1976–78 and 1989–91. The observations during 1976–78

Table 17. Photometric characteristics of UX Ari

Epoch	Amplitude	ΔV_{max}	ΔV_{min}	Phase Min	Refcrences
1972.2	0.11	0.865	0.975	0.14	Guinan et al. (1981)
1972.8	0.14	0.870	1.010	0.12	,,
1974.9	0.05	1.015	1.065	0.99	,,
1976.0	0.02	0.990	1.010	1.00	Sarma & Prakasa Rao (1984)
1976.8	0.05	1.005	1.055	0.80	Guinan et al. (1981)
1977.1	0.08	0.990	1.070	0.70	,,
1979.2	0.09	0.945	1.035	0.03	,,
1979.9	0.04	0.970	1.010	0.87	,,
1980.0	0.06	0.970	1.030	0.90	,,
1980.8	0.17	0.950	1.120	0.95	,,
1981.0	0.16	0.960	1.120	0.97	,,
1981.8	0.21	0.940	1.150	0.97	Zeilik et al. (1982a)
1982.0	0.16	1.000	1.160	1.00	Sarma & Prakasa Rao (1984)
1983.0	0.20	0.950	1.150	1.00	,,
1984.0	0.30	0.825	1.125	0.94±0.02	Stassmeier et al. (1989)
1984.9	0.28	0.890	1.170	0.90	Busso et al. (1986)
1985.0	0.30	0.842	1.142	0.86±0.01	Stassmeier et al. (1989)
1985.10	0.25	0.879	1.131	0.84±0.03	Present Study
1986.0	0.20	0.908	1.105	0.91±0.02	Stassmeier et al. (1989)
1986.06			1.072	0.93±0.01	Present Study
1987.0	0.15	0.944	1.089	0.91±0.04	Stassmeier et al. (1989)
1987.09	0.19	0.900	1.092	0.93±0.01	Present Study
1988.11	0.19	0.857	1.042	0.84±0.01	,,
1989.05	0.19	0.815	1.005	0.75±0.02	,,
1989.98	0.08	0.875	0.960	0.64±0.04	,,
1991.16	0.06	0.925	0.985	0.96±0.03	,,
				0.43±0.03	

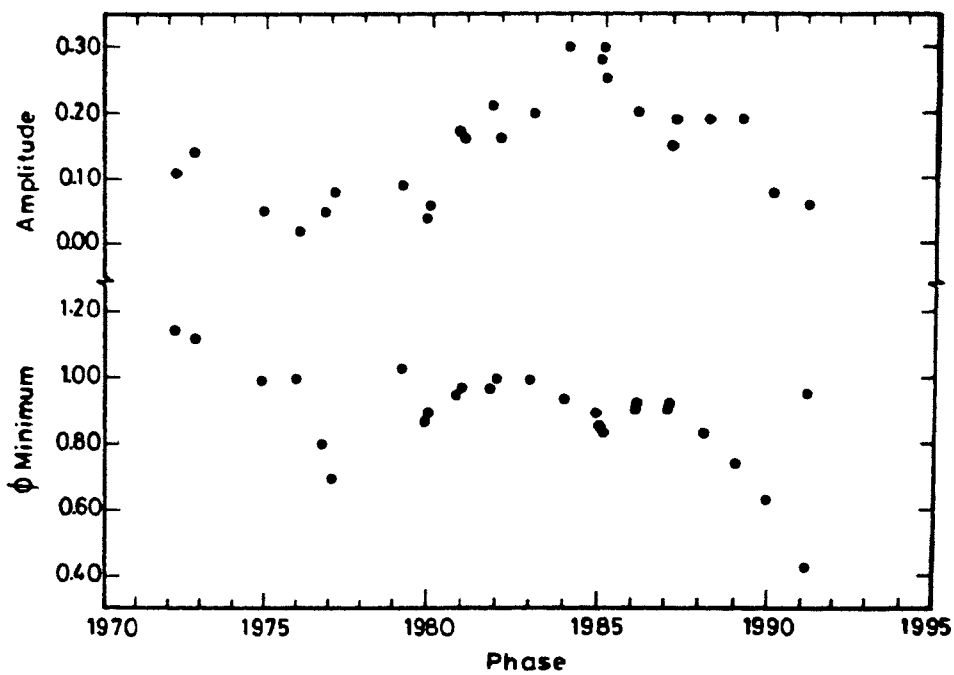

Figure 57. Plot of V amplitude and the phase of light minimum versus mean epoch of observation.

are a few in number making it difficult to say about the behaviour during that period. It is worth noting that these are the two periods during 1972–91 when the amplitudes of light variation are low. The minimum which appeared around 1980 can be traced upto 1991 and the appearance of a second minimum during 1991 reveals probably the beginning of another centre of spot activity.

39. $B-V$ variation

Wacker & Guinan (1987) have reported that both of the Villanova colour curves of UX Ari are phase dependent with the star being reddest at light maximum. Zeilik et al. (1982a) have also reported the phase dependence of the colour index. An inspection of Figs 52–56 makes it clear that $B-V$ is redder close to light maximum and bluer close to light minimum. The phase dependence of the colour index is prominently seen when the system shows comparatively larger amplitude of light variation and at fainter light minimum.

The components of UX Ari are classified by Carlos & Popper (1971) as G5 V and K0 IV and according to them in the visible region the spectrum is dominated by the G5 V component. The cooler component is not a normal subgiant since we would expect it to be more luminous by about 1.5–2.0 magnitude in V (Allen 1976).

As is known, the light variation of RS CVn stars is attributed to spot activity on the surface of the cooler component of the system. Starspots that are distributed on the cooler companion modulate the observed light as the star rotates, giving rise to the light curve. The conventional starspot model assumes that the spots are cooler than the surrounding photosphere and hence one would expect the star to be reddest at the light minimum. In chromospherically active single-lined RS CVn systems, it has been found that $B-V$ is redder or nearly constant at the light minimum (Chapters 4 and 5). With a view to investigating the phase dependence of $B-V$ in UX Ari, we have derived the expected $B-V$ of the cooler component at both the light maximum and minimum for a possible range of differences in V of both the components; the results are given in Fig. 58. The data used for

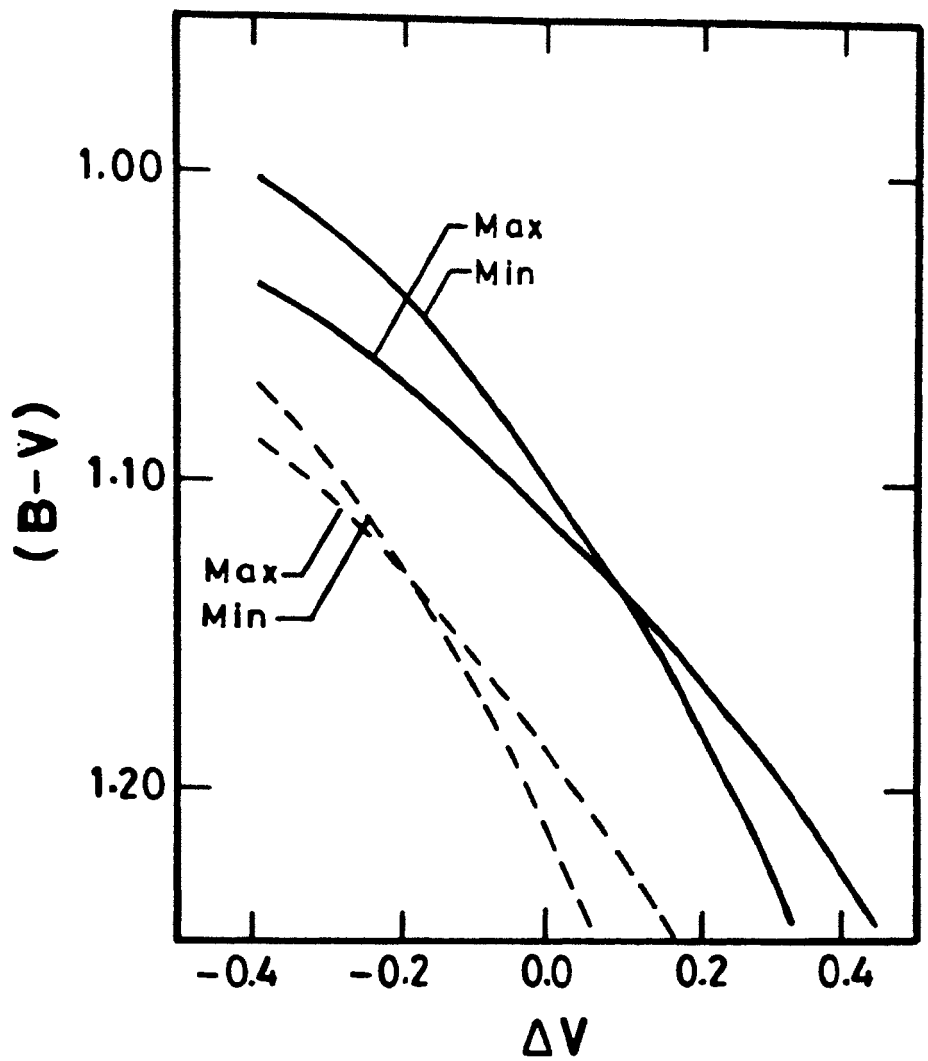

Figure 58. Derived $B - V$ values of the K0 IV component at maxima and minima for a possible range of the differences in V (K0 IV–G5 V). The two sets of curves are for the cases of assumed $B - V$ of 0.70 (continuous lines) and 0.65 (broken lines) for the G5 V component. The 1986–87 observations are used for the calculations.

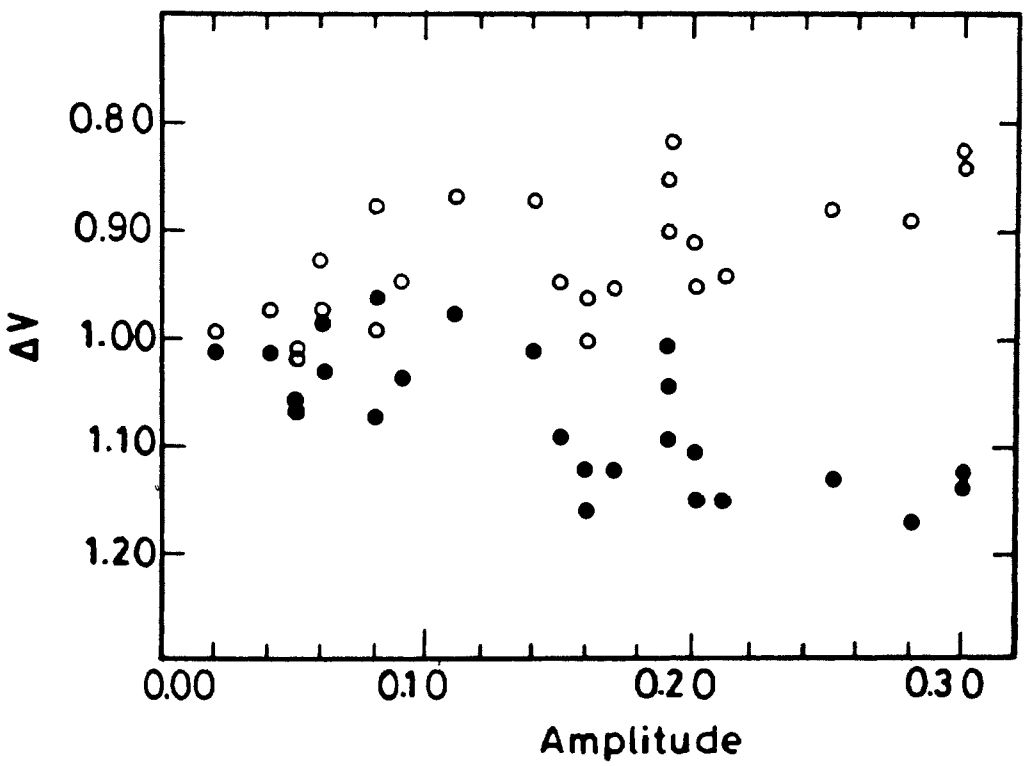

Figure 59. Plot of the brightness at light maximum (open circles) and light minimum (filled circles) against the V amplitude.

this purpose are that obtained during the 1986–87 observing season.

From Fig. 58 it is evident that the situation seen in the case of UX Ari as described above would arise only if the cooler and active component is fainter than the hotter component by around 0.2 magnitude in V for an assumed $B-V$ of 0.7 for the hotter component. A bluer colour for the hotter component is not possible because it would imply that either the cooler component is brighter than the hotter or both are of equal brightness, contrary to the observations. So the $B-V$ variations seen in this star arise as a result of the variable fractional contribution by the hotter component (G5 V) to the total light at shorter wavelengths.

40. Brightness at light maximum and minimum

We have plotted the values of ΔV_{max} and ΔV_{min} given in Table 17 against the corresponding amplitude in Fig. 59. The figure shows that at larger amplitudes the brightness at maximum increases and the brightness at minimum decreases, both converging to $\Delta V \approx 1.0$ at very low amplitudes as seen in the case of V711 Tau (Chapter 6). Sarma & Prakasa Rao (1984) have attributed the low amplitude in the light curve to a low spot activity and the high amplitude to high spot activity. The amplitude of the light curve depends only on the longitudinal asymmetry in the distribution of the spots on the rotating star. Since the brightness at light maximum and minimum converges at low amplitudes, it appears that most of the amplitude variation is essentially due to changes in the longitudinal distribution of spots rather than due to changes in the level of spot activity.

41. $H\alpha$ observations

Spectra of UX Ari in the $H\alpha$ region were obtained on a total of 14 nights during the 1990–91. Table 18 is the log of observations; it contains the Julian day of observation; $H\alpha$ emission equivalent width EW1; full width at half maximum of $H\alpha$ emission FWHM; height of the $H\alpha$ emission in terms of F_λ/F_c; phase reckoned from the ephemeris of Carlos & Popper (1971) and the equivalent width EW2 as described in Chapter 2.

Table 18. *Hα* data of UX Ari

Date	JD 2440000.+	Phase	EW1 Å	FWHM Å	Height	EW2 Å
08 Oct 1990	8173.4722	0.809	0.34	1.84	0.16	−1.35
10 Oct 1990	8175.4056	0.110	0.58	2.79	0.21	−0.90
23 Nov 1990	8219.2480	0.920	0.41	2.32	0.18	−0.84
28 Nov 1990	8224.3007	0.705	0.29	2.34	0.14	−1.19
29 Nov 1990	8225.2719	0.855	0.05	0.91	0.04	−1.88
30 Nov 1990	8226.2924	0.014	−0.26*		0.13*	−1.66
07 Jan 1991	8264.2417	0.909	−1.30*		0.31*	−2.17
08 Jan 1991	8265.1646	0.052	0.04	0.77	0.06	−1.48
08 Jan 1991	8265.2181	0.060	0.09	1.07	0.08	−1.41
08 Jan 1991	8265.2486	0.065	0.13	1.47	0.11	−1.35
06 Feb 1991	8294.1889	0.560	0.26	1.42	0.16	−1.08
07 Feb 1991	8295.1403	0.708	0.41	2.17	0.18	−0.99
07 Feb 1991	8295.1632	0.712	0.44	2.39	0.18	−0.77
08 Feb 1991	8296.1320	0.862	0.41	2.07	0.19	−0.93
06 Mar 1991	8322.1056	0.896	0.07	1.03	0.06	−1.86
07 Mar 1991	8323.1563	0.060	0.22	1.76	0.12	−1.56
08 Mar 1991	8324.0924	0.205	0.34	1.99	0.16	−1.30

* H_α absorption

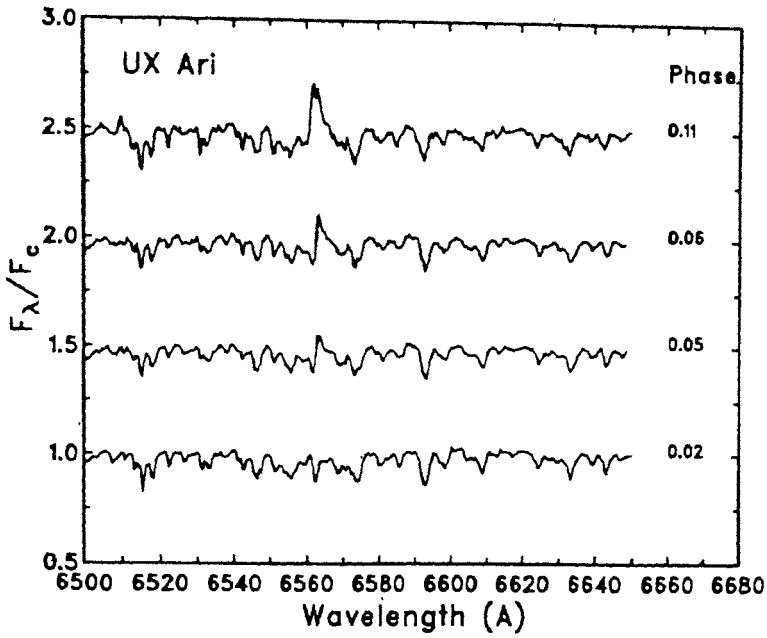

Figure 60. $H\alpha$ spectra of UX Ari. The spectra are adjusted on the rest wavelength of $H\alpha$. Each spectrum is normalized to continuum and shifted by 0.5. Phases are reckoned as in Fig. 52.

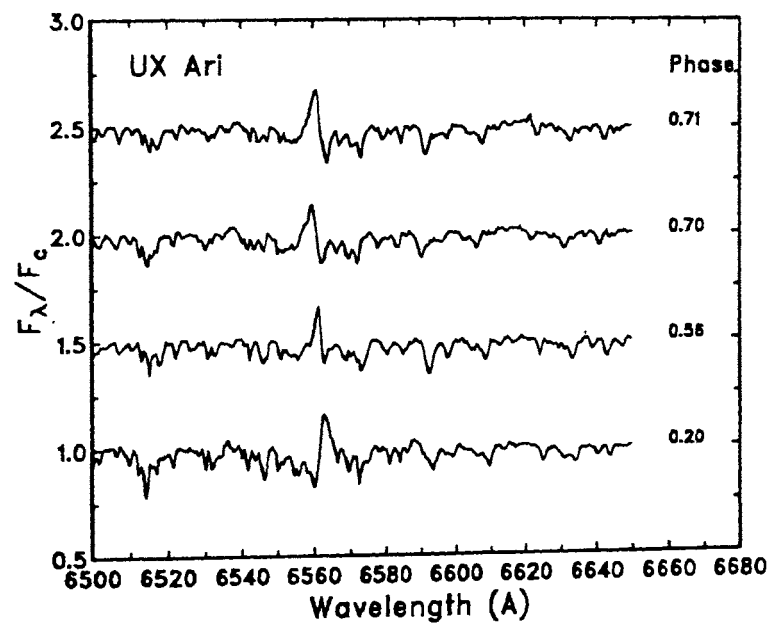

Figure 61. $H\alpha$ spectra of UX Ari. The descriptions are as in Fig. 60.

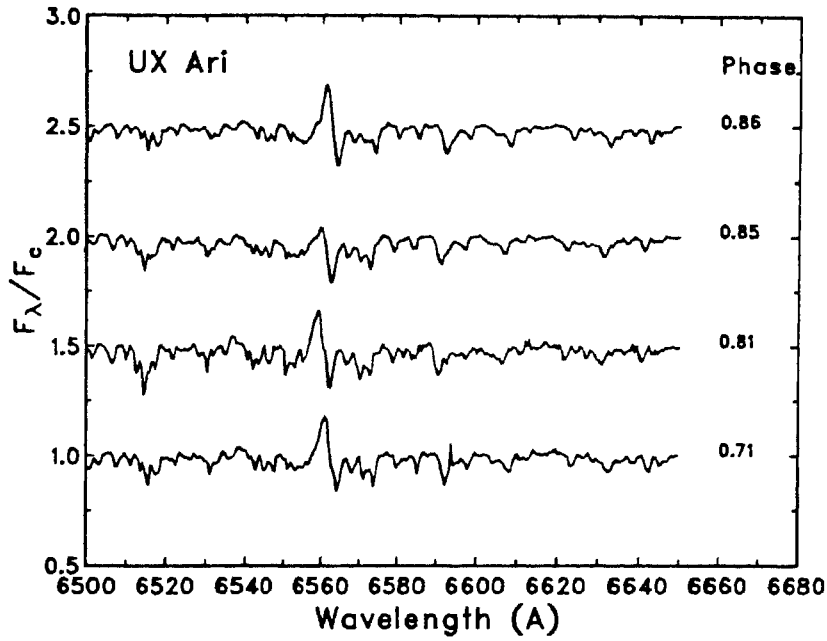

Figure 62. *Hα* spectra of UX Ari. The descriptions are as in Fig. 60.

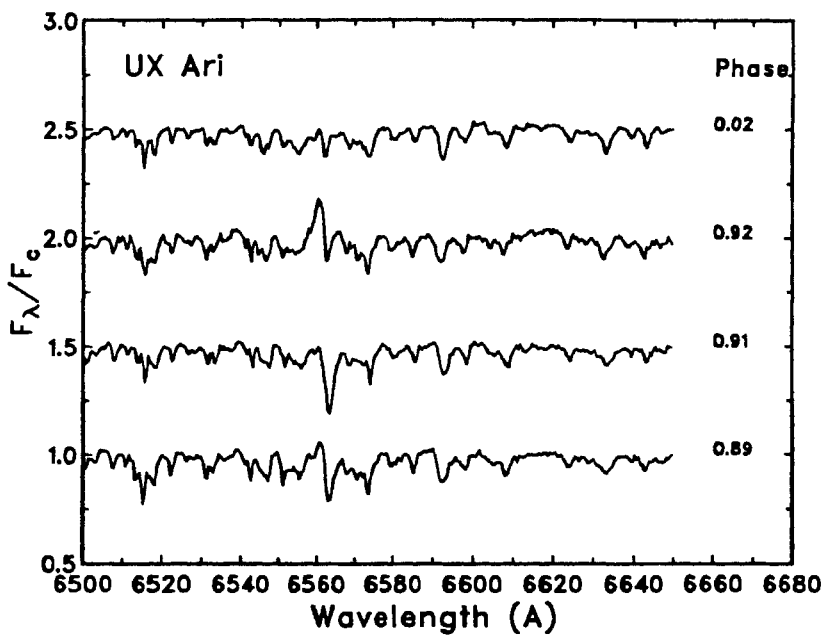

Figure 63. *Hα* spectra of UX Ari. The descriptions are as in Fig. 60.

The results of $H\alpha$ observations are plotted in Figs 60–63, which show that the emission is highly variable. It is interesting to note that the spectra obtained on any two nights are not similar in appearance. An inspection of the Figs 60–63 clearly reveals that UX Ari displays a variety of $H\alpha$ characteristics: an intense emission; a weak blue-shifted absorption line giving the emission the appearance of a P Cygni profile; a weak absorption line red-shifted from the emission; filled in absorption with out any emission or absorption; and pure absorption.

The spectrum obtained near the phase 0.20 shows a weak blue-shifted absorption feature giving the $H\alpha$ emission the appearance of a P Cygni profile. On the other hand, there are several spectra obtained around the phases 0.56–0.80 showing a weak absorption line red-shifted from the $H\alpha$ emission. These features may be the result of the superposition of $H\alpha$ absorption of the G5 V secondary star. Similar findings were reported by Nations & Ramsey (1986). We have another spectrum around phase 0.11 which shows the two emission components on both the red and violet sides of the $H\alpha$ line. The spectrum around the orbital phase 0.90 shows a pure absorption feature, whereas the spectrum obtained around 0.0 phase shows completely filled in emission line.

A spetroscopic study by Bopp & Talcott (1978) suggested that the equivalent width of $H\alpha$ was correlated with the orbital phase. They have also reported that the maximum strength of $H\alpha$ emission occurred near the orbital phase 0.6, whereas the photometric minimum was between $0^p.7$ and $0^p.8$. Another spectroscopic study by Nations & Ramsey (1986) indicated that the $H\alpha$ emission of the system is completely dominated by the G5 V secondary star. Fig. 64 is the plot of equivalent width of $H\alpha$ line EW1, along with the light curve obtained during the same period against the orbital phases. It is evident from the figure that the equivalent widths show a sudden drop around the phases 0.8–1.0. Here we note that the photometric light curve has its secondary minimum around these phases. Unfortunately, we do not have the spectroscopic observations during the main photometric minimum. Huenemoerder, Buzasi & Ramsey (1989) and Buzasi, Ramsey & Huenemoerder (1991) have reported that this star shows highly phase

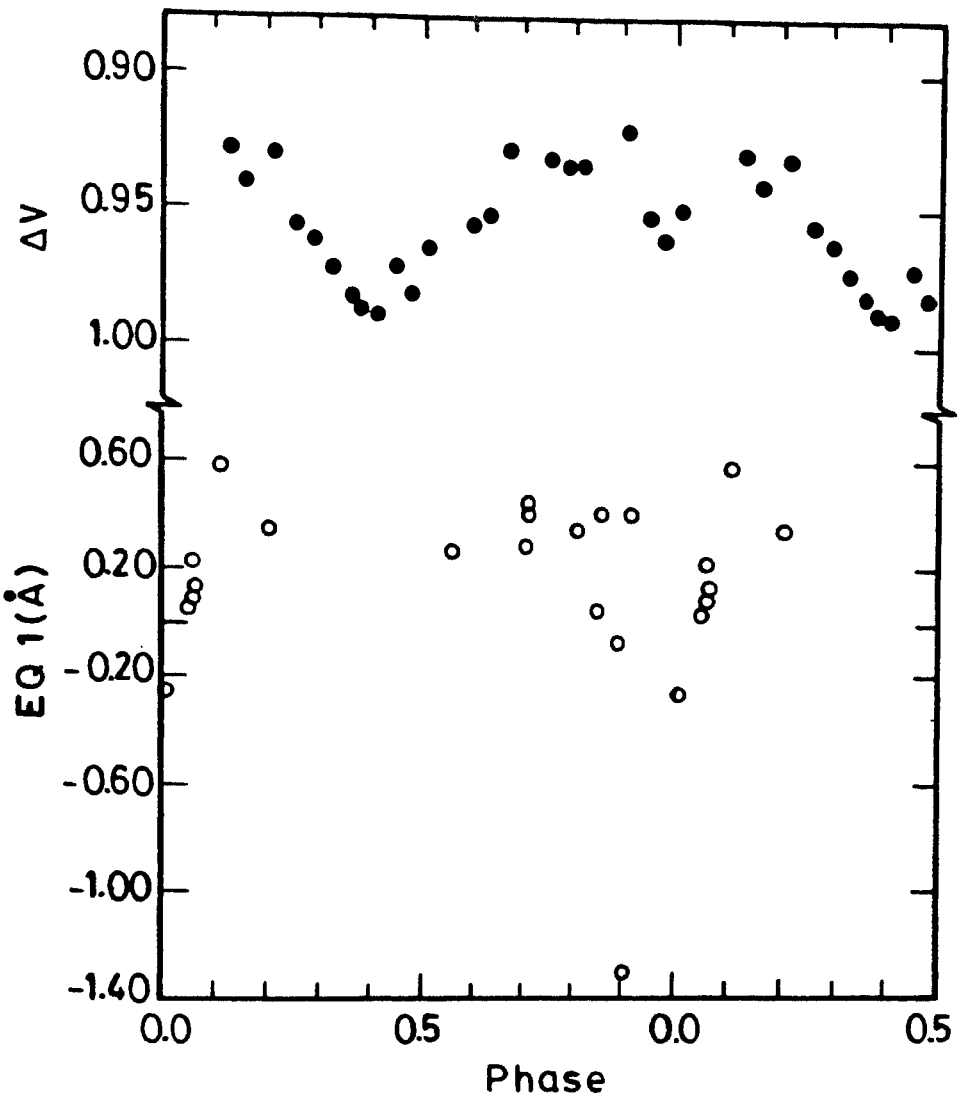

Figure 64. Top panel shows the V light curve and the bottom panel the variation of EW1. Phases are reckoned as in Fig. 52.

dependent excess absorption in $H\alpha$ and $H\beta$ and the absorption is seen to appear at the velocity of the G star. They have further argued that though the system shows a weak phase modulation in hydrogen and calcium emission lines from the chromospherically active component, the light variation may not be solely due to the activity of the primary alone.

8

Conclusions

42. Present work

BV photometric observations of four RS CVn systems – DM UMa (96 nights), II Peg (57 nights), V711 Tau (120 nights) and UX Ari (101 nights) – were obtained during 1984–91 using the 34-cm telescope at VBO. The photometric observations were supplemented with $H\alpha$ spectroscopy using the 102-cm telescope during the 1990–91 season.

All four stars are non-eclipsing close binary systems. DM UMa and II Peg are single-lined spectroscopic binaries. V711 Tau and UX Ari on the other hand are double-lined systems. We have analysed our database in conjunction with the published observations. Our analysis shows that all four stars have remarkably variable light curves. Appreciable changes occur even during time scales as short as a few orbital periods. For all the four systems the light curves obtained during any two seasons do not agree in any of the following: shape, amplitude, phases of the light maxima and minima, mean light level, brightness at the light maximum and minima.

Light curves

Astronomical interest in DM UMa is a recent occurence; its first light curve having been obtained a little more than a decade ago, in 1979. The

curve was rather smooth and nearly sinusoidal in shape. The amplitude of 0.32 mag obtained then has been the largest so far. The very next light curve, obtained during 1980 after a gap of 36 orbital periods, showed considerable changes. Brightness at light maximum dimmed by about 0.10 mag and light minimum brightened by about 0.03 mag, and the resultant light curve showed an amplitude of 0.20 mag only. Subsequently DM UMa showed both periods of small and large amplitudes with remarkable changes in the mean light level of the system. Apparently the amplitude of light variation does not depend on the mean brightness of the system. The object showed an amplitude of 0.23 mag during 1984 when the star was at its minimum brightness, and a similar amplitude during 1991 when the systems was at its maximum brightness.

The light curves of II Peg are mostly asymmetrical in shape and rapid changes occur in the mean light level of the system from season to season. Among the known RSCVn objects the largest amplitude of 0.50 mag is reported for II Peg. It maintained the maximum light level close to 7.35 mag during 1976–85 and has shown a secular increase in the maximum brightness from 1986 onwards.

The light curves of V711 Tau show a variety of shapes, like, sinusoidal, double-peaked and sometimes even flat. The change from larger to smaller amplitude is often followed by the appearance of two minima. The largest amplitude so far observed was during 1979. The system was then at its minimum mean light level (ΔV_{min} = 1.650). The mean light level during 1982–91 showed a rather erratic variation when compared to that seen during 1975–82.

The light curves of UX Ari are similar to that of V711 Tau in many respects. The shapes vary from nearly sinusoidal to nearly flat. During the period from 1974 to 1980 the amplitude values were less than 0.1 mag. The largest amplitude of 0.30 mag was observed during 1984–85; at that time the system's mean brightness was also the lowest (ΔV_{min} = 1.170). The earlier observations have indicated only weakly the simultaneous presence of two minima for this system, but the observations obtained by us during 1991.16 clearly shows the presence of a second minimum in the light curve.

$B-V$ variations

There is a significant correlation between the $B-V$ colour and the visual magnitude in the single lined systems DM UMa and II Peg. Both appear redder at fainter visual magnitudes. V711 Tau, which is a double-lined binary, does not show any significant modulation of $B-V$ colour with the photometric phase. UX Ari, the other double-lined binary observed, shows a colour modulation in the sense that $B-V$ colour is redder close to light maximum and bluer close to light minimum. The phase dependence of the colour index is prominently seen when the system shows comparatively larger amplitude of light variation. We find that the colour variations seen in UX Ari are as a result of the variable fractional contribution by the hotter component (G5 V) to the total light at shorter wavelength regions.

Brightness variations

Some of the parameters that characterize the observed brightness variations of these four stars are summarized in Table 19 which lists the period of observation; the brightest light maximum observed; the faintest light maximum; the brightest light minimum; the faintest light minimum and the total range in the brightness in the sense ΔV_{max} (brightest) minus ΔV_{min} (faintest). Both DM UMa and II Peg show a total range of about 0.60 mag whereas the double-lined objects UX Ari and V711 Tau show a range of 0.36 and 0.29 mag respectively. DM UMa and II Peg are single-lined spectroscopic binaries and their low mass companions have not been seen spectroscopically. So the light variations observed in these systems are exclusively from the visible primaries. In the case of double-lined systems UX Ari and V711 Tau the hotter components also contribute appreciable fractions to the total light of the systems. In the case of V711 Tau if we remove the contribution from the hotter component assuming both the star in the system to be equal in brightness, a change of 0.30 mag in the total brightness implies a change of about 0.65 mag for the cooler component. If the hotter component is fainter by about 0.2 mag, the change in the brightness of the cooler component would be around 0.60 mag which is comparable to the values obtained for

the single-lined spectroscopic binaries DM UMa and II Peg.

Table 19. Brightness variations of UX Ari, V711 Tau, II Peg and DM UMa

Star	UX Ari	V711 Tau	II Peg [1]	DM UMa
Period	1972–91	1975–91	1974–91	1979–91
ΔV_{max} (brightest)	0.815	1.364	7.200	0.135
ΔV_{max} (faintest)	1.015	1.542	7.530	0.439
ΔV_{min} (brightest)	0.960	1.506	7.424	0.350
ΔV_{min} (faintest)	1.170	1.650	7.800	0.655
Max. range[2]	0.355	0.286	0.600	0.520

[1] mag values refer to V.

[2]Max. range = ΔV_{max} (brightest)$-\Delta V_{min}$ (faintest).

In the case of UX Ari the total change in brightness observed is 0.355 mag which is larger than that of V711 Tau. If both the stars in UX Ari have the same magnitude at light maximum, our calculations show that the cooler component has to change by about 0.90 mag to account for the total range observed. UX Ari shows a bluer colour at light minimum due to an increase in the fractional contribution from the hotter component. This implies that the hotter component is brighter than the cooler component at light maximum. Hence the actual change in the brightness of the cooler component is larger than 0.90 mag which is significantly larger than in the case of other three systems studied.

Brightness at light maximum and minimum

It is generally accepted now that all the peculiarities seen in the light curves of RS CVn stars can be explained in terms of enhanced solar-type activity associated with the cooler component of the system. Starspots that are distributed on the cooler component modulate the observed light as the

star rotates, giving rise to the observed phenomena. The changes in the light curve are attributed to the changes in the location and distribution of starspots on the stellar surface.

The behaviour of ΔV_{max} and ΔV_{min} in relation to the amplitude of light variation is similar for UX Ari, V711 Tau and II Peg. At larger amplitudes the brightness at minimum decreases and the brightness at maximum increases, both converging to a particular value of ΔV at very low amplitudes. In terms of the starspot model this implies either of the following scenarios: (i) At lower amplitudes spots are evenly distributed in longitudes and are predominantly present at higher latitudes and hence are seen through out the rotational period. (ii) At higher amplitudes spots are more concentrated about some longitude and are predominantly located at lower latitudes and hence disappear from the field of view during the rotational period. In DM UMa the amplitude does not show any correlation with either ΔV_{max} or ΔV_{min}. Both of them show a large range of about 0.30 mag. In general an increase in ΔV_{max} is followed by an increase in ΔV_{min}, and a decrease in ΔV_{max} by a decrease in ΔV_{min}.

Phase of light minimum and lifetime of a centre of activity

The phase of light minimum is an important parameter that characterizes a light curve and is determined by the longitude of starspots on the photosphere of the active star. Its migration with respect to the orbital phases indicates a difference between the photometric period and the assumed orbital period. We have estimated the behaviour of the phase of light minimum over the years for the four systems. In DM UMa the phases of light minima lie on four well separated lines with different slopes. It is interesting to note that all the groups show migration towards decreasing orbital phases implying a smaller photometric period than the orbital period. II Peg shows both direct and retrograde migrations of the phase of light minimum. We could identify a total of six spot groups during the period 1974–91. On most occasions there were two prominent spot groups present. In the case of V711 Tau it is found that spots are confined predominantly to two different latitude belts as indicated by the grouping of the phases of light minima

on two independent near-straight lines. UX Ari shows a secular decrease in the phase of light minima superposed on two dips of short durations during 1976–78 and 1989–91.

We have determined approximate lifetimes for different active regions from the migration of the phase of light minima. In DM UMa we find that the lifetime of a spot or spot group can be as short as about two years. In V711 Tau the lifetime for a spot group is found to be more than 15 years. Observations of II Peg indicates a lifetime of about two to seven years and in UX Ari the lifetime is about 10 years.

$H\alpha$ variation

The $H\alpha$ emission equivalent widths in DM UMa and II Peg indicate a modulation with the photometric phase in the sense that the emission equivalent width is more intense near the minimum of the photometric light curve. The spectra of DM UMa obtained on the night of 1991 Jan 7 and of II Peg obtained on 1990 Nov 22 show strong evidences for optical stellar flare. Though the $H\alpha$ emission strengths are highly variable, V711 Tau and UX Ari do not show any modulation with the orbital phase during the period of our observations.

Numerical details

Our model assumes that the light variation is caused by a limited number of discrete spots and arrives at best fit values for the various spot parameters including the temperature. We use the method of least squares using differential correction. We have developed a computer program to solve multicolour light curves of spotted stars. In recent years several investigators have developed spot modelling techniques to reproduce observed light curves of spotted stars based on the approach outlined by Torres & Ferraz Mello (1973) and Friedemann & Gurtler (1975). In almost all the cases temperatures of the spots are fixed initially. The spot parameters are derived by systematically varying the different parameters until acceptable approximation to the observations is obtained. In the present method the presence of

a strict minimum in the sum of the squares of the deviations in the multi-dimensional parameter space is indicated by the absolute convergence of the solution on iteration. The problem of choosing the final parameters from a set of possible values does not arise in this method because all the spot parameters are simultaneously optimized instead of optimizing each one independently. Apart from avoiding any personal bias, this method also allows the simultaneous determination of the spot temperature when observations are available in more than one wavelength band.

Our Fortran program is fairly general; there is no restriction either on the number of discrete spots, or on their latitudes or longitudes; the temperature of the spots may be treated as either known, or unknown, in which case it may be either the same for all the spots or different for different spots. The determinancy of the spot parameters are indicated by their absolute convergence on iteration from the starting initial guess values; otherwise divergence occurs when the spot area or temperature finally becomes negative. Our trials with synthetic data indicate that the choice of the initial guess values are not critical for achieving the convergence of the solution.

We have applied the method to DM UMa for which a larger database is available, most of which comes from the same telescope set-up thus ensuring minimum systematic errors. The results of modelling indicate the presence of spots at high latitudes at all times except in one case where there is an indication of an additional low latitude spot. Only large discrete cool spots are required to reproduce all of the photometric light curves of DM UMa; their radii range from 22 to 36°. Modelling shows a gradual decrease in the spot area from 1984 onwards. The derived spot temperatures range from 2800 to 3720 K with a mean value of 3400±60 K.

43. Future prospects

The present analysis of the four RS CVn systems confirms that the peculiaities seen in the light curve of a RS CVn star can be explained in terms of starspots associated with the active component of the system. However, the observations do not indicate a strong relationship between the spot activity implied by the light curve and chromospheric activity implied by the

$H\alpha$ emission equivalent width.

The uniqueness of spot modelling is severely constrained by the following two parameters: (i) The inclination of the rotational axis to the line of sight for non-eclipsing systems, and (ii) the magnitude of the unspotted star. The fact that there is always a clear rotational modulation, in most cases with well-defined one or two minima, indicates that most of the light variation is due to one or two prominent spot groups. Effectively replacing a spot or spot group of irregular shape by an equivalent circular spot may not be always possible. Sometimes, this would imply a larger fractional area for the spots if it extends beyond the visible hemisphere. Note that a large fraction of observed light curves of spotted stars is nearly sinusoidal indicating that in general the shape of a spot or spot group cannot be far from circular.

Doppler imaging technique is a very powerful method of studying starspots of rapidly rotating stars. It exploits the correspondence between wavelength position across a rotationally Doppler-broadened spectral line and spatial position across the stellar disc to derive a two dimensional image of the star. Cool spots on a rotating star produce distortions in the star's spectral line profiles. If the line profiles are dominated by rotational broadening, a high degree of correlation exists between the position of a given distortion in a line and the stellar longitude of the feature which produces it. A high resolution spectrum of the line is thus, to first order, a one dimensional image of the star in longitude, but completely blurred in latitude. The observation of the star at other rotational phases provides additional similar images. All these sets of one dimensional images can be combined into a two dimensional image of the star provided the inclination, rotation period and other basic physical parameters of the star are known (Vogt et al. 1987; Vogt & Hatzes 1990). The Doppler imaging technique is an independent method for obtaining the distribution of starspots across the stellar surface, and can be used to test the accuracy and uniqueness of spot modelling based upon broadband photometry (cf. Linsky 1988).

The observations of RS CVn stars at wide wavelength regions have given information on the different temperature zones of the stellar atmosphere from cool photospheric spots to multi-million degree corona (Byrne et al. 1989 and

references therein). The spatial correspondence between the spots as indicated by the light curve and the active regions as indicated by the various chromospheric emission features is not well established in RS CVn systems. Simultaneous multiwavelength coordinated observations, well distributed in rotational phases spread over many observing seasons, will be useful in determining whether spots and active regions are spatially correlated.

References

Adams, W. S., Joy, A. H. & Sanford, R. F. (1924) P. A. S. P. **36**, 137.

Allen, C. W. (1976) in *Astrophysical Quantities* (ed. : C. W. Allen) The Athlone Press, Univ. of London p. 204.

Andrews, A. D. et al. (1988) Astr. Ap. **204**, 177.

Appenzellar, I. & Mundt, R. (1989) Astr. Ap. Rev. **1**, 291.

Arevalo, M. J., Lazaro, C. & Fuensalida, J. J. (1985) Inf. Bull. Var. Stars No. 2840.

Ayres, T. R. & Linsky, J. L. (1982) Ap. J. **254**, 168.

Ayres, T. R., Simon, T. & Linsky, J. L. (1984) Ap. J. **279**, 197.

Baliunas, S. L., Hartmann, L., Vaughan, A. H. & Dupree, A. K. (1981) Ap. J. **246**, 473.

Baliunas, S. L. & Dupree, A. K. (1982) Ap. J. **252**, 668.

Baliunas, S. L., Guinan, E. F. & Dupree, A. K. (1984) Ap. J. **282**, 733.

Baliunas, S. L. (1986) in *Cool Stars, Stellar Systems, and the Sun* (eds: M. Zeilik & D. M. Gibson) Springer–Verlag, p. 3.

Bartolini, C. et al. (1978) Astr. J. **83**, 1510.

Bartolini, C. et al. (1983) Astr. Ap. **117**, 149.

Bohusz, E. & Udalski, A. (1981) Acta Astr. **31**, 185.

Bookbinder, J.A. (1988) in *Activity in Cool Star Envelopes* (eds: O. H. Havnes, B. R. Pettersen, J. H. M. M. Schmitt & J. E. Solheim) Kluwer, p. 257.

Bopp, B. W. & Fekel, F. C. (1976) Astr. J. **81**, 771.

Bopp, B. W. et al. (1977) Astr. J. **82**, 47.

Bopp, B. W. & Fekel, F. C. (1977) Astr. J. **82**, 490.

Bopp, B. W. & Talcott, J. C. (1978) Astr. J. **83**, 1517.

Bopp, B. W. & Noah, P. V. (1980) P. A. S. P. **92**, 333.

Bopp, B. W. & Stencel, R. E. (1981) Ap. J. **247**, L. 131.

Bopp, B. W. (1983) in *IAU Coll. No.* **71***: Activity in Red–Dwarf Stars* (eds: P. B. Byrne & M. Rodono) Reidel, p. 363.

Bopp, B. W. et al. (1989) Ap. J. **339** 1059.

Bopp, B. W. (1990) Mem. S. A. It. **61**, 723.

Boyd, P. T. et al. (1987) Inf. Bull. Var. Stars No. 3089.

Budding, E. & Zeilik, M. (1987) Ap. J. **319**, 827.

Busso, M., Scaltriti, F. & Cellino, A. (1986) Astr. Ap. **156**, 106.

Buzasi, D. L., Ramsey, L. W. & Huenemoerder, D.P. (1987) Ap. J. **322**, 353.

Buzasi, D., Ramsey, L. W. & Huenemoerder, D.P. (1991) (preprint)

Buzasi, D. L., Huenemoerder, D. P. & Ramsey, L. W. (1991) (preprint).

Byrne , P. B. et al. (1984) in *Proc. Fourth European IUE Con.* ESA SP–**218**, p. 343.

Byrne, P. B. (1986) Inf. Bull. Var. Stars No. 2951.

Byrne, P. B. et al. (1989) Astron. Ap. **214**, 227.

Cano, J. A. et al. (1987) Inf. Bull. Var. Stars No. 3107.

Carlos, R. C. & Popper, D. M. (1971) P. A. S. P. **83**, 504.

Casas, R. et al. (1989) Inf. Bull. Var. Stars No. 3330.

Catalano, S. & Rodono, M. (1967) Mem. Soc. Astr. Ital. **38**, p. 395.

Catalano, S. & Rodono, M. (1969) in *IAU Coll. No.* **4***: Non–Periodic Phenomena in Variable Stars* (ed. : L. Detre) Academic Press, Budapest, p. 435.

Chambliss, C. R. et al. (1978) Astr. J. **83**, 1514.

Chambliss, C. R. & Detterline, P. J. (1979) Inf. Bull. Var. Stars No. 1591.

Charles, P., Walter, F. & Bowyer, S. (1979) Nature **282**, p. 691.

Charles, P. (1983) in *IAU Coll.* **71***: Activity in Red–Dwarf stars* (eds: P. B. Byrne & M. Rodono) Reidel, p. 415.

Chisari, D. & Lacona, G. (1965) Mem. Soc. Astr. Ital. **36**, p. 463.

Chugainov, P. F. (1976) Bull. Crim. Astr. Obs. **54**, 89 (Russian).

Chugainov, P. F. (1977) Bull. Crim. Astr. Obs. **57**, 22.

Cousins, A. W. J. (1963) M. N. A. S. S. Africa **22**, 58.

Crampton, D., Dobias, J. & Margon, B. (1979) Ap. J. **234**, 993.

Cutispoto, G. et al. (1987) Inf. Bull. Var. Stars No. 3034.

Cutispoto, G. et al. (1989) Inf. Bull. Var. Stars No. 3379.

Donati, J. F. et al. (1990) Astr. Ap. **232**, L. 1.

Dorren, J. D. et al. (1981) Astr. J. **86**, 572.

Dorren, J. D. & Guinan, E. F. (1982) Ap. J. **252**, 296.

Dorren, J. D., Guinan, E. F. & Wacker, S.W. (1986) in *New Insights in Astrophysics: Eight Years of UV Astronomy with IUE* ESA SP−263, p. 201.

Doyle, J. G. et al. (1988) Astr. Ap. **192**, 275.

Eaton, J. A. & Hall, D. S. (1979) Ap. J. **227**, 907.

Eaton, J. A. (1986) Acta Astr. **36**, 79.

Eggen, O. J. (1968) R. Obs. Bull. No. 137.

Evren, S. (1988) Ap. Sp. Sci. **143**, 123.

Evren, S. (1990) in *Active Close Binaries* (eds. : Cafer Ibanoglu) Kluwer, p. 561.

Fekel, F. C. (1983) Ap. J. **268**, 274.

Fekel, F. C., Moffett, T. J. & Henry, G. W. (1986) Ap. J. Suppl. **60**, 551.

Feldman, P. A., Taylor, A. R. & Gregory, P. C. (1978) Astr. J. **83**, 1471

Fraquelli, D.A. (1984) Ap. J. **276**, 243.

Friedemann, C. & Gurtler, J. (1975) Astr. Nachr. **296**, 125.

Gibson, D. M., Hjellming, R. M. & Owen, F. N. (1975) Ap. J. **200**, L. 99.

Gondoin, P. (1986) Astr. Ap. **160**, 73.

Gratton, L. (1950) Ap. J. **111**, 31.

Guinan, E. F. et al. (1981) P. A. S. P. **93**, 495.

Hall, D. S. (1972) P. A. S. P. **84**, 323.

Hall, D. S. (1976) in *IAU Coll. No.29: Multiple Periodic Variable Stars* (ed. : W. S. Fitch) Reidel, p. 287.

Hall, D. S. & Henry, G. W. (1983) Inf. Bull. Var. Stars No. 2307.

Hall, D. S. (1989) Sp. Sci. Rev. **50**, 219.

Hall, D. S. (1990) in *Active Close Binaries* (ed. : Cafer Ibanoglu) Kluwer, p. 377.

Halliday, I. (1952) J. R. Astr. Soc. Can. **46**, 103.

Hardie, R. H. (1962) in *Astronomical Techniques* (ed. : W.A.Hiltner) Univ. of Chicago Press, London, p. 178.

Hartmann, L., Londono, C. & Phillips, M. J. (1979) Ap. J **229**, 183.

Heckert, P. A. et al. (1988) Inf. Bull. Var. Stars No. 3274.

Henry, G. W. (1983) Inf. Bull. Var. Stars No. 2309.

Hiltner, W. A. (1947) Ap. J. **106**, 481.

Huenemoerder, D. P. & Ramsey, L. W. (1987) Ap. J. **319**, 392.

Huenemoerder, D. P., Ramsey, L. W. & Buzasi, D. L. (1989) Astr. J. **98**, 2264.

Huenemoerder, D. P., Buzasi, D. L. & Ramsey, L. W. (1989) Astr. J. **98**, 1398.

Horne, K. (1986) P. A. S. P. **98**, 609.

Jeffers, H. M. & van den Bos, W. H. (1963) Pub. Lick Obs. **21**, 1.

Johnson, H. L. (1963) in *Basic Astronomical Data* (ed. : K.A.Strand) Univ. of Chicago Press, Chicago, p. 204.

Johnson, H. L. (1966) Ann. Rev. Astr. Ap. **4**, 193.

Kaluzny, J. (1984) Inf. Bull. Var. Stars No. 2627.

Kholopov, P. N. (1984) Sov. Sci. Rev. E. Astrophys. Space Phys. **3**, p. 98.

Kimble, R. A., Kahn, S. M. & Bowyer, S. (1981) Ap. J. **251**, 585.

Kopal, Z. (1959) in *Close Binary Systems* Chapman & Hall, London. p. 450.

Kron, G. E. (1947) P. A. S. P. **59**, 261.

Kron, G. E. (1952) Ap. J. **115**, 301.

Landis, H. J. et al. (1978) Astr. J. **83**, 176.

Lang, K. R. & Willson, R. R. (1988) Ap. J. **328**, 610.

Liller, W. (1978) IAU Circ. No. 3176.

Lines, R. D. et al. (1983) Inf. Bull. Var. Stars No. 2308.

Linsky, J. L. (1980) Ann. Rev. Astr. Ap. **18**, 439.

Linsky, J. L. (1983) in *IAU Coll. No.* **71***: Activity in Red–Dwarf Stars* (eds: P. B. Byrne & M. Rodono) Reidel, p. 377.

Linsky, J. L. (1984) in *Cool Stars, Stellar Systems and the Sun* (eds: S. L. Baliunas & L. Hartmann) Springer–Verlag, p. 244.

Linsky, J. L. (1988) in *Multiwavelength Astrophysics* (ed. : F. A. Cordova) Cambridge Univ. Press, p. 49.

Liu, X-f. & Tan, H-s. (1987) Chin. Astr. Ap. **11**, 64.

Manduca, A., Bell, R. A. & Gustafsson, B. (1977) Astr. Ap. **61**, 809.

Marstad, N. et al. (1982) in *Advances in Ultraviolet Astronomy: Four years of IUE Research* NASA Conf. Pub. No **2238**, p. 554.

Mekkaden, M. V., Raveendran, A. V. & Mohin, S. (1982) J. Astr. Ap. **3**, 27.

Mekkaden, M. V. (1987) Inf. Bull. Var. Stars No. 3043.

Mohin, S. et al. (1982) Inf. Bull. Var. Stars No. 2190.

Mohin, S. et al. (1985) Ap. Sp. Sci. **115**, 353.

Mohin, S., Raveendran, A. V. & Mekkaden, M. V. (1986) Bull. Astr. Soc. India **14**, 48.

Mohin, S. & Raveendran, A. V. (1989) J. Ap. Astr. **10**, 35.

Morgan, J. G. & Eggleton, P. P. (1979) M. N. R. A. S. **187**, 661.

Morris, D. H. & Mutel, R. L. (1988) Astr. J. **95**, 204.

Mutel, R. L. et al. (1987) Astr. J. **93**, 1220.

Nations, H. L. & Ramsey, L. W. (1980) Astr. J. **85**, 1086.

Nations, H. L. & Ramsey, L. W. (1981) Astr. J. **86**, 433.

Nations, H. L. & Ramsey, L. W. (1986) Astr. J. **92**, 1403.

Nicolet, B. (1978) Astr. Ap. Suppl. **34**, 1.

Oliver, J. P. (1974) Ph. D. Thesis, Univ. of California, Los Angeles.

Oke, J. B. (1965) Ann. Rev. Astr. Ap. **3**, 23.

Owen, F. N., Jones, T. W. & Gibson, D. M. (1976) Ap. J. **210**, L. 27.

Owen, F. N. & Gibson, D. M. (1978) Astr. J **83**, 1488.

Parthasarathy, M., Raveendran, A. V. & Mekkaden, M. V. (1981) Ap. Sp. Sci. **74**, 87.

Pajdosz, G. et al. (1989) Inf. Bull. Var. Stars No. 3292.

Plavec, M. & Grygar, J. (1965) Kleine Veroff. Remeis Sternw, Bamberg, **4**, No. 40, p. 213.

Poe, C. H. & Eaton, J. A. (1985) Ap. J **289**, 644.

Popper, D. M. (1970) IAU Colloq. No. **6**, p. 13.

Popper, D. M. & Ulrich, R. K. (1977) Ap. J. **212**, L. 131.

Popper, D. M. (1980) Ann. Rev. Astr. Ap. **18**, 115.

Prabhu, T. P. & Anupama, G. C. (1991) Bull. Astr. Soc. India **19**, 97.

Ramsey, L. W. & Nations, H. L. (1980) Ap. J. **239**, L. 121.

Ramsey, L. W. & Nations, H. L. (1984) Astr. J. **89**, 115.

Ramsey, L. W. (1990) in *Cool Stars, Stellar Systems, and the Sun* (ed. : George Wallerstein) Astronomical Society of the Pacific, p. 195.

Raveendran, A. V., Mohin, S. & Mekkaden, M. V. (1981) M. N. R. A. S. **196**, 289.

Raveendran, A. V. & Mohin, S. (1987) Kodaikanal Obs. Bull. **8**, 13.

Rodono, M., Romeo, G. & Strazzula, G. (1980) *Proc. Second European IUE Conference* ESA–SP **157**, p. 55.

Rodono, M. et al. (1983) in *IAU Coll. No.* **71***: Activity in Red–Dwarf Stars* (eds: P. B. Byrne & M. Rodono) Reidel, p. 179.

Rodono, M. et al. (1986) Astr. Ap. **165**, 135.

Rodono, M. et al. (1987) Astr. Ap. **176**, 267.

Rucinski, S. M. (1977) P. A. S. P. **89**, 280.

Sanford, R. F. (1921) Ap. J. **53**, 201.

Scarborough, J. B. (1964) in *Numerical Mathematical Analysis* Oxford Book & Stationery Co. Calcutta, p. 539.

Schwartz, D. A. et al. (1979) Astr. J. **84**, 1160.

Schwartz, D. A. et al. (1980) Bull. Am. Astr. Soc. **12**, 513.

Sarma, M. B. K. & Ausekar, B. D. (1980) Acta Astr. **30**, 101.

Sarma, M. B. K. & Ausekar, B. D. (1981) Acta Astr. **31**, 103.

Sarma, M. B. K. & Prakasa Rao, B. V. N. S. (1984) J. Ap. Astr. **5**, 159.

Simon, T., Linsky, J. L. & Schiffer. F. H. III. (1980) Ap. J. **239**, 911.

Simon, T. & Linsky, J. L. (1980) Ap. J. **241**, 759.

Simon, T. et al. (1985) Ap. J. **293**, 551.

Simon, T. & Sonneborn, G. (1987) Astr. J. **94**, 1657.

Skumanich, A. (1972) Ap. J. **171**, 565.

Slee, O. B. et al. (1987) M. N. R. A. S. **229**, 659.

Soderblom, D. R. (1982) Ap. J. **263**, 239.

Spangler, S. R., Owen, F. N. & Hulse, R. A. (1977) Astr. J. **82**, 169.

Strassmeier, K. G. et al. (1989) Ap. J. Suppl. **69**, 141.

Struve, O. (1946) Ann. d'Astrophys. **9**, 1.

Tan, H. & Liu, X. (1985) Inf. Bull. Var. Stars No. 2669.

Torres, C. A. O. & Ferraz Mello, S. (1973) Astr. Ap. **27**, 231.

Vogt, S. S. (1979) P. A. S. P. **91**, 616.

Vogt, S. S. (1981) Ap. J. **247**, 975.

Vogt, S. S. & Penrod, G. D. (1983) P. A. S. P. **95**, 565.

Vogt, S. S., Penrod, G. D. & Hatzes, A. P. (1987) Ap. J. **321**, 496.

Vogt, S. S. & Hatzes, A. P. (1991) in *IAU Coll. No.* **130** (eds: T. D. Moss & G. Rudiger) Springer–Verlag, p. 297.

Wacker, S. W. & Guinan, E. F. (1986) Inf. Bull. Var. Stars No. 2970.

Wacker, S. W. & Guinan, E. F. (1987) Inf. Bull. Var. Stars No. 3018.

Walter, F. M., Charles, P. & Bowyer, S. (1978) Nature **274**, 569.

Walter, F. M. et al. (1980) Ap. J. **236**, 212.

Weiler, E. J. (1978) M. N. R. A. S. **182**, 77.

Weiler, E. J., Owen, F. N. & Bopp, B. W. (1978) Ap. J. **225**, 919.

White, N. E., Sanford, P. W. & Weiler, E. J. (1978) Nature **274**, 569.

Wilson, O. C. (1963) Ap. J. **138**, 832.

Wilson, O. C. (1964) P. A. S. P. **76**, 238.

Wilson, O. C. (1978) Ap. J. **226**, 379.

Zeilik, M. et al. (1982a) Inf. Bull. Var. Stars No. 2168.

Zeilik, M. et al. (1982) Inf. Bull. Var. Stars No. 2177.

Zeilik, M. et al. (1988) Ap. J. **332**, 293.

Zeilik, M. et al. (1990) Ap. J. **354**, 352.